Separation and speciation of biodegradable complexes using capillary zone electrophoresis

by

Lindiwe Eudora Khotseng

Dissertation submitted for the degree of

Doctor of Philosophy

(Chemistry)

at the Faculty of Science at the University of Stellenbosch, Republic of South Africa.

Promoter: **Prof. A. M. Crouch**

Co-promoter: **Prof. P. Sandra**

December 2004

Declaration

I, the undersigned, hereby declare that the work contained in this dissertation is my own original work and that I have not previously in its entirety or in part submitted it at any university for a degree.

Signature:

Date:

ABSTRACT

Separation of the metal ions Cu^{2+}, Pb^{2+}, Cd^{2+} Mn^{2+}, Cr^{3+}, Fe^{3+} and Zn^{2+} with poly ethylenediamine tetra-acetic acid (EDTA), ethylenediamine disuccinic acid ([S,S']-EDDS) and ethylenediamine dimalonic acid (EDDM) was performed by Capillary Electrophoresis.

The electropherograms obtained by Capillary Electrophoresis were validated with a speciation model Joint Expert Speciation System (JESS). Excellent agreement was observed for the speciation diagrams for these species with the pH curves determined by capillary electrophoresis with those determined by speciation modelling using JESS.

The ligands EDDS and EDDM are readily biodegradable. They have been proposed as substitute ligands for EDTA.

Detection of the above species was performed using both an electrochemical and a UV detector. The obtained electropherograms were used for the determination of the detection limits of these species. The electrochemical detector has a lower detection limit for these species than the UV detector in conformity with reported literature for these detectors.

OPSOMMING

Skeiding van die metaal ione Cu^{2+}, Pb^{2+}, Cd^{2+}, Cr^{3+}, Fe^{3+} en Zn^{2+} met behulp van etileendiamientetra-asyn suur (EDTA), etileendiamiendisuksien suur ([S,S']-EDDS) en etileendiamiendimaleen suur (EDDM) was gedoen deur kapilêre elektroferose.

Die elektroferogramme, verkry deur kapilêre elektroferose was gebruik om die spesiasie model "Joint Expert Speciation System (JESS)" te valideer. Uitstekende ooreenstemming was waargeneem vir die verspreidings diagramme van hierdie spesies as 'n funksie van pH wat verkry was deur kapilêre elektroferose met die' wat vasgestel was deur die spesiasie modeleeringsproses van JESS.

Die ligande EDDS en EDDM toon onmiddelike biodigradeerbaarheid. Hulle was voorgehou as alternatiewe ligande vir EDTA.

Bepaling van die bogenoemde spesies was ook gedoen deur beide elektrochemiese en UV deteksie. Deur gebruik te maak van hierdie detektore was die deteksie limiete van hierdie spesies bepaal. Die elektroochemiese detektor het 'n laer deteksie limiet vir hierdie spesies in vergelyking met die UV detector. Dit stem ooreen met die literatuur vir hierdie detektore.

GLOSSARY OF SYMBOLS

AD - Amperometric detection

AEAA - N(2-aminoethyl)aspartic acid

CAS - Chemical abstracts services

CCE - Carbon composite working electrode

CD - Conductivity detection

CE - Capillary electrophoresis

CEEC - Capillary electrophoresis with electrochemical detection

CGE - Capillary gel electrophoresis

CIEF - Capillary isoelectric focusing

CMC - Critical micelle concentration

CME - Chemically modified electrode

CZE - Capillary zone electrophoresis

CITP - Capillary isotachophoresis

CTAB - Cetyltrimethylammonium bromide

DAD - Diode array detection

DetMP - Detritus from nanophytoplankton c

DOC - Dissolved organic carbon

DTPA - Diethylenetriamine penta-acetic acid

EC - Electrochemical detection

EDDA - Ethylenediamine diacetic acid

EDDM - Ethylenediamine dimalonic acid

EDDS - Ethylenediamine disuccinic acid

EDTA - Ethylenediamine tetra-acetic acid

EDTMP - Ethylenediamine tetramethylenephosphonic acid

EOF - Electro-osmotic flow

EPR - Electron paramagnetic resonance

HPCE - High-performance capillary electrophoresis

HPLC - High-performance liquid chromatography

HSAB - Hard and soft acid and base

HV - High voltage

ICE - In-capillary electrode

i.d. - Inner diameter

JESS - Joint expert speciation system

MEKC - Micellar electrokinetic capillary chromatography

NTA - Nitrilotriacetate

OCE - On-capillary electrode

o.d. - Outer diameter

OECD - Organization for Economic Co-operation and Development

PD - Potentiometric detection

pI - Isoelectric point

PLS - Partial least squares

STP - Pentasodium tripolyphosphate

WHO - World Health Organisation

WJE - Wall jet electrode

ACKNOWLEDGEMENTS

The author wishes to express her appreciation to:

- Prof. A. M. Crouch, for his support, patience, help and encouragement throughout my postgraduate years of study.
- The Electricity Supply Commission (ESKOM), University of Stellenbosch (US) and National Research Foundation (NRF) for their financial support.
- S. Woolley and M. Brewer of Associated Octel Co. Ltd (U.K.) for supplying us with the ([S,S']-H_4EDDS) ligand.
- Prof. D. Williams and Dr. Paul W. Jones from the University of Cardiff, Cardiff, UK, for assistance with the speciation data.
- Prof. Sandra, Prof. H. Lauer Dr. A. De Villiers and Dr. F. Lynen for their contribution in the project

CONTENTS

LIST OF FIGURES

CHAPTER 2

CHAPTER 3

CHAPTER 4

CHAPTER 5

LIST OF TABLES

CHAPTER 2

CHAPTER 3

CHAPTER 4

CHAPTER 5

CHAPTER 1

MOTIVATION AND GOALS

1.1 Background

The rapid increase in the levels of environmental pollution over recent decades has resulted in increasing concern for people's well being and for global ecosystems. The need to determine different species of trace elements in environmental and biological materials is beyond question since the effects or toxicity of an element and its behaviors depend to a great extent on its chemical form and concentration[1]. The hexadentate chelating agent ethylenediamine-*N,N,N',N'*-tetra-acetic acid [H_4EDTA] is widely used in industry due to its ability to complex with various transition metal ions in 1:1 ratio[2]. The importance of EDTA is exemplified by its diversity of applications in many spheres, such as imaging agents[3], ion-exchange materials[4] and metal ion sequestering agents in the H_2O_2 bleaching of paper pulp[5,6], to name a few. Like other aminopolycarboxylic acids, its release into the environment may affect the distribution of metals within the aquatic ecosystem and may remobilize heavy metals from sediments[7]. Hence, with increasing concern for the welfare of the environment, it is necessary to replace some, if not all, of the ligands currently preferred in industrial processes, as they and their complexes with toxic heavy metal ions are not readily biodegradable and thus tend to accumulate in the biosphere[8].

[*S,S'*]-ethylenediamine-*N,N'*-disuccinic acid [H_4EDDS] and ethylenediamine-N,N'-dimalonic acid [H_4EDDM] have been proposed as potential biodegradable substitutes for EDTA. Of importance is, on one hand, the development of analytical techniques allowing the easy monitoring of EDTA and its biodegradable analogues in the complexed and free

chelate form, but also the availability of a technique able to a make a distinction between the different ligand species.

1.2 Project motivation

Studies of speciation of trace metals have been focused on the interpretation of their roles in recent environmental and biological studies. The chemical and physical properties of a metal species depend very much on its oxidation state. Thus, an accurate determination of each metal species is usually important to evaluate environmental risk.

Chemical speciation is the chemical form or compound in which an element occurs in a living system or environment. It may also refer to the quantitative distribution of an element, therefore speciation can be defined as the oxidation state, concentration and composition of each of the species in the chemical sample[9]. Speciation modelling is essential when trying to understand complex systems, and various methods to study speciation have been used *i.e.* stripping voltammetry, ion selective electrodes, UV-Vis spectroscopy[1]. As far as can be ascertained there is nothing in the literature describing the use of CE to study speciation of biodegradable ligands.

The focus of this thesis was to develop analytical techniques which could speciate metal ligand complexes and ligands by making use of CE in the capillary zone electrophoresis mode. A further objective was to develop a more sensitive and cost effective detector like EC for the detection of metal complexes.

1.3 Aims and objectives

The aim of this study is the detailed evaluation of the common aminopolycarboxylic acid, which is EDTA and its structural isomers EDDM and [S,S']-EDDS as derivatizating reagents for the separation of metal ions using CZE. Attention was paid to the effect of carrier electrolyte parameters (*i.e.* pH) on the migration behavior of metal complexes. Several samples were selected to demonstrate the feasibility of the method. The results obtained using CZE were to be validated with speciation calculations obtained using joint expert speciation system (JESS).

1.4 Methodology

Capillary Electrophoresis (CE) was the method selected. It is probably the most rapid growing analytical technology that has appeared in the last two decades and has been used widely in all branches of analytical chemistry[10]. Introduced by the fundamental papers of Mikkers *et al.*[11] and Jorgenson and Lukacs[12], CE has rapidly evolved as an independent technique, expanding beyond the application field of slab gel electrophoresis, traditionally limited to the separation of biopolymers, to include the analysis of inorganic anions and cations, metal chelates, pharmaceuticals and drugs (including enantiomers), hydrocarbons, organic acids, amines, carbohydrates, polymers and particles, fuels, dyes, explosives, *etc.*, which traditionally were typical applications of chromatography. In recent years, the application of CE to speciation studies has become an important research area[13].

The great interest raised by CE is undoubtedly due to its high efficiency, mass sensitivity, minimum needs of solvent and sample volumes, *etc.*, but particularly to the high

versatility in terms of separation modes, which, based on different physicochemical principles, display different selectivity. As it is well known, without changes in the instrumental hardware, CE separations can be carried out using capillary zone electrophoresis (CZE), micellar electrokinetic capillary chromatography (MEKC), capillary electrochromatography (CEC), capillary isoelectrokinetic focusing (CIEF), capillary gel electrophoresis (CGE) and capillary isotachophoresis (CITP).

Recently more and more studies related to CE separation of metal ions as their complexes have been carried out to the advantages of the combination of high performance separation technique and high sensitivity derivatization agents[14]. Separation of metal ions complexed with a chelating reagent by capillary zone electrophoresis (CZE) is influenced by the charge, the size and the stability of chelate, and pH and some properties of the buffer[15]. Capillary zone electrophoresis (CZE) methods provide efficient separations with high resolution and can have excellent detection limits for small sample sizes [16]. Complexation of the cations to be separated with auxiliary ligands is used to change the selectivity of the separation and/or to facilitate the detection[1].

In order to realize these advantages in practice, detection systems must be available which are both highly sensitive and fully compatible with the small physical scale of CE capillaries. UV-Visible absorption, which is clearly the most widely used detection approach in HPLC and should have many attractive features for CE, is restricted by its sensitivity in CE due to the short optical pathlengths afforded by the small inside diameter (i.d.) of the capillaries.[6] Additionally, many interesting analytes do not absorb strongly or at long enough wavelengths and therefore are only after derivatization good candidates for UV-Visible detection [5].

Electrochemical detection (EC), an alternative to conventional spectroscopic methods, is ideally suitable to CE characterized by its small injection volume, high separation efficiency, rapid speed,[7] high selectivity and sensitivity[17] as well as the variety of configurations and materials that can be employed[9]. Since its introduction in 1987 by Wallingford and Ewing[18], capillary electrophoresis with electrochemical detection (CEEC) has attracted a great deal of interest with an increasing number of publications each year[19]. With amperometry, which is mostly used in the direct mode (*i.e.*, for electroactive species), very low detection limits can be achieved[20]. The successful application of an electrochemical detection scheme is strongly dependent on the choice of the working electrode materials, which have been fabricated from a number of conventional electrode materials such as carbon, platinum, gold, nickel and copper. Chemically modified electrodes which have been developed through the introduction of a catalyst or redox mediator, extend the applicability of CE with EC to compounds that could not be detected electrochemically or that must be detected at high over-potential. However, selection of most electrode materials is still being focused on carbon-based materials owing to their low background, low cost, high stability and resistance to passivation[21].

The developed analytical technique was to be improved further to be able to detect samples at very low concentrations *e.g.* micromolar (μM). Hence, an electrochemical detector was to be developed during this study in order to speciate the polyaminocarboxylic acid complexes with much lower concentration compared to the UV-Visible detector.

1.5 Layout of the thesis

- The analysis of the different species of polyaminocarboxylic acid ligands which are [(S, S')-EDDS]$^{4-}$, [EDDM]$^{4-}$ and [EDTA]$^{4-}$ at different pH values using capillary zone electrophoresis.
- The separation of the metal ligand complexes of EDDS^{4-}, EDDM^{4-} and EDTA^{4-} with Cu^{2+}, Zn^{2+}, Cd^{2+}, Pb^{2+}, Cr^{3+}, Mn^{2+} and Fe^{3+} using the same method.
- The validation of the results with the speciation graphs obtained using JESS speciation graphs.
- The development of an electrochemical detector to study the detection limit of the metal ligand complexes mentioned above.

References

1. Kot A., Namiesnik J., *Trends in Analytical Chemistry*, 2000, **19(2),** 69.
2. Kim M. H., Birke R. L., *Analytical Chemistry*, 1983, **55**, 1735.
3. Lauffer R. B., *Chemical Review*, 1987, **87**, 901.
4. Sahni S. K., Reedijk J., *Journal of Coordination Chemistry Review*, 1984, **1**, 59.
5. Lapierre L., Bouchard J., Berry R. M., Van Lierop B. J., *Pulp and Paper Science*, 1995, **21**, J628.
6. Bryant P. S., Edwards L. L. J., *Pulp and Paper Science*, 1998, **22**, J37.
7. Williams D. R., *Chemistry in Britain*, January 1998, 48.
8. Loonen H., Lindgren F., Hansen B., Karcher W., Rorije E., Struijs J., *Environmental Toxicology Chemistry,* 1999, **18**, 1763.
9. Taylor D. M., Williams D. R, *Trace Element Medicine and Chelation Therapy,* 1995, RSC.
10. Mikkers F.E.P., Everaerts E., Verheggen Th. P.E.M., *Journal of Chromatography*, 1979, **169**, 11.
11. Jorgenson W., Lukacs K.D., *Analytical Chemistry*, 1981, **53**, 1298.
12. Jorgenson W., Lukacs K.D., *Journal of Chromatography*, 1981, **218**, 209.
13. Tagliaro F., Turrina S., Pisi P., Smith F. P., Marigo M., *Journal of Chromatography B,* 1998, **713**, 27.
14. Liu B-F., Liu F-B., Cheng J-K., *Journal of Chromatography A*, 1999, **834**, 277.
15. Yakoyama T., Tsuji H., Zenki M., *Analytica Chimica Acta*, 2000, **409**, 555.

16. Okemgbo A.A., Hill H. H., Metcalf S. G., Bachelor M., *Analytica Chimica Acta*, 1999, **396**, 105.

17. Bryant P. S., Edwards L. L. J., *Pulp and Paper Science*, 1998, **22**, J37.

18. Loonen H., Lindgren F., Hansen B., Karcher W., Rorije E., Struijs J., *Environmental Toxicology Chemistry,* 1999, **18**, 1763.

19. Nowack B., Kari F. G., Hilger S. U., Sigg L., *Anaytical Chemistry,* 1996, **68(3)**, 561.

20. Kari F. G., Giger W., *Water Resources*, 1996, **30 (1)**, 122.

21. Taylor D. L., Jardine P. M., *Journal of Environmental Quality,* 1995, **24(4)**, 789.

CHAPTER 2

METALS AND METAL LIGAND COMPLEXES

2.1 Metals and their distribution

Transition metal chelates are used in a variety of consumer products and processes, *e.g.* in the pulp and paper, textile, metal, photographic, leather, cosmetic and detergent industries. Their prime purpose is to control trace amounts of iron, manganese, copper, *etc.* that would otherwise be deleterious to product performance or commercial process. The molecular design requirements for an effective chelator (*e.g.* hexadendate ligand derived from a diamine with carboxylate or phosphate moieties) are well known and exemplified in current commercially available materials, such as, aminopolycarboxylates (EDTA, DTPA, *etc.*) or aminophosphonates (EDTMP, DETPMP, *etc.*).

These chelators are, however, essentially non-biodegradable or require special environmental conditions for degradation to occur. Hence, with increasing concern for the welfare of the environment, it is necessary to replace some, if not all, of the ligands currently preferred in industrial processes, as they and their complexes with toxic heavy metal ions are not readily biodegradable and thus tend to accumulate in the biosphere[1,2].

The metals investigated in this study are transition metals, including four metals (Cu^{2+}, Pb^{2+}, Zn^{2+}, Cd^{2+}) of prime environmental concern, commonly referred to as heavy metals. Certain heavy metals, such as Hg, Cd, and Pb, are considered toxic even at very low levels. Potentially toxic metals, *e.g.* Cu, Zn, and Ni, also have essential properties with different threshold levels[3] for various plants[4] and organisms, including man[3].

2.2 Metal ligands

A complex is a species formed by the association of two or more simpler species, each capable of independent exististence[5]. The word ligand is derived from the Latin verb *ligare,* meaning bind. Ligands are Lewis bases (electron pair donors) because they always bear at least one atom having a lone pair of electrons accessible for bonding to another atom. The process of donating electrons is also known as complexation and the ligands undergoing this process are known as metal complexing agents. Ligands can be either monodentate *i.e.* possess a single donor atom or polydentate if they appear to chelate the metal between two or more donor atoms. A metal ligand complex is made up of a central metal ion and one or more ligands donating at least one pair of electrons to the metal ion, forming a coordinate bond.

Werner was the first to develop the concept of metal complexes[6]. He concluded that a metal ion is characterized by two valencies primary and auxiliary. The principal valency is now termed the oxidation number of the metal. The auxiliary valency represents the number of ligand atoms associated with the central metal atom, *i.e.* the coordination number. Later, the bonding of transition metal complexes was described using electrostatic attraction. Crystal field and molecular orbital theories were developed to explain the bonding and electronic properties of transition metal complexes[6].

Metals and ligands can be classified using the Hard and Soft Acid and Base (HSAB) theory developed by Pearson[7]. Hard acids are small metal ions and are not very polarisable; these prefer hard ligands and bases, which are also small and not very polarisable. Similarly, soft acids and the ligands they prefer, soft bases, are larger and polarizable[8].

Complexing agents can often be added to a solution to prevent one or more customary reactions of a metal ion without actually removing it from the solution. For example, a metal ion that interferes with a chemical analysis can often be complexed and its interference thereby prevented. In a sense, the complexing agent hides the metal ion and is therefore referred to as a sequestering agent. Because chelates perform this role more effectively than do monodentate ligands, the term sequestering agent is usually reserved for chelates[9].

There are two main forces controlling the nature of a ligand:

- when the adducts formed are electrostatic, and
- hydrogen bond interaction (intermolecular)[9].

The ability of metals to form complexes normally increases as the positive charge of the metal increases and as its size decreases. As the ligand gets larger, fewer can coordinate to the metal. As the ligand approaches a metal ion, a ligand lone electron pair forms a π bond with the metal through an interaction between the lone pair orbital and an empty orbital on the metal ion or atom, *e.g.*

$M^{n+} + :NH_3 \rightarrow [M \leftarrow NH_3]^{n+}$

2.3 Chelates

A chelate is a polydentate ligand, *i.e.* it can bind to the metal ion with more than one atom, forming a ring. The word chelate is derived from the Greek word *chele*, meaning a lobster's claw[4], describing the way in which the ligand binds by wrapping itself around the metal ion. Chelating ligands form much more stable complexes and have higher formation constants with metal ions than unidentate ligands do. This is known as the

"chelate effect" and is due partly to the reduction in entropy of subsequent donor atoms, as their movement is restricted, after the initial donor atom has bound to the metal ion[5].

2.4 Chelating agents in industry

Metal ions play a role in virtually all aqueous processes. A common phenomenon is the scale formation by precipitation of alkaline earth and of heavy metal salts, which blocks pipes and valves. Transition metal ions also catalyze unwanted degradation reactions, rendering formulations useless[6]. The most effective solution is to use chelates to mask the metal ions, thus keeping them in solution or preventing them from catalyzing unwanted reactions.

The applications of chelates range from the use in detergents, the pulp and paper industry, pharmaceuticals and agrochemicals.

The following is a list of the classes of industrial chelates:

1. Polyphosphates (*e.g.* pentasodium tripolyphosphate (STP) and potassium diphosphate).
2. Aminocarboxylates (*e.g.* ethylenediamine tetra-acetic acid (EDTA) and nitrilo triacetate (NTA)).
3. Hydroxycarboxylates (*e.g.* citric acid and gluconic acid).
4. Phosphonates (*e.g.* ethylenediamine tetramethylene phosphonate (EDTMP) and aminotriethylene phosphonate (ATMP).

The main problems with the current chelating agents are that they cause environmental problems and/or are not readily biodegradable. Biodegradation is the metabolism of

organic chemicals as sources of carbon and energy by microorganisms to form microbial mass and simple end products, such as methane and carbon dioxide[8].

Phosphates contribute to eutrophication, an excessive growth of algae in natural waters, resulting in the loss of other plant and animal life. Thus, many phosphates have been replaced by aminocarboxylates, but many aminocarboxylates are not readily biodegradable as well. The need for biodegradability is probably the reason why hydroxycarboxylates, such as citric acid are found in many applications even though they are less effective at complexing metal ions compared with the other types.

Aminocarboxylates, also known as "complexones", are highly effective chelating ligands. They are essentially derived from the simple amino acid glycine and they contain several carboxylalkyl groups bound to one or more nitrogen atoms, with the result that coordination of a single metal ion establishes several chelate rings[9]. It is estimated that the annual worldwide production of aminocarboxylate chelates is about 166,000 tones, two-thirds of which is (ethylenediamine tetra-acetic acid) EDTA[10].

The aminocarboxylic acid ligands used in this study are (ethylenediamine tetra-acetic acid) EDTA, ethylenediamine dimalonic acid (EDDM) and ethylenediamine disuccinic acid (EDDS). All the above ligands are polydentate since they contain more than one Lewis base, hence they are called sequestering agents or chelating agents. One of the common applications of sequestering agents is in complexing cations in natural waters to keep them from interfering with the action of soap or detergent molecules. The Mg^{2+} and Ca^{2+} ions react with soap to form a precipitate commonly known as soap scum. Although these and other ions do not precipitate detergent molecules, they do complex with them, thereby interfering with their cleansing action [11].

Chelates and chelating agents have also been used as drugs[11]. For example, they have been used to destroy bacteria by depriving them of essential metals. In this fashion the drug mimics the body's natural defenses. Chelating agents are also used to remove metals such as Hg^{2+}, Pb^{2+} and Cd^{2+} that are detrimental to health. For example, one method of treating lead poisoning is to administer Na_2[CaEDTA]. The EDTA chelates the lead, allowing its removal from the body in urine[11]. In Finland, the pulp and paper industry is the main user of chelating agents; chelates are used to inactivate metal ions, which catalyze the decomposition of added bleach.

2.5 Ethylenediamine tetra-acetic acid (EDTA) and the environment

$EDTA^{4-}$ is a hexadentate ligand, which combines with metal ions in a 1:1 ratio regardless of the charge of the cation[11]. The reagent is remarkable, not only because it forms chelates with all cations, but also because most of these chelates are stable. This is confirmed by the stability constants. The large entropy value represents a large contribution to the stability of the metal-EDTA complex. This great stability undoubtedly results from the several complexing sites within the EDTA molecule that give rise to a cage-like structure in which the cation is effectively surrounded and isolated from solvent molecules. Figures 2.01a and 2.01b show the structure of $EDTA^{4-}$ and the structure of M-$EDTA^{2-}$, respectively. The chelation of $EDTA^{4-}$ gives four five-membered chelation rings, which are the preferred size for most metal ions.

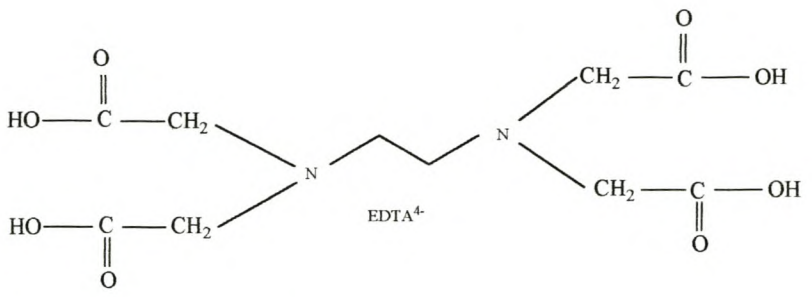

Figure 2.01a Structure of $EDTA^{4-}$

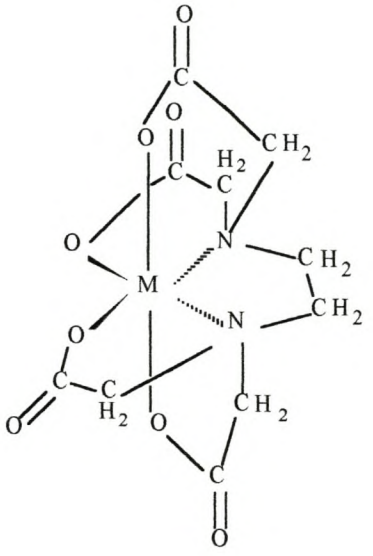

Figure 2.01b Structure of $M\text{-}EDTA^{2-}$

EDTA was first patented in Germany in 1935, and then in the US in 1946. It is now marketed under more than 30 different trade names[12]. It can also be found in almost all effluents of sewage plants and enters our creeks, rivers and lakes[13]. EDTA forms very stable complexes with metals and has therefore often been suspected to remobilize adsorbed or precipitated heavy metals from river sediments or aquifers. EDTA is used to bind metal ions in industrial and agricultural applications. Metals can interfere, at least to some extent, with the esterification step[14].

The determination of the concentrations, and especially the specification of EDTA are important to understand its environmental fate[15]. After 60 years of use, EDTA and related ligands are now beginning to come under closer scrunity. The main concerns about these compounds are:

- poor biodegradability.
- significant contribution to reduced quality of drinking water.
- high pollution of surface water with EDTA[16].

EDTA is not readily biodegradable under groundwater and sewage conditions and is building up in the environment. There is, however, some evidence that under certain conditions EDTA may be degraded. For example, the ferric chelate of EDTA has shown to photodegrade in UV light[17], and particular microbial cultures may be able to slowly degrade some metal EDTA complexes[18]. The microbes present in typical groundwater and sewage conditions, are, however, incapable of degrading EDTA.

A few studies have been carried out to investigate the concentrations and effects of EDTA in the environment. A survey of concentrations of nitrilotriacetate (NTA) and EDTA in the UK rivers and sewage works was carried out by Warren Spring Laboratory[19]. The calculated concentration of EDTA in UK rivers ranged from 2 μgl^{-1} to 129 μgl^{-1} and in sewage effluents from 60 μgl^{-1} to 1640 μgl^{-1}. Although these concentrations are relatively high, EDTA is continuously being used and ending up in the environment.

The presence of EDTA in sewage treatment and surface waters gives rise to the potential for disrupting equilibria and mobilizing heavy metals from sewage sludge, thereby indirectly causing humans to be increasingly exposed to EDTA via drinking water. A

study of the concentration of EDTA in drinking water carried out in Germany discovered the concentration of EDTA to be about 15 μgl^{-1} leading to a human intake of 30 μgl^{-1}, which is 17% of the maximum level recommended by the World Health Organization (WHO)[20].

There have been investigations carried out on the potential toxicity of EDTA. Na_2H_2EDTA has been shown to damage rat kidney cells[20], although a study using cells related to human keratinocytes showed Na_2H_2EDTA to have little effect[21]. EDTA may also affect the toxicity of metal ions when bound to them.

EDTA is used for the decontamination of nuclear power plant equipment. If EDTA is not removed from waste before dumping, it can mobilize heavy metals *e.g.* the radionuclides in nuclear waste dumps[18].

Although with the present concentration of EDTA in the environment there is little cause for concern, there has been increasing concern over the rising concentrations of EDTA in the environment and increasing pressure to replace it with a readily biodegradable alternative. Biodegradability has become an increasingly important factor when designing organic chemicals. A biodegradable model has been developed to predict biodegradability from the chemical structure of compounds and this could become a useful technique in the early process of chemical design[22]. The development of the model comprised five steps: a large database was assembled of experimentally measured biodegradation data; a set of predefined structural fragments was selected and a descriptor matrix was developed indicating the absence or presence of each fragment in the chemicals; biodegradability was correlated with the structural descriptors using Partial Least Squares (PLS) discriminant analysis; the influence of interactions between

fragments within the same molecule was investigated; and the model was extensively validated using large sets of compounds not included in the development of the model[22].

2.6 Ethylenediamine disuccinic acid (EDDS)

EDDS is a structural isomer of EDTA. It has two amine donor atoms and four carboxylate oxygen donors. It is, however, distinct in several important respects[23].

i. EDDS has secondary rather than tertiary amines.

ii. EDDS carboxylate arms can be divided into two groups: one, which forms six membered chelate rings upon coordination and the other, which forms five membered rings.

iii. EDDS has two chiral carbon atoms, and has three stereoisomers: [S,S']-EDDS, [S,R']-EDDS or [R,S']-EDDS and [R,R']-EDDS, the structures of which are given in figure 2.02.

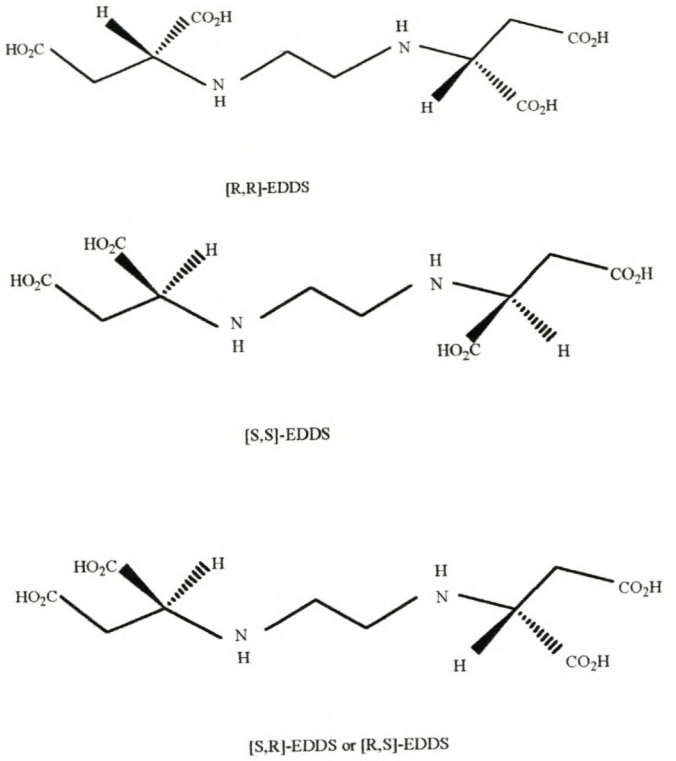

Figure 2.02 Chemical structure of the stereoisomers of EDDS[26]

2.6.1 Synthesis of EDDS

EDDS was first mentioned in a patent in 1964[24]. It was synthesized from ethylenediamine and maleic acid anhydride, giving a mixture of the stereoisomers consisting of 25% [S,S'], 50% [R,S']/[S,R'] and 25% [R,R'].

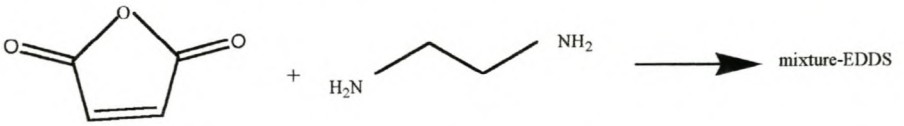

Alternatively, single isomers of EDDS may be prepared using 1,2-dibromoethane and a pure enantiomeric form of aspartic acid, *i.e.* L-aspartic acid gives the [S,S']-EDDS isomer and D-aspartic acid gives the [R,R']-EDDS isomer. Neal and Rose discovered this stereoselective method in 1968[23].

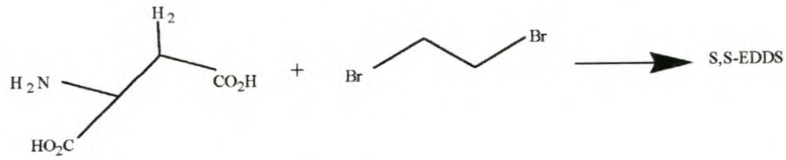

It has also been reported that [S,S']-EDDS can be produced naturally by a number of microorganisms[25] such as *Amycolatopsis japonicum sp. nov.*[26] This was observed in an antibiotic screening programme due to its ability to inhibit activity of the Zn^{2+}-dependent Phospholipase C.

2.6.2 Biodegradability of EDDS

The biodegradation tests (modified sturm (OECD 301B), SCAS (OECD 302A), CAS (OECD 303)) executed following the respective OECD (Organization for Economic Cooperation and Development) guidelines[18] have shown [S,S']-EDDS to be readily biodegradable. The [R,R']-EDDS isomer is not readily biodegradable and [R,S']- or [S,R']-EDDS, lies in between the two [26,27].

The screening tests used to determine the ready biodegradability of a chemical in sewage sludge involves measuring carbon dioxide evolution, oxygen consumption and decrease in dissolved organic carbon (DOC)[31]. Figure 2.03 and table 2.01 compares the biodegradability of EDDS enantiomers using a modified sturm test (OECD 301B), SCAS and CAS testing, respectively.

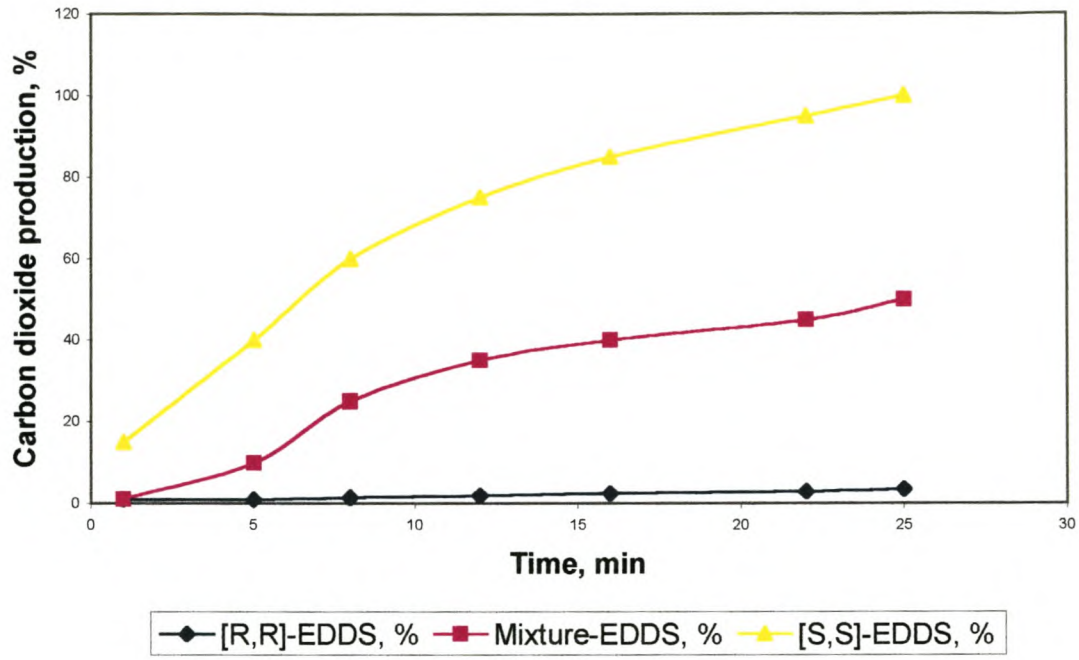

Figure 2.03 Modified sturm CO_2 production (OECD 301B) with [S,S']-, [R,R']-, and mixture-EDDS (20 mg/l each)

Table 2.01 Summary of the DOC removal of mixture and single isomers of EDDS in SCAS and CAS testing[31]

	Test Type	
Test Material	**SCAS in %**	**CAS in %**
[S,S']-EDDS	97	96
[R,R']-EDDS	2	-
Mixture EDDS	27	35

Mixture of EDDS contains [S,S']-, [R.R']-, and [R,S']- or [S,R']- EDDS isomers in a ratio of 1:1:2. The [S,S']-EDDS isomer is selectively biodegraded in the mixture and then the [S,R'-/[R,S']-isomer may slowly degrade. Stereochemistry is an important factor affecting

the biodegradability and metabolite formation of a chemical. Takahashi *et al.* suggested that chelates having N-substituted aspartic acid residues are biodegradable.[27] Figure 2.04 is a proposed biodegradation pathway for the isomers of EDDS.

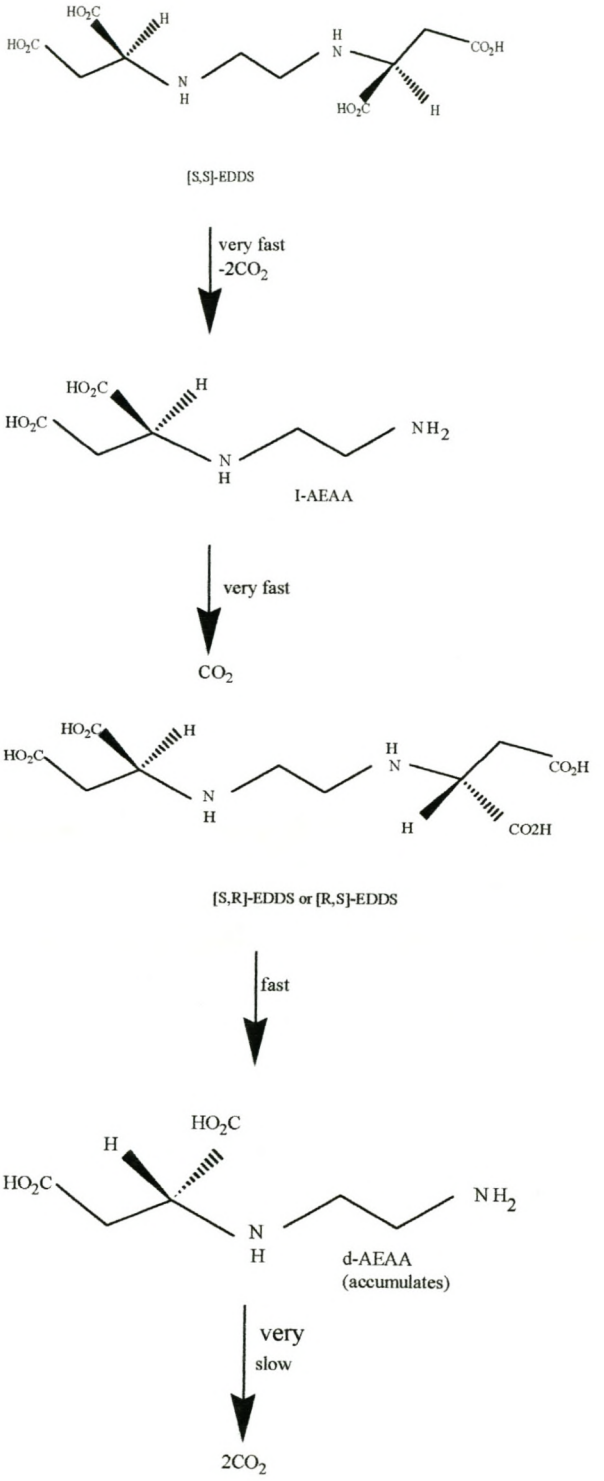

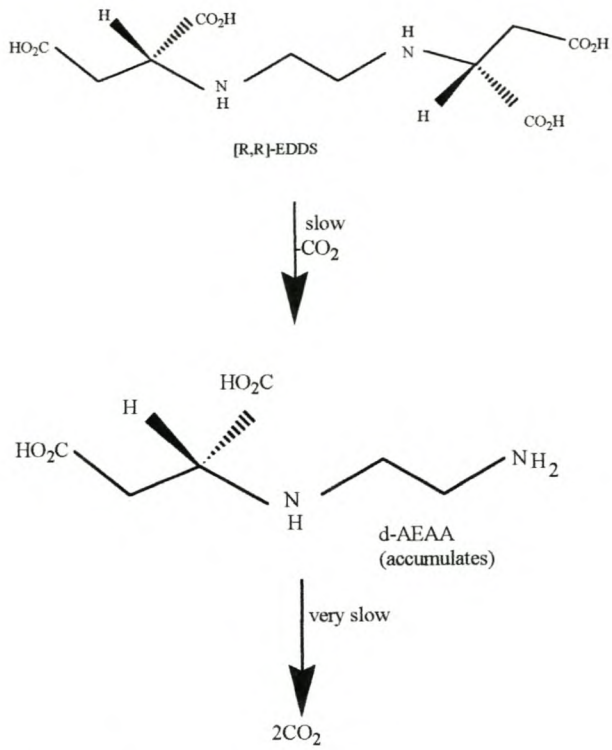

AEAA=N(2-aminoethyl)aspartic acid

Figure 2.04 Proposed biodegradation pathway of the EDDS isomers[26]

[S,S']-EDDS is the only isomer that undergoes complete biodegradation and thus, from an environmental perspective, it is the only isomer recommended for large volume applications[26]. In the present study only [S,S']-EDDS has been considered hence whenever EDDS is mentioned, it refers to the [S,S']-isomer.

Jaworska *et al.* proposed an environmental risk assessment for the use of EDDS in detergent applications[28]. From projected use volumes in detergent applications it was predicted that the steady-state concentration of EDDS in rivers leaving the mixing zone would be below 5 μgl^{-1} due to rapid biodegradation. EDDS exhibits low toxicity to fish. Toxicity was observed with algal tests, but this was demonstrated by Schowanek *et al.* to be a chelation effect of trace elements, leading to a deficiency of nutrients, rather than

toxicity *sensu stricto*[29]. Using speciation modelling to conduct the risk assessment, it was predicted that this chelation effect would be insignificant.

2.6.3 Metal-EDDS complexes

EDDS is a good metal chelator, particularly with regard to transition metal ions, which are the critical problem with ions in the pulp and paper process[31]. EDDS was not industrially manufactured until fairly recently, when a relatively effective method was developed[30]. It can be used to treat both mechanical and chemical pulps and shows excellent performance in comparison with the currently used chelates under appropriate conditions[31]. It has, however, not been widely used due to its poor ability to chelate calcium and magnesium. Although not all applications involve the chelation of alkaline earth metals and with the increasing environmental pressures for a biodegradable chelate, EDDS has recently received more recognition.

EDDS is capable of forming two absolute configurations with metal ions. EDDS forms five- and six-membered chelate rings, which can either be on the equatorial or axial position. Figure 2.05 shows the structure of the two configurations. Type I complex has both six-membered carboxylate rings serving equatorial sites with the five-membered rings at the axial sites, whereas type II has the five-membered rings in the equatorial site with the six-membered ones in the axial. In both conformations the metal ion will be present as an asymmetric center.

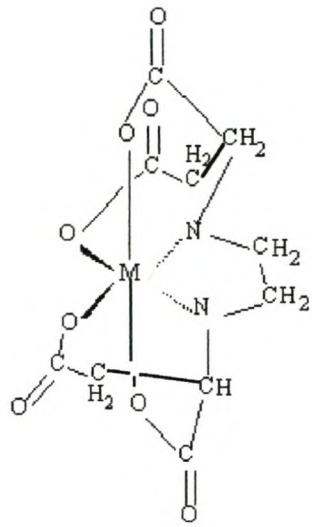

Type I

5-membered axial

6-membered equatorial

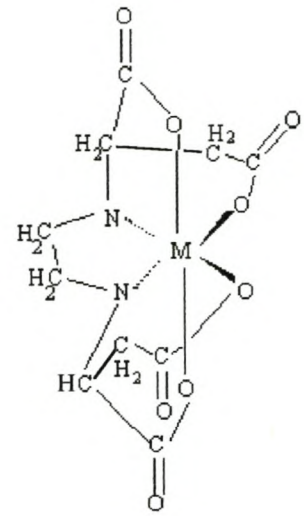

Type II

5-membered equitorial

6-membered axial

Figure 2.05 Absolute configurations of MEDDS[23]

It has been suggested by Neal and Rose that complexes of EDDS with cobalt (II), nickel (II) and rhodium (III) prefer type I configuration[23,33]. It has been observed that $[CoEDTA]^-$ showed marked strain in the equatorial five-member position, which may explain why the configuration of EDDS around cobalt (III) favors the six-member ring in the equatorial position[23].

When an acidic aqueous solution of EDDS is heated its complexing power weakens, due to the intermolecular stylization of EDDS[34, 35]. EDDS forms lactam rings, either six- or seven-membered, as shown below in Figure 2.06.

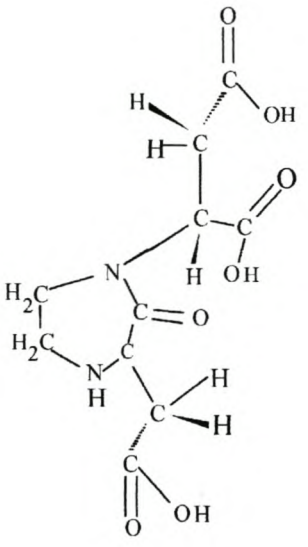

Figure 2.06 Structure of EDDS lactam ring[34]

The loss of complexing ability is observed because formation of the lactam ring prevents chelation of a metal ion and also the charge on the ionized species is only 3- rather than $EDDS^{4-}$ [34].

2.7 Ethylenediamine dimalonic acid (EDDM)

EDDM was investigated by Schwarzenbach in 1973[36]. EDDM has three functional groups in metal chelate function. However, it is sterically impossible for these three groups to coordinate to the metal ion forming two chelate rings. This is because the stability of the metal chelates of aminomalonic acid is lower than that of iminodiacetic acid, which can act as a terdentate ligand to form two chelate rings with metal ions[36].

EDDM is a tetrabasic acid having six donor groups including two basic nitrogen atoms. However, it is considered to act as a quadridentate ligand in metal chelate formation as in

aminomalonic acid, and expected to exhibit behavior analogous to that of ethylenediamine diacetic acid (EDDA)[36].

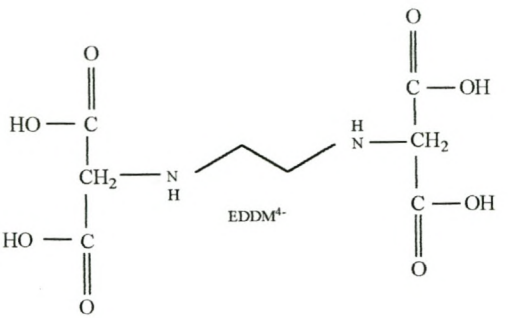

Figure 2.07 Structure of $EDDM^{4-}$

2.7.1 Synthesis of EDDM

EDDM is synthesized in three steps:

Step 1:

Malonic acid and bromine are mixed together to give bromomalonate

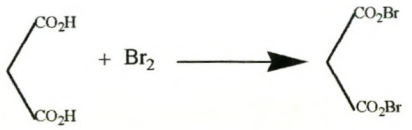

Step 2:

The bromomalonate, is mixed with a saturated solution of KOAc to give dipotassium bromomalonate.

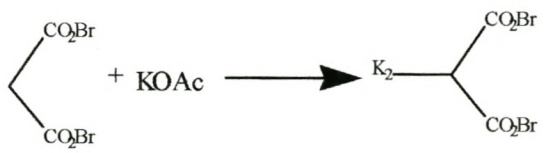

Step 3:

The obtained dipotassium bromomalonate is mixed with ethylenediamine to afford ethylenediamine-N,N'-dimalonic acid (23%).

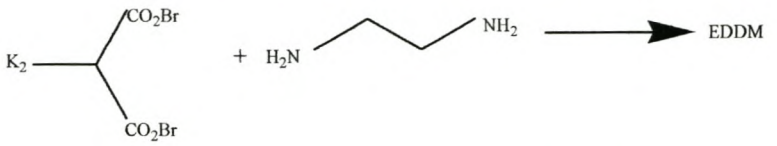

The EDDM ligand used in this study was synthesized according to the procedure as outlined in the experimental section.

2.7.2 Metal-EDDM Complexes

Titration of EDDM, indicated relatively weak chelate formation with alkaline earth metals but strong interaction with transition metals[32]. A recent theoretical study using a semi-empirical approach showed its relative stability compared to that of other ligands on the assumption that all six coordination centers of the ligand bind to the metal ions of interest[36].

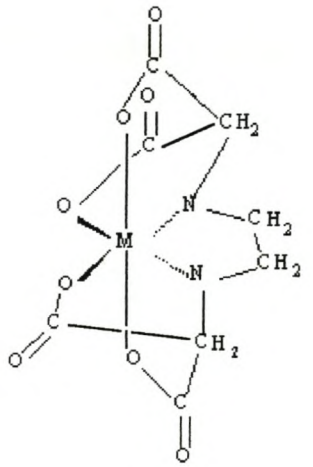

Figure 2.08 Structure of M-EDDM^{2-}

References

1. Nurnberg H. W., *Analytica Chimia Acta* ,1984, **164,** 1.
2. Jianguo C., Chakrabrit C. L.I., Back M. H., Schroender W. H., *Analytica Chimica Acta,* 1994, **288**,141 .
3. Van Leeuwen H. P., Buffle J., *Journal of Electroanalytical Chemistry*, 1990, **296**, 359.
4. Hetland S. M. I., Radzuk B., Thomassen Y., *Analytical Sciences,* 1991, **7**, 1029.
5. Dwyer F. P., Mellor D. P., *Chelating Agents and Metal Chelates.*, Academic Press, 1964.
6. Hedley E. P., *New Ideas on Inorganic Chemistry*, London, 1911.
7. Taylor D. M., Williams D. R., *Trace Element Medicine and Chelation Therapy*, Royal Society of Chemistry, London, 1998.
8. Pearson R. G., *Inorganic Chemistry*, Chapman Hall, London, 1994.
9. Bell C. F., *Principles and Applications of Metal Chelation,* Clarendon Press, Oxford, 1977.
10. Beck M. T., Nagypal I., Williams D. R., *Polyhedron Chemistry of Complex Equilibria* , Ellis Horwood Limited, Chichester, 1990.
11. Kotz J. Purcell K., *Chemistry and Chemical Reactivity*, CBS College Publishing, USA, 1987.
12. Nowack B., Kari F. G., Sabine U. H., Sigg L., *Fresenius Journal of Analytical Chemistry,* 1996, **68**, 561.
13. Vema P., Saxena R. C., Jayaraman A., *Fresenius Journal of Analytical Chemistry,* 1997, **357**, 56.

14. Noboru O., Hiroaki M., *Journal of Electroanalytical Chemistry*, 1997, **78**, 103.

15. Killa H. M., Mercer E. E., Phillip Jr. R., H., *Analytical Chemistry*, 1984, **56**, 2401.

16. Ciszkowska M., Osteryoung J. G., *Journal of Physical Chemistry*, 1994, **98**, 11791.

17. Hill-Cottingham D. G., *Nature*, 1955, **175**, 347.

18. Thomas R. P. A., Lawlor K., Bailey L. E., Macaskie L. E., *Applied and Environmental Microbiology,* 1998, **64 (4)**, 1319.

19. Garland J. H. N., Capon J., Cox J., Collier A., Kibblewhite M. G., *Survey of Concentrations of NTA and EDTA in UK Rivers and Sewage Treatment Works,* Stevenage, Warren Spring Laboratory, 1992.

20. Hugenschmidt S., Planas-Bohne F., Taylor D. M., *Arch Toxicology*, 1993, **67**, 76.

21. Williams D. R., *Chemistry in Britain*, January 1998, 48.

22. Loonen H., Lindgren F., Hansen B., Karcher W., Niemela J., Hiromatsu K., Takatsuki M., Peijnenburg W., Rorije E., Struijs J., *Environmental Toxicology. and Chemistry* 1999, **18(8)**, 1763.

23. Neal J. A., Rose N. J., *Inorganic Chemistry*, 1968, **7(11),** 2405.

24. Kezerian C., Ramsey W. M., *US Patent*, 3158635, November 1864.

25. Kovalyova I. B., Mitrofanova N. D., Martynenko L. I., Samohina M. V., Felin M. G., *Inorganic Chemistry*, 1991, **36(3)**.

26. Schowanek D., Feijtel T. C. J., Perkins C, M., Hartman F. A., Ferdele T.W., Larson R. J., *Chemosphere*, 1997, **34 (11)**, 2375.

27. Takahashi R., Fujimoto N., Suzuki M., Endo T., *Bioscience Biotechnology and Biochemistry.*, 1997, **61 (11)**, 1957.

28. Jaworska J. S., Schowanek D., Feijtel T. C. J., *Chemosphere*, 1999, **38 (15)**, 3597.

29. Schowanek D., McVoy D., Versteeg D., Hanstveit A., *Aquatic Toxicology*, 1996, **36**, 255.

30. Cowton E. L. M., Bassett D. A., *UK Patent*, 2299809, October 1996.

31. *Technical Bulletin*, **(23)**, The Associated Octel Company Limited, Perfomance Chemicals Group.

32. Wang J., Lu J., Murase I., *Bulletin of Chemical Society Japan*, 1973, **46**, 844.

33. Neal J. A., Rose N. J., *Inorganic Chemistry*, 1973, **12(6)**.

34. Kolleganov M.Y., Kolleganova I.G., Mitrofanova D., Martynenko L. I., Nazarov P. P, Spitsyn V. I., Plenum Publishing, Translated from Izvestiya Akademii Nauk, SSSR, *Khimicheskaya*, 1983, **6**, 1293.

35. Vasiliev V. P., Orlova T. D., Ledenkov S. F., *Journal of General Chemistry*, 1989, **59 (8)**.

36. Crouch A. M., Polhuis M., *Journal of Molecular Structure*, 2000, **530**, 171.

CHAPTER 3

SPECIATION

3.1 Speciation

Chemical speciation is the chemical form or compound in which an element occurs in a living system or in the environment[1]. It may also refer to the quantitative distribution of an element, therefore speciation can be defined as the oxidation state, concentration and composition of each of the species in the chemical sample[2].

The chemical speciation of an element, not just the total concentration of an element, is crucial in the understanding of the element's behavior, reactivity and toxicity. For example, arsenic (III) is highly toxic, whereas V (III) is more tolerated. The speciation of an element that is consumed as a food or drug, influences whether it is absorbed into the blood stream from the intestine and speciation of a pollutant determines whether or not it will be mobile in the environment. Clearly, speciation is essential in a better understanding of reactions in the environment and industry.

There are various methods of studying speciation. These include[3]:

- Potentiometry
- Anodic stripping voltammetry
- Atomic absorption
- Bioassay
- Computer simulated modelling
- Electron paramagnetic resonance
- Solvent extraction

- Ion selective electrodes
- UV-Vis spectroscopy

3.2 Computer simulated speciation modelling

Modelling chemical speciation is essential when trying to understand complex systems. Computer simulated modelling uses known thermodynamic constants for all the relevant reactions to calculate a mathematical model to match the specified conditions. All types of chemical equilibria must be considered including protonation, complex formation, redox, solubility and absorption.

3.2.1 Advantages of speciation modelling

- Speciation modelling does not disturb the chemically labile equilibria, as it is a non-invasive method.
- Direct analytical measurements are often time-consuming, expensive and complicated.
- Variable parameters, such as temperature, pH and ionic strength may be altered and the system may be readily remodelled.
- It is possible to model components with concentrations lower than those detectable by other analytical methods.

Speciation modelling is a very powerful tool and works well in conjunction with other analytical methods. Modelling may prevent or reduce unnecessary experimental work and it can be used to select the most effective experiments. Experiments can then be used to validate results predicted by the models.

3.2.2 Disadvantages of speciation modelling

According to Duffield *et al*[4] there are three major sources of errors with speciation modelling:

1. Modelling uncertainties: - these arise from an inaccurate understanding of the processes being modelled and/or from numerical approximations used in the mathematical representations.
2. Data uncertainties: - this is a result of poor quality and/or not fitting the conditions of the data and parameters used in the mathematical model.
3. Completeness uncertainties: - these refer to possible omissions from the model due to lack of knowledge.

The main source of errors lies in the quality of the measured formation constants and solubility products, which depend upon time-consuming and accurate experimental work. Most of the formation constants measured to date have been done through potentiometric measurements[6], but there is a large variation in the data[7].

3.3 Computer speciation modelling

Conditional formation constants can be useful to predict the relative complexing abilities of ligands with various metal ions, but when the system becomes more complex there are too many competing reactions and too many species present to calculate all the conditional formation constants. This is where computer simulated speciation modelling can be used to predict speciation quantitatively. Speciation modelling takes into account all of the reactions occurring in the system as long as adequate data are available.

A number of assumptions are made in calculating a model, such as:

- the thermodynamic database is complete and accurate
- the component concentrations are correct
- the thermodynamic theory adequately describes the system of interest
- equilibrium or steady-state conditions prevail.

Figure 3.01 is a flow chart of the modelling procedure[6] used in this work. The model was continuously refined until the speciation results either make chemical sense or agree with experimental validation.

There are a number of computer programs available for the simulation of metal ligand equilibria in aqueous systems, *e.g.* AQUASIM, which is used for simulation of hydraulic processes, FITEX which can simultaneously account for the surface electric field of both bacterial and mineral surfaces, and SQUAD which has been used successfully in geochemical studies. In this study work, the computer program JESS (Joint Expert Speciation System)[8,9,10] was used.

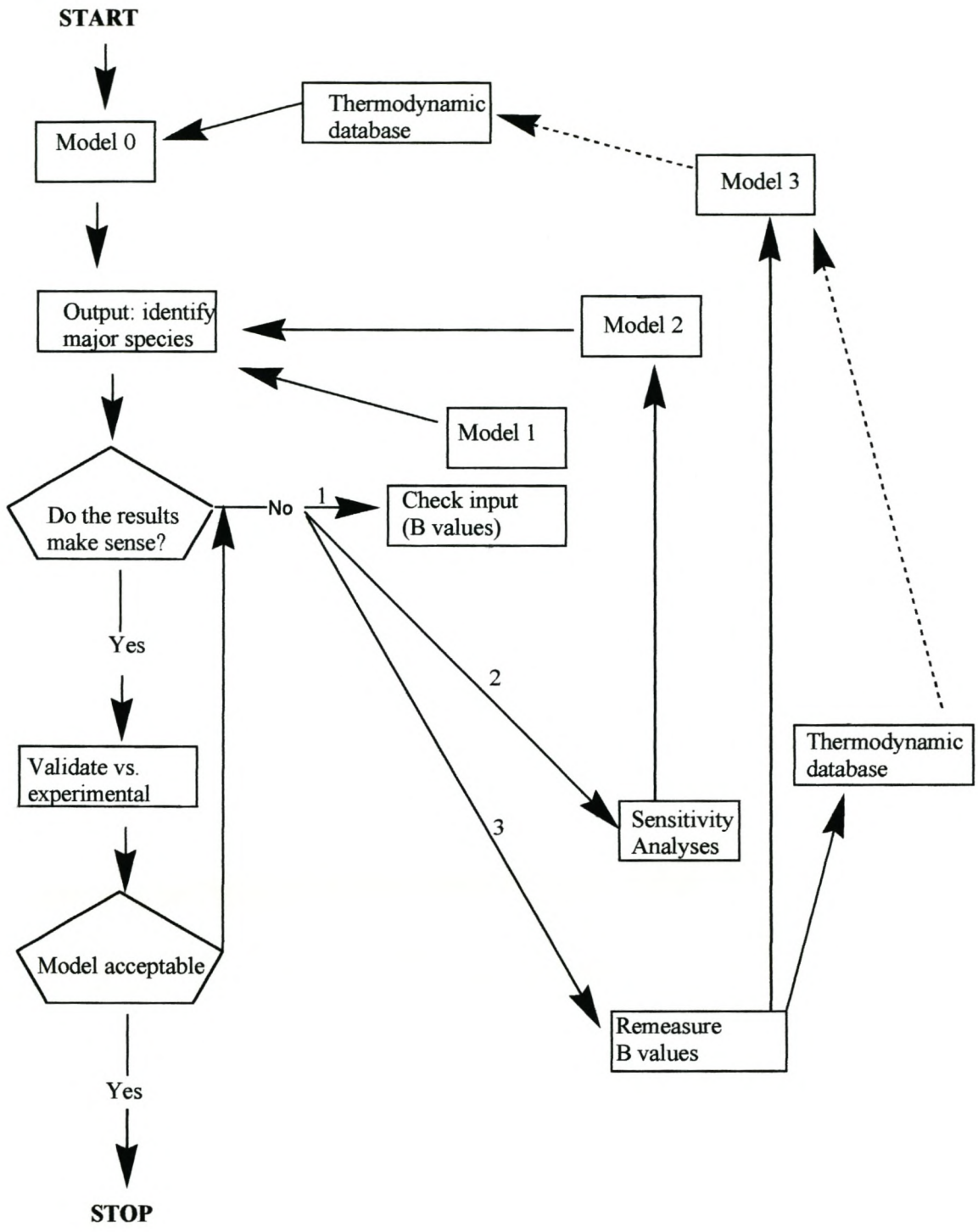

Figure 3.01 Flow chart of the modelling process[6]

JESS [7,8,9], for Joint Expert Speciation System, is a computer package used for modelling chemical systems in solution and performing numerical analyses of the corresponding data, *e.g.* input formation constants determined using potentiometric titration. This package was developed to solve problems requiring specialist knowledge of chemical speciation, and comprises over 150 programs, 1 200 subroutines and 120 000 lines of Fortran code.

The thermodynamic database of JESS overcomes many existing problems with solution chemistry databases, and is a fully interactive system. Reactions can be expressed in almost any form and can be associated with any number of equilibrium constants, enthalpy, entropy and Gibbs free energy values. Supplementary data, *e.g.* ionic strength, temperature, background electrolyte, method of determination and original literature reference are also stored in the database. The database distributed with JESS contains over 12 000 reactions and more than 20 000 formation constants, including spanning interactions in aqueous solution of some 100 metal ions with more than 650 ligands.

Using a series of commands, the user can interactively select the desired ligand and metal(s) to be speciated, as well as define the conditions under which the data are to be modelled, *e.g.* ionic strength of the medium, temperature, concentrations of reactants and desired pH range over which the speciation is to be calculated. The final data output are fields corresponding *e.g.* to pH and the respective species that have been modelled over the pH range of interest. This output can then be readily manipulated and graphed in most spreadsheets and graphics programs for facile visual representation of the speciation curves.

The approach taken by JESS towards speciation modelling is distinct to the speciation modelling programs in four main areas[11]:

1. Thermodynamic parameters appear in the database just as they appear in the literature.
2. The procedure involves many independent computer programs.
3. The effects of kinetics on equilibrium calculations are more easily handled and are kept explicit.
4. Theoretical corrections for changes in ionic strength and temperature are minimized.

The speciation curves depicted in this dissertation were modelled using the JESS thermodynamic database of the Chemistry Department at the University of Wales, Cardiff, United Kingdom.

A model is a simplified representation of a real life system. There are six steps in the sequence that comprises a JESS equilibrium calculation. These are called GEM, Generalised Equilibrium Modelling, and stages and consist of SUB, RNG, BAS, CCC and QED stages. Table 3.1 describes each stage.

Table 3.01 GEM Stages of JESS Modelling[11]

GEM Stage	
SUB	Creating a sub-database. Specify the chemical elements in the model
RNG	Specify ranges of conditions, (ionic strength, temperature, solvent and background electrolytes).
BAS	Determines basis sets.
CCC	Determines constant correction coefficients, determine functions for log K corrections.
QED	Quasi-equilibrium calculation, specify scan info, fixed and free concentrations, solids, temp. and ionic strength.
OUT	Producing output.

Each GEM stage is subdivided into several distinct operations. The prefix TEL is used to specify the input, the prefix DO is used to carry out the stages operation and VEW is used to inspect the output of the stage. The QED stage actually performs the equilibrium calculation, the stages before preparing the input.

When calculating a model, JESS will select the constants having the highest weighting, which are closest to the conditions selected, and then take an average if there is more than one constant. If there are no constants measured at the selected temperature and ionic strength, JESS will adjust the closest, most accurate constants by using the Van't Hoff

equation to adjust the temperature and by applying various extensions of the Debye-Huckel theory for adjustments to ionic strength.

JESS uses the formation constants and solubility products along with the variables selected, *i.e.* concentration, temperature, pH and ionic strength, to calculate a mathematical model of the speciation. JESS uses the Newton Raphson iteration to solve the sets of simultaneous equations generated from the prevailing condition of mass balance and chemical equilibria.

3.4 Results and discussion

The speciation curves obtained using JESS are discussed below. Firstly, the polyaminocarboxylic acid ligands were modelled and analysed. Thereafter the metal complexes of these ligands were also modelled.

3.4.1. Speciation diagrams for EDTA, EDDS and EDDM

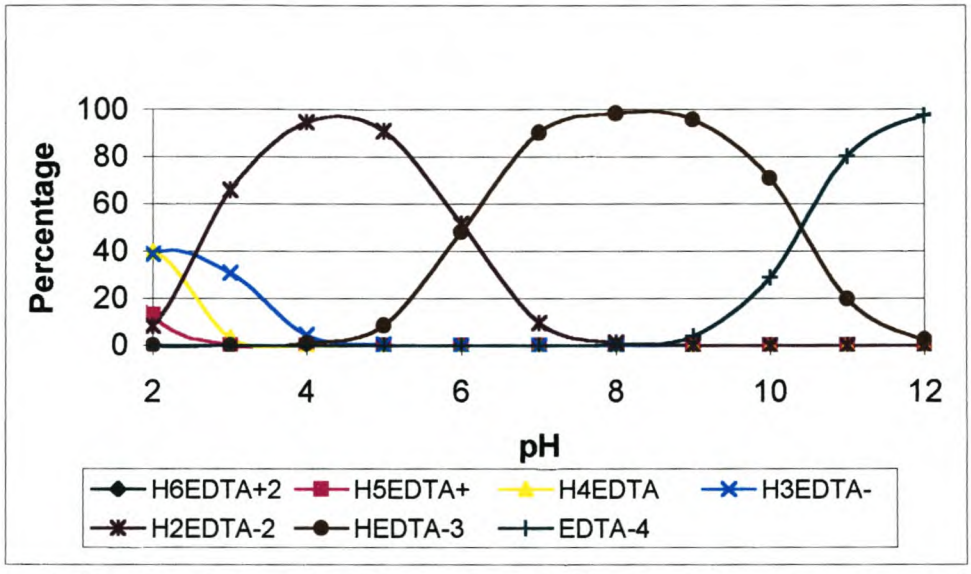

Figure 3.02 Speciation of EDTA using JESS. Total ligand concentration 0.1M, ionic strength I = 0, temperature 25°C.

Figure 3.02 illustrates how the relative amounts of the species derived from EDTA vary as a function of pH. From the speciation curves it can be seen that at pH values above 11 the $[EDTA]^{4-}$ is the fully deprotonated ion. Also at pH above 11, the $[EDTA]^{4-}$ ion becomes a major component of EDTA solutions. The first and second steps in the dissociation process involve successive loss of protons from the two carboxylic groups to form $[H_3EDTA]^-$, and $[H_2EDTA]^{2-}$, and the third and forth steps involve dissociation of the protonated amine groups to form $[HEDTA]^{3-}$, and $[EDTA]^{4-}$. Note also that the $[H_4EDTA]$ species is also formed. It's net charge is zero and it contains four dissociatable protons, two associated with two carboxyl groups and the other two with the two amine groups. Generally, the double zwitterions are formulated.

Figure 3.03 illustrates how the relative amounts of the species derived from EDDS vary as a function of pH formed. From the speciation profile it is observed that the EDDS ligand behaves like EDTA, where at pH values above 9 the $[EDDS]^{4-}$ is the fully deprotonated ion. Above pH 8, the $[EDDS]^{4-}$ ion becomes a major component of EDDS solutions. The first and second steps in the dissociation process involve successive loss of protons from the two carboxylic groups to form $[H_3EDDS]^-$ and $[H_2EDDS]^{2-}$(at pH 5 to 10). The third step involves dissociation of the protonated amine groups to form $[HEDDS]^{3-}$ and $[EDDS]^-$. Hence EDDS also formulates double zwitterions.

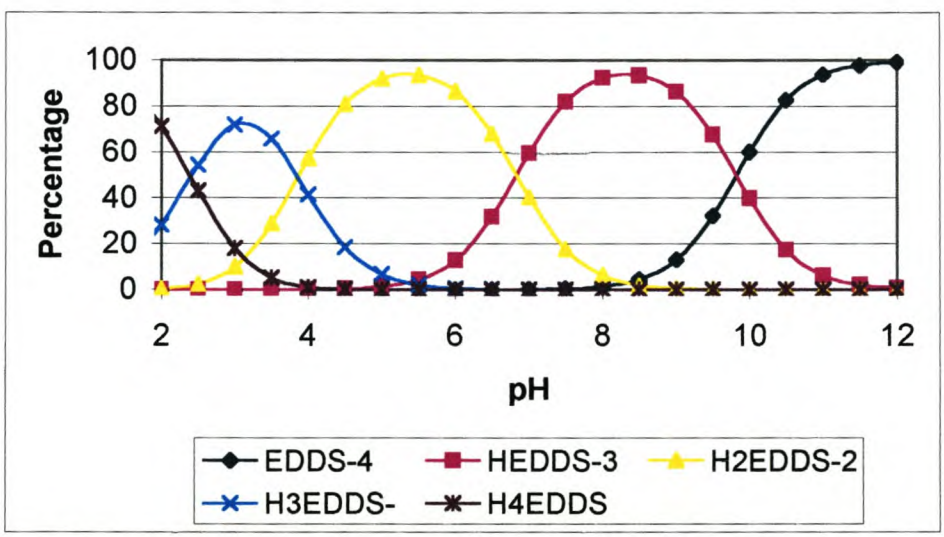

Figure 3.03 Speciation of [S,S']-EDDS using JESS. Total ligand concentration 0.1M, ionic strength I = 0, temperature 25°C.

For EDDM, which is also a biodegradable ligand the same species, were noted as for EDDS. The chemical speciation of EDDM can be seen in Figure 3.04 .

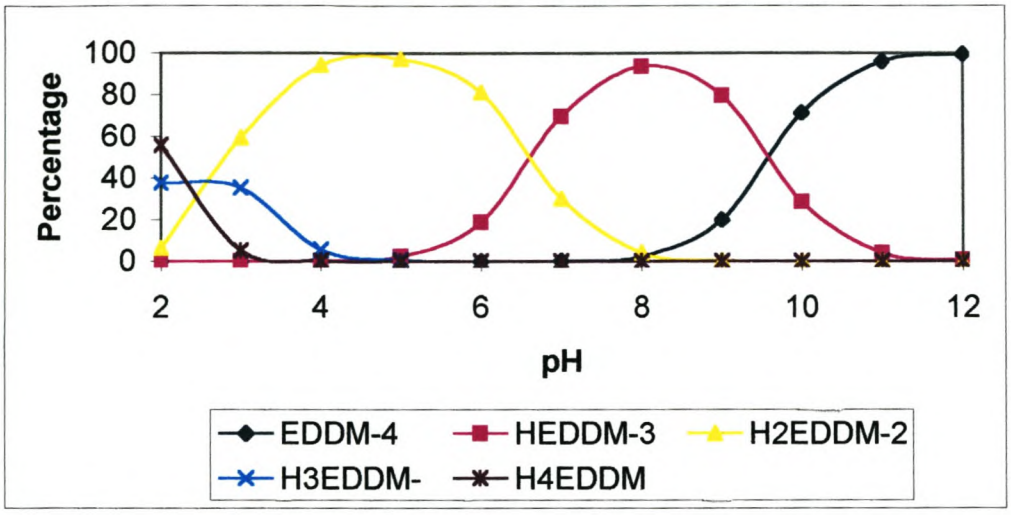

Figure 3.04 Speciation of EDDM using JESS. Total ligand concentration 0.1M, ionic strength I = 0, temperature 25°C.

All the above ligands *i.e.* EDTA, EDDS and EDDM at low pH undergo protonation to form the protonated species while at high pH they undergo deprotonation. It is also observed that EDTA undergoes further protonation to form a cationic species between pH 2 and 12, while the biodegradable ligands only undergo protonation to form the neutral species between 2 and 12, the cationic species are not observed. All the above ligands formulate double zwitterions.

3.4.2 Speciation diagrams for CuEDTA, PbEDTA and CdEDTA

Figure 3.05 illustrates how the relative amounts of the species derived from CuEDTA vary as a function of pH. From the speciation profile it is observed that the main species found at pH values between 4.0 and 10.0 is the fully deprotonated $[CuEDTA]^{2-}$ ion which become a major component of CuEDTA. Above pH 10, hydroxy species start to form, *e.g.* $[CuOHEDTA]^{3-}$, $[Cu(OH)_4]^{2-}$ and $[CuOH]^{3-}$, and below pH 4.5 the metal complex undergoes protonation to form CuH_2EDTA and $[CuHEDTA]^{-}$.

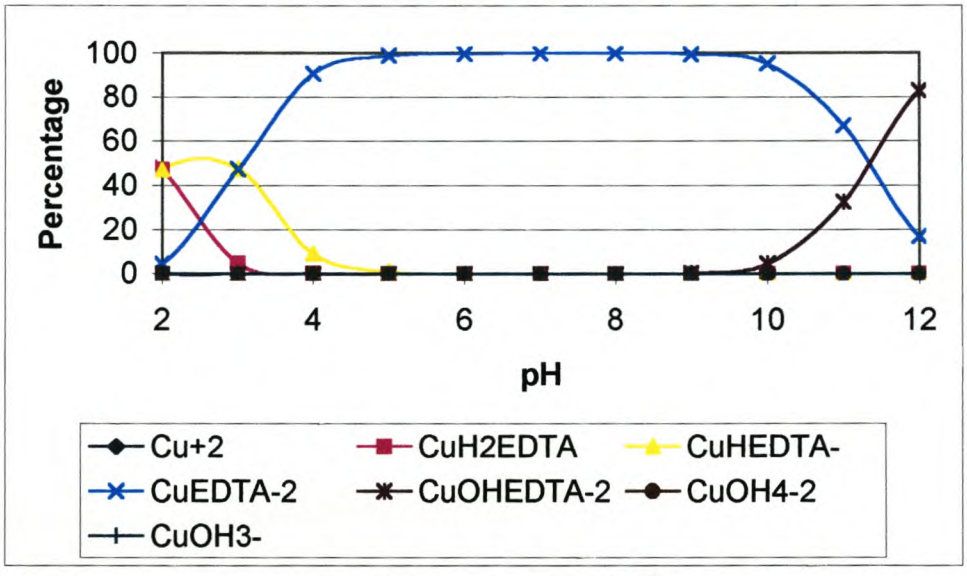

Figure 3.05 Speciation of CuEDTA using JESS. Total metal concentration 100 ppm, total ligand concentration 0.1M, ionic strength I = 0, temperature 25°C.

The Pb^{2+} and Cd^{2+} metal ions were also complexed with EDTA to form PbEDTA and CdEDTA. Figures 3.06 and 3.07 shows the obtained chemical speciation profiles.

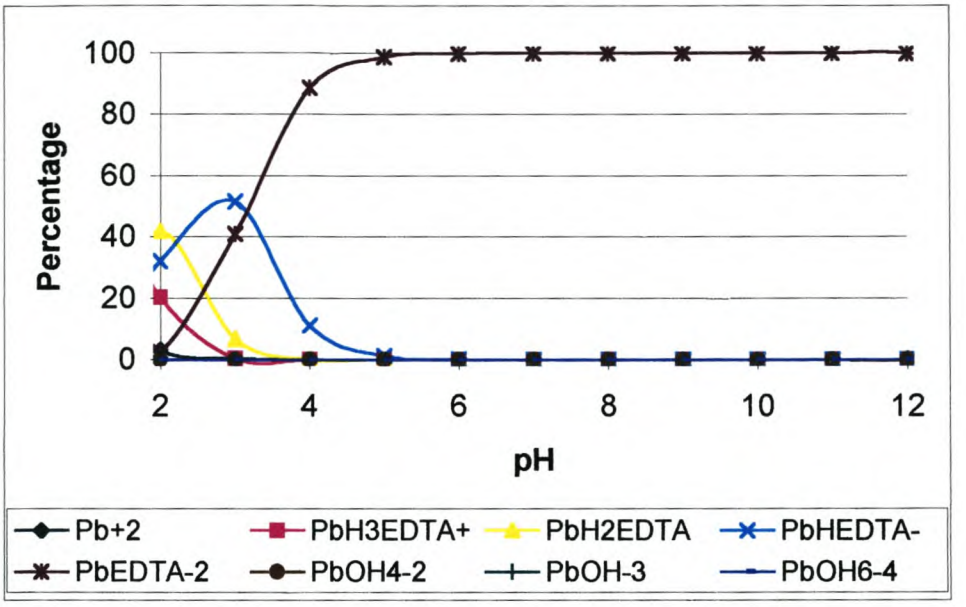

Figure 3.06 Speciation of PbEDTA using JESS. Total metal concentration 100 ppm, total ligand concentration 0.1M, ionic strength I = 0, temperature 25°C.

The chemical speciation of PbEDTA shows that the main species found between pH 4.0 and 10.0 is the fully deprotonated $[PbEDTA]^{2-}$ ion, which becomes a major component of PbEDTA. Above pH 10 hydroxy species start to form, *e.g.* $[Pb(OH)_6]^{4-}$, $[Pb(OH)_4]^{2-}$ and $[PbOH]^{3-}$, and below pH 4.5 the metal complex undergoes protonation to form $[PbH_3EDTA]^{+}$, $[PbH_2EDTA]$ and $[PbHEDTA]^{-}$. This is similar to what was observed for CuEDTA. For CuEDTA, the major component species $[CuEDTA]^{2-}$ ion decreases after pH 10 while for PbEDTA the major component species $[PbEDTA]^{2-}$ ion, the distribution remains 100% at pH values above 10. Similar chemical speciation was obtained for CdEDTA.

Figure 3.07 illustrates how the relative amounts of the species derived from CdEDTA vary as a function of pH.

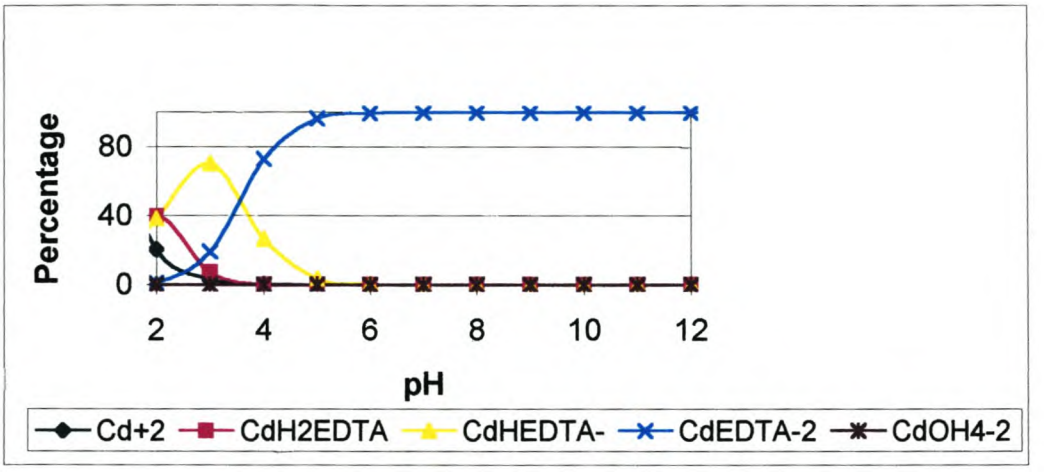

Figure 3.07 Speciation of CdEDTA using JESS. Total metal concentration 100 ppm, total ligand concentration 0.1M, ionic strength I = 0, temperature 25°C.

All the above metal ligands *i.e.* CuEDTA, PbEDTA and CdEDTA undergo protonation to form the protonated species at low pH while at high pH they undergo deprotonation.

3.4.3 Speciation diagrams for CuEDDS, PbEDDS, CdEDDS, ZnEDDS, FeEDDS, and CrEDDS

Figure 3.08 illustrates how the relative amounts of the species derived from CuEDDS vary as a function of pH. The species obtained for CuEDDS are similar to what was observed for CuEDTA. From the chemical speciation of CuEDDS only one protonated species is observed which is $[CuHEDDS]^-$ while the other protonated species could not be observed since their distribution is below 10 %.

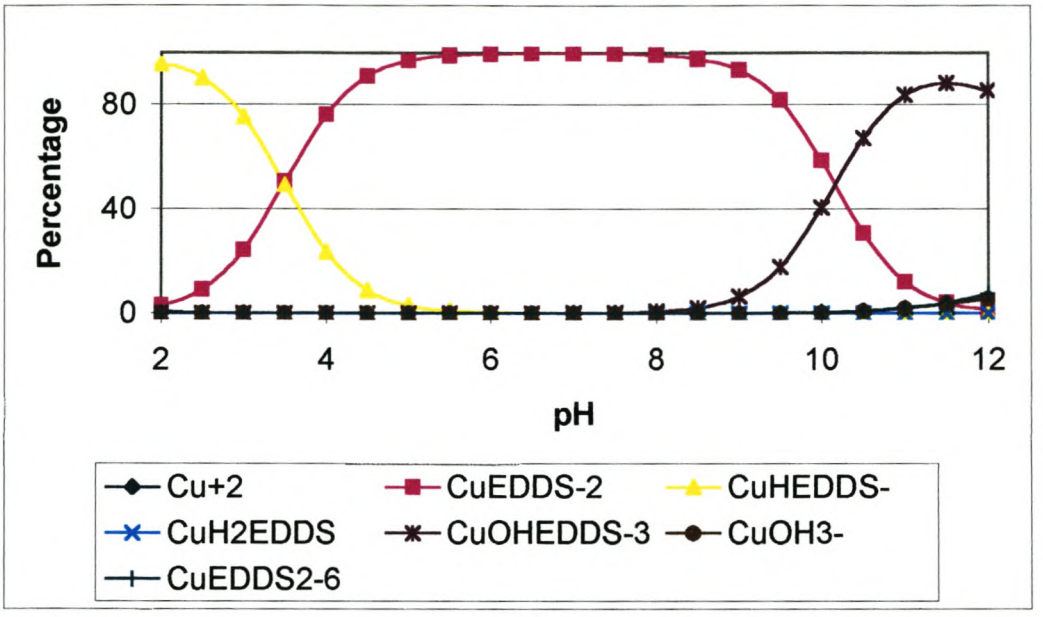

Figure 3.08 Speciation of CuEDDS using JESS. Total metal concentration 100 ppm, total ligand concentration 0.1M, ionic strength I = 0, temperature 25°C.

The chemical speciation of PbEDDS is shown in Figure 3.09. The species obtained for PbEDDS are similar to what was observed for PbEDTA. For PbEDTA the hydroxy species was not observed in the chemical speciation since the distribution is below 10%, while for PbEDDS only one protonation peak is observed compared to PbEDTA.

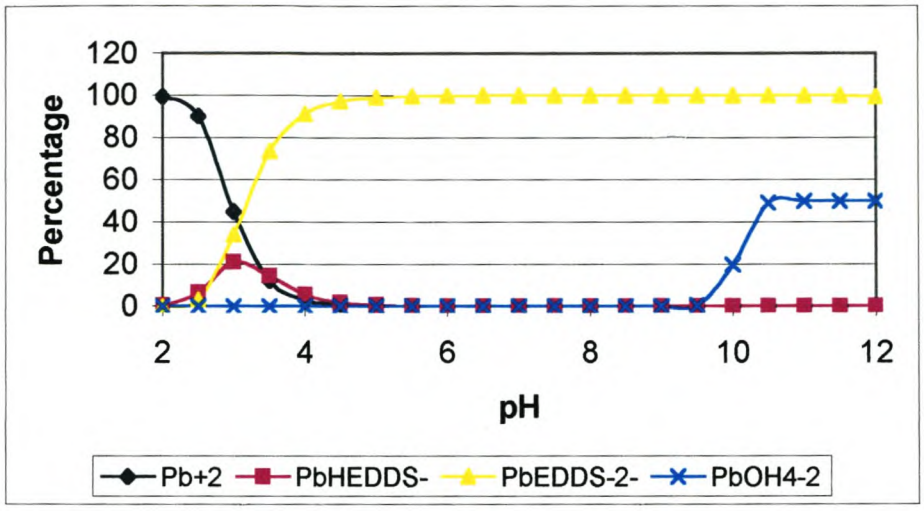

Figure 3.09 Speciation of PbEDDS using JESS. Total metal concentration 100 ppm, total ligand concentration 0.1M, ionic strength I = 0, temperature 25°C.

The chemical speciation of CdEDDS is shown in Figure 3.10. For CdEDDS no protonation or hydroxyspecies were observed from pH 2 to 12, while for CdEDTA these species were observed.

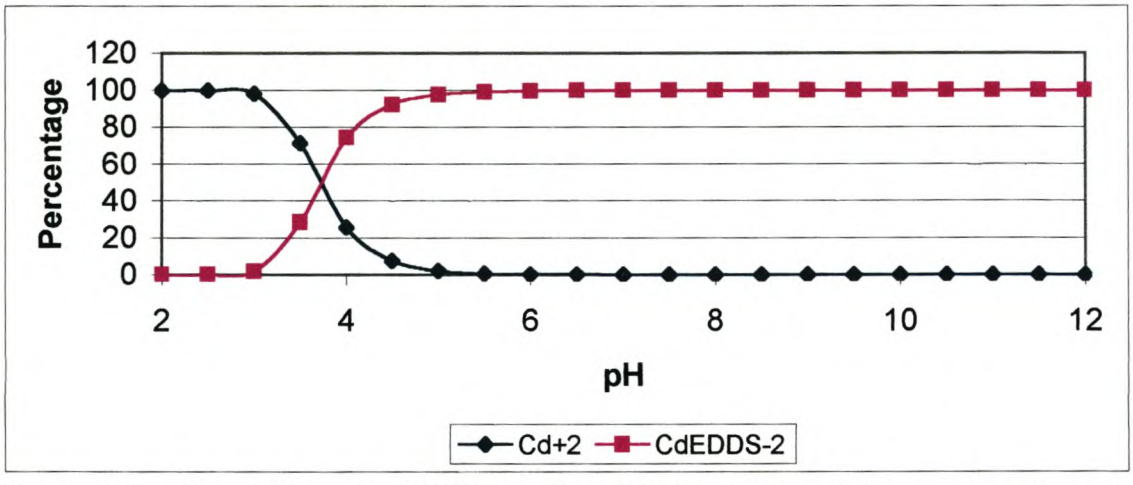

Figure 3.10 Speciation of CdEDDS using JESS. Total metal concentration 100 ppm, total ligand concentration 0.1M, ionic strength I = 0, temperature 25°C.

The same was noted for ZnEDDS as for CdEDDS. The chemical speciation of ZnEDDS is shown in Figure 3.11.

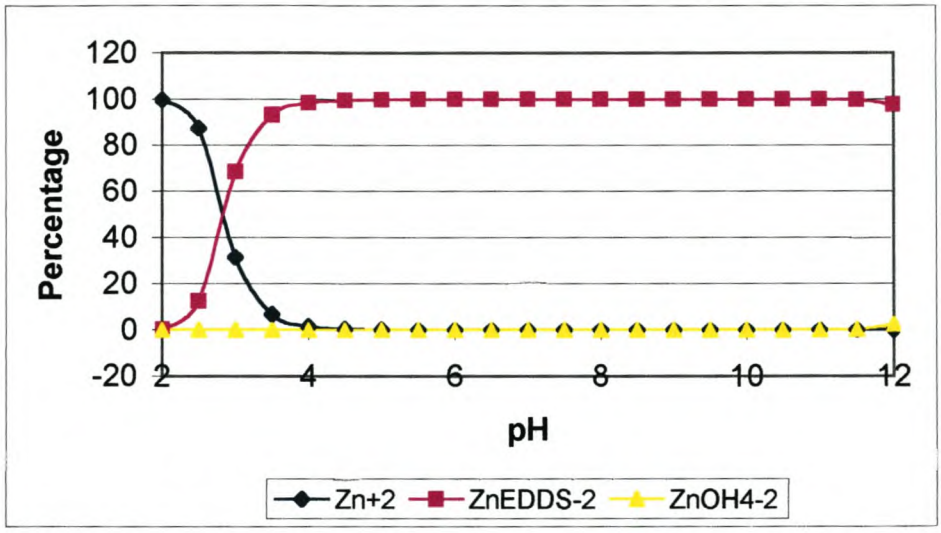

Figure 3.11 Speciation of ZnEDDS using JESS. Total metal concentration 100 ppm, total ligand concentration 0.1M, ionic strength I = 0, temperature 25°C.

Figure 3.12 shows the chemical speciation of the trivalent ion Fe^{3+}, when it complexes with EDDS forms $[FeEDDS]^-$. From the speciation curves the hydroxy species are observed, but no protonation peaks are noted. This might be due to the fact that the distribution of these species is less than 5 %. This chemical speciation differs from the one for Cr^{3+}, which is also a trivalent ion, in the fact that both protonation and hydroxyl species can be observed in the chemical speciation of CrEDDS. The obtained chemical speciation of CrEDDS is shown in Figure 3.13.

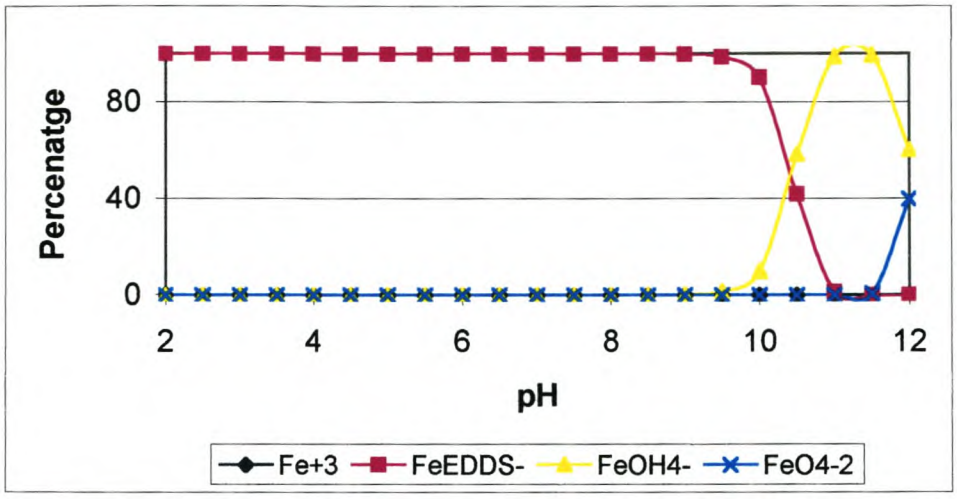

Figure 3.12 Speciation of FeEDDS using JESS. Total metal concentration 100 ppm, total ligand concentration 0.1M, ionic strength I = 0, temperature 25°C.

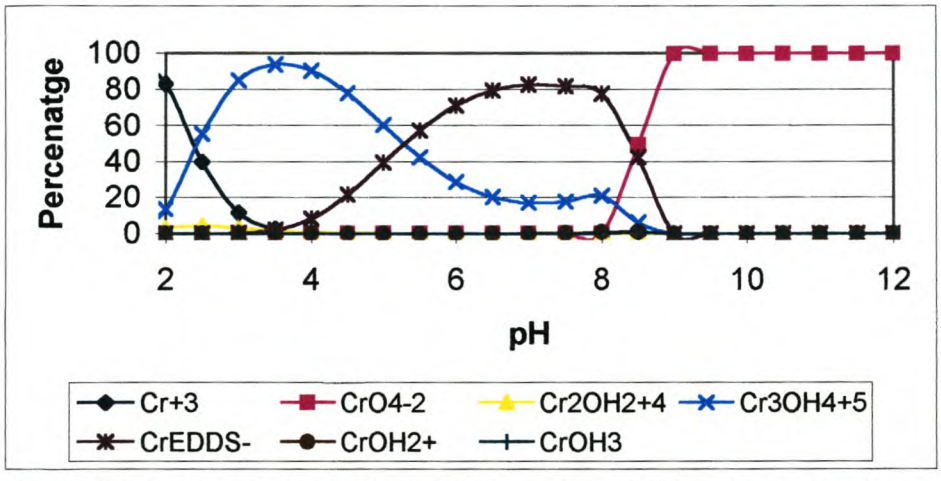

Figure 3.13 Speciation of CrEDDS using JESS. Total metal concentration 100 ppm, total ligand concentration 0.1M, ionic strength I = 0, temperature 25°C

3.4.4 Speciation diagrams for CuEDDM and PbEDDM

EDDM metal complexes were also modelled using JESS since the EDDM ligand was also to be used in the next *Chapter* for capillary electrophoresis. Figure 3.14 shows the obtained chemical speciation of CuEDDM. Like CdEDDS and ZnEDDS, only the major

species of CuEDDM which is $[CuEDDM]^{2-}$ ion has a high distribution that can be observed from the chemical speciation, the other species could not be observed since their distribution was less than 5 %.

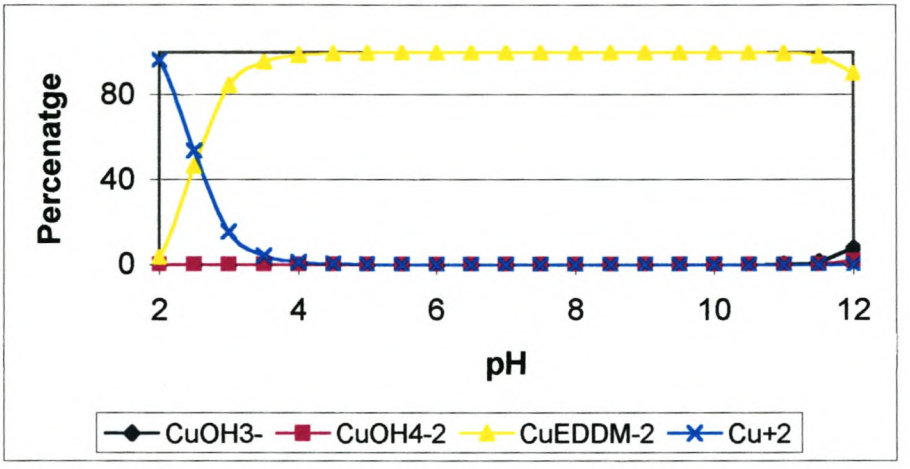

Figure 3.14 Speciation of CuEDDM using JESS. Total metal concentration 100 ppm, total ligand concentration 0.1M, ionic strength I = 0, temperature 25°C

The obtained chemical speciation of the PbEDDM is the same as for PbEDTA. The chemical speciation of PbEDDM is shown in Figure 3.15.

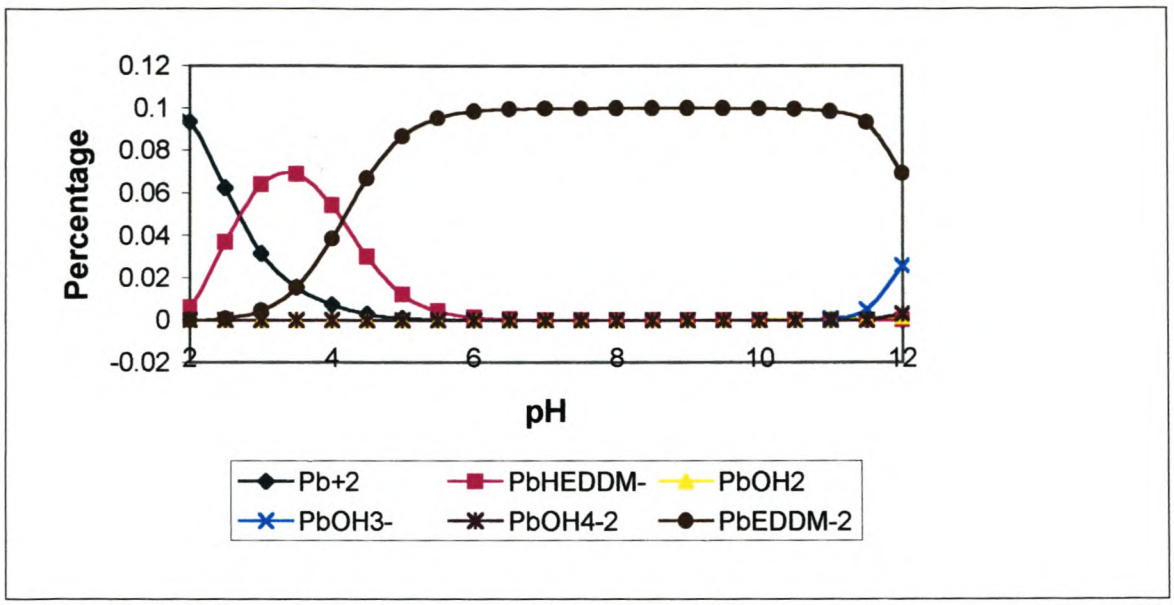

Figure 3.15 Speciation of PbEDDM using JESS. Total metal concentration 100 ppm, total ligand concentration 0.1M, ionic strength I = 0, temperature 25°C

Table 3.02 shows the pH regions where the metal ion is fully sequestered by the chelating agents

Table 3.02 pH regions in which the transition metal-ion is completely sequestered by the chelating agents

Metal-ion	[S,S']-EDDS	EDTA	EDDM
Cu	4.0-9.0	4.0-10.0	4.0-12.0
Fe	2.0-10.0	-	-
Pb	4.0-12.0	4.0-10.5	5.0-10.0
Cd	5.0-12.0	4.0-12.0	-
Zn	5.0-12.0	5.0-12.0	-
Cr	6.0-8.0	-	-

3.5 Conclusions

This chapter has described the fundamental theory behind speciation and the computational approaches used to analyze it based upon formation constants. The speciation models were considered at various pH values and were used to validate the electropherograms obtained using Capillary Electrophoresis (CE). The comparisons are discussed in detail in *Chapter 4.*

Simple computer simulated speciation models were created to analyse the order of complexation of $EDTA^{4-}$, $EDDM^{4-}$ and $EDDS^{4-}$ with various metal ions i.e. Cu^{2+}, Pb^{2+}, Zn^{2+}, Cd^{2+}, Ni^{2+}, Cr^{3+} and Fe^{3+}. From the speciation graphs it can be concluded that all the species undergo protonation at low pH while they deprotonate at high pH.

References

1. IUPAC Glossary of Terms used in Bioinorganic Chemistry, *Pure and Applied Chemistry*, 1997, **69(6),** 1251.
2. Taylor D. M., Williams D. R, *Trace Element Medicine and Chelation Therapy,* Royal Society of Chemistry, London, 1998.
3. Williams D. R., *An Introduction to Bioinorganic Chemistry*, C.C. Thomas Publishers, Springfield, Illinois, 1976.
4. Williams D. R., *Chemical Speciation and Bioavailability.*
5. Duffield J. R., Marsicano F., Williams D. R, *Polyhedron,* 1991, **10(10),** 1105.
6. Duffield J. R., Marsicano F., Waters M., Williams D. R, *Polyhedron*, 1991, **10(10),** 1113.
7. May P. M., Murray K., *Talanta*, 1991, **38(12),** 1409.
8. May P. M., Murray K., *Talanta*, 1991, **8(12),** 1419.
9. May P. M., Murray K., *Talanta*, 1993, **40(6),** 819.
10. May P. M, Murray K., *Jess Primer*, 1996.
11. Sawyer C. T., *Experiments for Instrumental Method*, A Laboratory Manual, McGraw-Hill Book Co, 1991
12. The thermodynamic constants are included in the Jess thermodynamic database. http://jess.murdoch.edu.au/jess/jess_home.htm.

CHAPTER 4

CAPILLARY ELECTROPHORESIS

4.1 Electrophoresis -Overview

Electrophoresis, in general, describes the transport of charged species in an electric field. The separation capability of electrophoresis is based on recognition of the differences in electrophoretic mobilities of charged species. The electrophoretic mobility is proportional, in a simple picture, to the ratio of the effective ion charge to its friction[1].

Capillary Electrophoresis (CE) was born of the marriage of the powerful separation mechanisms of electrophoresis with the instrumentation and automation concepts of chromatography. The early phases of its evolution were mostly concerned with determining its characteristics and learning about some inherent capabilities of the technique. This separation technique was first developed by the Swedish chemist Arne Tiselius in the 1930s for the study of cerium proteins. He was subsequently awarded the 1948 Nobel Prize for his work[2].

Electrophoresis has been applied to a variety of difficult analytical separation problems: inorganic anions and cations, amino acids, catecholamines, drugs, vitamins, carbohydrates, peptides, proteins, nucleic acids, nucleotides, polynucleotides and numerous other species[2].

A key feature of CE is the overall simplicity of the instrumentation. In addition, CE offers the following advantages; simple method development, minimal sample volume requirements, short separation time, high number of theoretical plates, low electrolyte and column material consumption, low capital and running costs and absence of organic waste. CE also has a uniform flow and hence high separation efficiency and versatility

have been obtained for large molecules, such as proteins with small diffusion coefficients. A schematic diagram of a generic capillary electrophoresis system is shown in Figure 4.01[3].

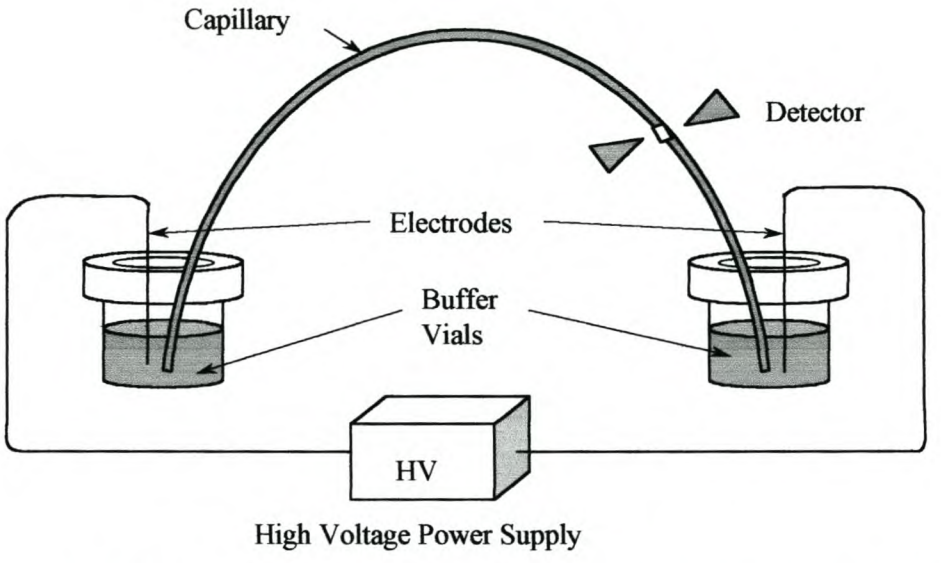

Figure 4.01 Schematic drawing of a capillary electrophoresis instrument[3]

Briefly, the ends of a narrow-bore, fused-silica capillary (10-100 μm i.d.) are placed in buffer reservoirs. The content of the reservoirs is identical to that within the capillary. The reservoirs also contain electrodes used to make electrical contact between the high-voltage power supply and the capillary. Sample is loaded onto the capillary by replacing one of the reservoirs (usually at the anodic side) with a sample reservoir and applying either an electric field or external pressure. After replacing the buffer reservoir, the electric field is applied and separation performed. Optical detection can be made at the opposite end, directly through the capillary wall. The details regarding capillary and injection are discussed briefly.

4.1 1 Instrumentation

Ideal properties of the capillary material include being chemically and electrically inert, UV-Visible transparent, flexible and robust, and inexpensive. Meeting most of these requirements, fused silica is the primary material employed today. Fused-silica capillaries are coated with a protective layer of polyimide to make them strong and easy to handle. For detection, an optical window can easily be made in the capillary by removal of a small section of the protective polyimide coating. This is accomplished by burning off a few millimetres of polyimide using an electrical arc or electrically heated wire, or by scraping with a razor blade.

Teflon is another material used in CE, although not to the extent of fused silica. Teflon is transparent to UV and thus requires no special optical window. Although uncharged, it also exhibits a significant electro-osmotic flow (EOF). Unfortunately, it is difficult to obtain teflon with homogenous inner diameters. Moreover it exhibits sample adsorption problems and has poor heat transfer properties. These disadvantages have limited its use.

4.1.2 Sample injection

There are two methods of sample injection in CE namely: hydrodynamic and electrokinetic injection.

4.1.2.1 Hydrodynamic injection

Hydrodynamic sample injection is the most widely used method[2]. It can be accomplished by application of pressure at the injection end of the capillary, vacuum at the exit end of the capillary, or by a siphoning action obtained by elevating the injection reservoir

relative to the exit reservoir. With hydrodynamic injection, the quantity of sample loaded is virtually independent of the sample matrix.

4.1.2.2 Electrokinetic injection

Electrokinetic, or electromigration injection is performed by replacing the injection-end reservoir with a sample vial and applying a voltage. Usually a field strength 3 to 5 times lower than that used for separation is applied. In electrokinetic injection, analytes enter the capillary both by electro-migration and by the pumping action of the EOF[4]. A unique property of electrokinetic injection is that the quantity loaded is dependent on the electrophoretic mobility of the individual solutes. Discrimination thus occurs for ionic species since the more mobile ions are loaded to a greater extent than those that are less mobile.

For electrokinetic injection, sample loading is dependent on the EOF, sample concentration, and sample mobility. Variations in conductivity, which can be due to matrix effects such as a large quantity of an undetected ion such as sodium or chloride, result in differences in voltage drop and quantity loaded. Due to these phenomena electrokinetic injection is generally not as reproducible as its hydrodynamic counterpart.

4.2 Electroosmotic flow

When a voltage is applied between the ends of an insulating tube that contains a liquid, the liquid moves along the entire length of the tube as a plug. This motion is called electroosmosis, electroendoosmosis, or electroosmotic flow (EOF)[5]. The flow rate is proportional to the voltage applied and the buffer viscosity, and depends on the charge at

the inner surface of the capillary. Control of the EOF is essential to obtain reproducible results in capillary electrophoresis. A schematic illustration of the generation of EOF is shown in Figure 4.02.

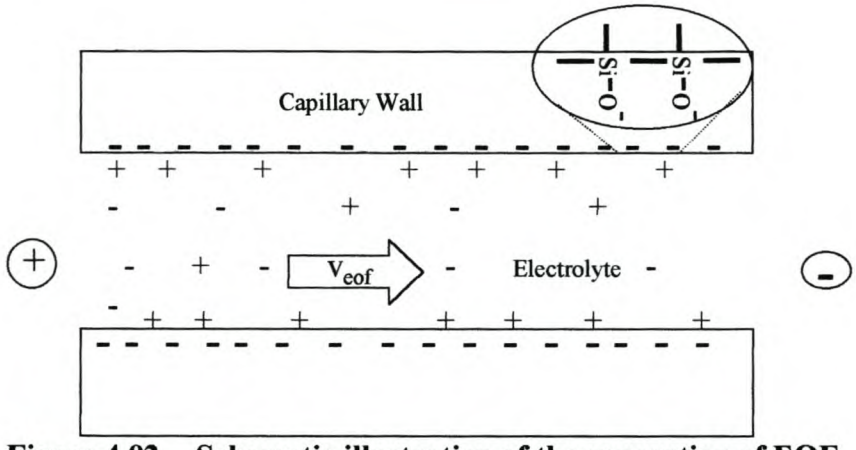

Figure 4.02 Schematic illustration of the generation of EOF

Buffer pH is one of the most significant factors influencing the EOF in a fused-silica capillary because of the development of charge at the silica wall surface due to dissociation of the residual silanol sites on the capillary wall. The pK_a for the silanol group is about 5.9, depending on the solution composition in contact with the fused silica wall. Typically, EOF for the fused-silica capillary is high in a basic buffer, it decreases significantly at about pH 6 and is low in a more acidic buffer solution. Even with an acidic buffer, analyte migration is towards the negative electrode, but is sharply decreased because of the low EOF under the acidic conditions. Depending on the specific conditions, the EOF can vary by more than an order of magnitude between pH 2 and 12. Also, a change in EOF is dependent on buffer composition[6,7] and on the experimental process used to condition the fused-silica capillary wall[8-10].

Other experimental variables can be changed to optimize EOF and improve resolution, alter analyte migration time or direction, and/or change analysis time. Increasing the buffer ionic strength decreases the EOF while an EOF change can also be correlated to the viscosity, dielectric properties, solvent composition, and temperature of the buffer solution[11]. Coating the fused-silica capillary wall and/or derivatization of the wall silanol sites, for example, with monomeric or polymeric hydrocarbons, alcohols, diols, glycols, carbohydrates, amides, ethers, and oxides[12], can mask or alter the influence of the residual silanol sites. While these techniques often minimize analyte capillary wall interactions, they will also affect capillary wall surface charge and viscocity and also therefore, the EOF. Adding ionic or nonionic surfactants to the buffer below critical micelle formation affects the EOF due to interactions between the surfactant and the capillary wall surface. For example, for quaternary ammonium salts the decrease in EOF is dependent on concentration and alkyl chain length of the tetra-alkyl ammonium cation[13,14]. For long alkyl chain lengths an EOF reversal is observed[13,15,16].

Modification of the fused-silica capillary wall with a highly ionized group, compared to the silanol group, should offer several advantages. Extensive ionization, which is less sensitive to buffer pH, whether due to anionic or cationic groups, should lead to a more constant surface change. The dependence of the EOF on pH should be minimized and, therefore, should result in a more constant, reproducible EOF, which should lead to better reproducibility in CZE separations. In addition, wall-analyte interactions should be minimized, depending on the analyte and the type of charged wall modification. These advantages have been realized in studies where anionic surfaces are generated by attaching a sulfonated group[12,17-20] or a boronate group on a fused-silica capillary wall

and where cationic surfaces are generated via the introduction of cationic groups on the wall[21-24].

A unique feature of EOF in the capillary is the flat profile of the flow. This flow profile is beneficial since it does not directly contribute to the dispersion of solute zones. This is in contrast to that generated by an external pump, which yields a laminar or parabolic flow due to the shear forces at the wall.

The flow rate drops off rapidly at the wall. This quiescent solution layer is caused by friction against flow at the surface. Since this layer extends a short way into the solution, it is relatively unimportant to the overall separation process (that is, other dispersion processes dominate). Further, the flow rate and profile are generally independent of capillary diameter. The profile will be disrupted, however, if the capillary internal diameter is too wide ($\geq$ 200 to 300 μm).

One great benefit of having electroosmotic flow present is that electrophoretic separations and detection can be run for anions and cations simultaneously. Without EOF, either only anions or only cations would migrate toward the detector. The oppositely charged ion would migrate back out of the injection end, and the neutral ions would remain and spread by diffusion. Under normal conditions (that is, negatively charged capillary surface), the flow is from the anode to the cathode. Anions will be flushed towards the cathode since the magnitude of the flow can be more than an order of magnitude greater than their electrophoretic mobilities. Thus cations, neutral ions, and anions can be electrophoresed in a single run since they all "migrate" in the same direction. Cations migrate fastest since the electrophoretic attraction towards the cathode and the EOF are in the same direction, neutrals are all carried at the velocity of the EOF

but are not separated from each other, and anions migrate slowest since they are attracted to the anode but are still carried by the EOF toward the cathode.

For the analysis of small ions (for example, sodium, potassium, chloride) the magnitude of EOF is usually not greater than the solute mobilities. In addition, modification of the capillary wall charge can decrease the EOF while leaving solute mobility unaffected. Under these circumstances, anions and cations can migrate in the opposite direction.

While the EOF is usually beneficial, it often needs to be controlled. Methods to control EOF are listed in Table 4.01.

Table 4.01 Methods to control EOF

Variable	Result	Comment
Electric field	Proportional change in EOF.	• Efficiency and resolution may decrease when lowered. • Joule heating may result when increased.
Buffer pH	EOF decreased at low pH and increased at high pH.	• Most convenient and useful method to change EOF. • May change charge or structure of solute.
Ionic strength or buffer concentration	Decreases zeta potential and EOF when increased.	• High ionic strength generates high current and possible Joule heating. • Low ionic strength problematic for sample adsorption. • May distort peak shape if conductivity different from sample conductivity. • Limits sample stacking if reduced.
Temperature	Changes viscosity 2-3% per °C.	• Often useful since temperature is controlled instrumentally.
Organic modifier	Changes zeta potential and viscosity (usually decreases EOF).	• Complex changes, effect most easily determined experimentally. • May alter selectivity.
Surfactant	Adsorbs to capillary wall via hydrophobic and/or ionic interactions.	• Anionic surfactants can increase EOF. • Cationic surfactant can decrease or reverse EOF. • Can significantly alter selectivity.
Neutral hydrophilic polymer	Adsorbs to capillary wall via hydrophobic interactions.	• Decreases EOF by shielding surface charge and increasing viscosity.
Covalent coating	Chemical bonding to capillary wall	• Many modifications possible (hydrophilicity or charge). • Stability often problematic.

4.3 Modes of operation

The versatility of CE is derived from its numerous modes of operation. The separation mechanisms of each mode are different and thus can offer orthogonal and complementary information. The basic methods encountered by CE include capillary zone electrophoresis (CZE), micellar electrokinetic chromatography (MEKC), capillary gel electrophoresis (CGE), capillary isoelectric focusing (CIEF), and capillary isotachophoresis (CITP). The separation mechanisms of each mode are described in Table 4.02. For the most part, the different modes are accessed simply by altering the buffer composition.

Table 4.02 Modes of CE

Mode	**Basic operation**
Capillary zone electrophoresis (CZE)	Free solution mobility
Micellar electrokinetic chromatography (MEKC)	Hydrophobic/ionic interactions with micelles
Capillary gel electrophoresis (CGE)	Size and charge
Isoelectric focusing (IEF)	Isoelectric point
Isotachophoresis (ITP)	Moving boundries

Capillary zone electrophoresis is by far the most widely used operation mode in CE. Its mechanism is based on the differences in the electrophoretic mobility of analytes. The analytes with different electrophoretic mobility will migrate in separated zones, which is the origin for the name *zone*. Capillary zone electrophoresis was first described by

Jorgenson *et al.* in 1981[7]; using 75 μm i.d. fused-silica capillaries, narrow band injection by electromigration, sensitive fluorescence detection and suitable samples. They were able to show fast and excellent separations with symmetrical peaks and efficiencies in excess of 400,000 plates.

The major fundamental properties that determine analyte migration in capillary zone electrophoresis (CZE) are electrophoretic mobility, μ_{ep}, and electroosmotic flow (EOF), μ_{EOF}. The former is primarily influenced by analyte structure, capillary dimensions and electrical field conditions, while the latter is a function of the properties of the solution in contact with the capillary wall and the surface charge that develops at the wall[7].

Successful CZE separations require one to carefully control and reproduce the EOF, which is present in the capillary because of surface charge on the capillary wall. Because of its high resolution, short analysis time, and low consumption of reagents[7], CZE has received a great deal of attention for the determination of inorganic ions.

In addition, CZE in free buffer solution needs only minute sample volumes, which are customary in life sciences, and the separation is mainly based on charge discrimination, which can provide additional information about the possible structure of the molecules[3].

To date the most promising injection techniques for CZE that do not discriminate between different components in a sample are those, which use a controlled pressure differential over the separation capillary.

Recently, Ballou *et al.* reported the application of capillary zone electrophoresis for the determination of chelating agents in the Hanford tank waste stimulant. Although many other publications on CZE measurements involving other aminopolycarboxylic acids have appeared in recent years [7-12], there have been only few reports on capillary

electrophoretic investigations involving EDTA and nothing on biodegradable ligands such as [S,S']-EDDS and EDDM.

4.4 Experimental procedures

4.4.1 Instrumentation

The CE analyses were performed on a HP^{3D} CE capillary electrophoresis system Hewlett-Packard (Waldbronn, Germany) equipped with diode array detection with wavelengths between 190-820 nm. Fused-silica capillaries (Polymicro Technology, Phoenix, AZ, USA) of 50 µm i.d. and 50 cm long (42 cm to the detector) were used. Before use, capillaries were washed with 0.1 M NaOH, followed by triple distilled water and the separation buffer. Data analysis was executed with ChemStation (REV. A.06.01) software, also from Hewlett Parkard. All experiments were conducted at 25°C.

The following parameters were generally used throughout:

Potential	-25 kV
Injection time	2 s
Pressure	100 mbar
Wavelength	200 nm

4.2.2 Reagents and chemicals

All chemicals and reagents were purchased commercially and used as received. Ultra-pure water was prepared in a Milli-Q water-purification system (Millipore, Eschborn, Germany).

CHEMICALS	**MANUFACTURER AND GRADE**
Zinc nitrate Solution (1000 ppm)	Merck (Spectrosol)
Lead nitrate Solution (1000 ppm)	Merck (Spectrosol)
Copper nitrate Solution (1000 ppm)	Merck (Spectrosol)
Cadmium nitrate Solution (1000 ppm)	Merck (Spectrosol)
Iron nitrate Solution (1000ppm)	Merck (Spectrosol)
Chromium Solution (1000ppm)	Merck (Spectrosol)
EDTA	N.T. Laboratory Supplies (Analytical Reagent)
Thiourea	Aldrich (99%)
[S,S']-EDDS	Associated Octel UK Ltd. (only 33%)
Bromine	Merck (extra pure)
Ethanol	Aldrich (extra pure)
KOAc	Merck (analytical grade)
CCl_4	Aldrich (photometric grade)
NaOH	Merck (analytical reagent)
Diethyl Ether	Aldrich (extra pure)
Malonic Acid	Aldrich (analytical reagent)
Nitric Acid	Riedel-de Haen (65%)
Mercury metal triple-distilled	SAAR CHEM (Univar)
Borate	Merck (analytical grade)
CTAB	Fluka (analytical grade)

4.4.3 Preparation of standard solutions

Preparation of borate buffer solution, 20 mM $Na_2B_4O_7.10H_2O$. 0.7762 g of borate was weighed and diluted with distilled water in a 100 ml volumetric flask.

Preparation of HNO_3 solution, 0.1 M. Dilute 0.7 ml of HNO_3 (65%) with distilled water in a 100 ml volumetric flask.

Preparation of NaOH solution, 0.1 M. Dilute 10 ml of NaOH (1M) with distilled water in a 100 ml volumetric flask.

Preparation of mercury solution, 0.015 M Hg^{2+}. 0.3 g of triple distilled mercury was dissolved with several drops of concentrated nitric acid (in the hood) and diluted with distilled water in a 100 ml volumetric flask.

Preparation of metal standard solutions (i.e. Cu^{2+}, Pb^{2+}, Zn^{2+}, Cd^{2+}, Fe^{3+}, Cr^{3+}, Mn^{2+}), 10 ppm. Dilute 1.0 ml of metal standard solution with 20 mM borate in a 10 ml volumetric flask.

Preparation of [S,S']-EDDS, 1 mM. [S,S']-EDDS (0.03 g, $1x10^{-4}$ mol) was weighed and added to the standard solution.

Preparation of EDDM, 1 mM. EDDM (0.025 g, $1x10^{-4}$ mol) was weighed and added to the standard solution.

Preparation of EDTA, 1 mM. EDTA (0.04 g, $1x10^{-4}$ mol) was weighed and added to the standard solution.

Preparation of CTAB, 0.3 mM. CTAB (0.018 g, 5×10^{-5} mol) was weighed and mixed with borate (30 mM) in a 50ml volumetric flask.

4.4.4 Synthesis of EDDM

A 50 ml sample of bromine (0.0976 mol) was dissolved in CCl_4 (30.0 ml). A 10.16 g sample of malonic acid (0.0976 mol) was dissolved in 20.0 ml diethyl ether. The malonic acid/ether solution was placed in an ice bath with magnetic stirring, and the Br_2/CCl_4 was added dropwise. At the end of the reaction, the solvents were evaporated off under reduced pressure, with the flask still in the ice bath. The yellowish product was dissolved in about 10.0 ml of water and added to a saturated solution of 30.0 g KOAc in approximately 500.0 ml EtOH. This yielded the dipotassium salt of bromomalonic aid. The white dipotassium bromomalonate was separated from the ethanol by filtration. The product was then further purified by dissolving it in about 100 ml of water and precipitating with approximately 500 ml EtOH, followed by filtration. This procedure was carried out two or three times to afford dipotassium bromomalonate (27.11 g, 0.105 mol, 44%), m.p. 207-209°C (decomp) (lit. m.p. 208°C (decomp)).

4.5 Results and discussion

The results below show the obtained electropherograms for the polyaminocarboxylic acid ligands, which are EDTA, [S,S']-EDDS and EDDM and their complexes at different pH values. From the electropherograms the graphs of area vs. pH were plotted and compared with the speciation graphs obtained using JESS in *Chapter 3*. First, separation under coelectroosmotic conditions was determined since that was the mode to be used in these experiments. In this separation mode a cationic surfactant, cetyltrimethylammonium bromide is added which has the effect of reversing the direction of the EOF so that it flows from the negative electrode to the positive electrode. Thiourea was used as the marker to check if the direction of the EOF was reversed. The analysis of the metal complexes was to be done at varying pH. Hence, considering that the effect of the pH on the presence of the different species investigated in the study, it was attempted to obtain a stable EOF over the whole pH range. This facilitates the follow up of the relative amounts of the species. Under the used buffer composition (30 mM borate buffer with 0.3 mM CTAB), the pH of electrolyte was varied over the range from 2.0 to 12.0

4.5.1 Separation under coelectroosmotic conditions

Figure 4.03 shows a plot of the migration time for the thiourea marker vs. pH. A higher pH (>12) was not considered as speciation would then become more complicated due to increased hydrolysis of metal ions. Likewise a much lower pH (<2) was not investigated as the separation time became longer in spite of a decrease in the EOF velocity.

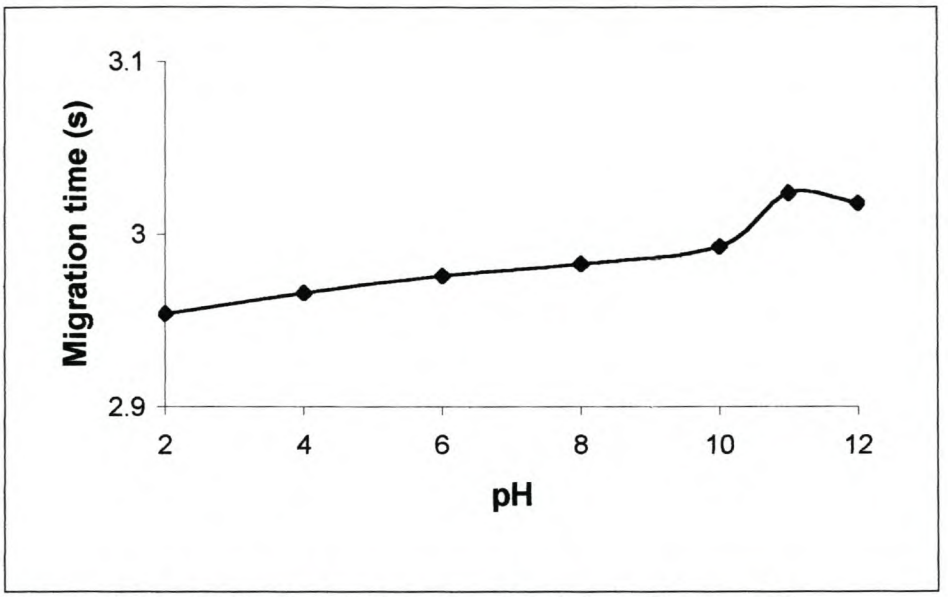

Figure 4.03 Plot of migration time for the marker vs. pH

From the graph it can be observed that the migration time increased almost linearly over the pH range 2.0-10.0. Migration times varied by 0.1 s over a pH range of 10. From these observations it can be concluded that the EOF increases with an increase in pH.

The pH value of the carrier electrolyte solution in CZE is the most important separation parameter for changing the selectivity of the system. The pH effect observed in our system could result from the following factors. First, the EOF decreases with a decreasing pH owing to the suppression of dissociation of capillary surface silanol groups, which lead to lowering of the charge density in the double layer. The effect of the EOF on the separation selectivity is given by the following equation:

$$\Delta t = \frac{L_d}{E} \cdot \frac{\mu_1 - \mu_2}{(\mu_{eo} - \mu_1)(\mu_{eo} - \mu_2)} \qquad (4.1)$$

where Δt is the difference of the migration times between two ions

μ_1 and μ_2 is the migration mobilities of these analytes

μ_{eo} is the electroosmotic mobility

L_d is the capillary length between the points of sample introduction and detection

E is the applied electric field strength

From equation (4.1) it follows that an increase of μ_{eo} with pH will decrease the value of Δt for these analytes.

In the pH range investigated, the EOF velocity is only slightly affected by the pH (Table 4.03). The most probable reason for this is that the pH effect and the ionic strength effect on the EOF are opposite.

Table 4.03 Obtained mobility values for the marker

pH	μ_{EOF} (cm^2/Vs)	Migration times (min.)
2	2.81×10^{-2}	2.954
4	2.80×10^{-2}	2.966
6	2.79×10^{-2}	2.976
8	2.78×10^{-2}	2.983
10	2.75×10^{-2}	3.018
12	2.74×10^{-2}	3.024

4.5.2 Speciation of EDTA using capillary zone electrophoresis

First, the background electropherogram was obtained for, thiourea, which was used as the marker, and then for 8 mM EDTA. The ligand was then examined by varying the pH of the solution by adding aliquots of 0.1 M NaOH to increase the pH and aliquots of 0.01 M HNO_3 to lower the pH. Figure 4.04 shows some obtained electropherograms of EDTA at different pH values.

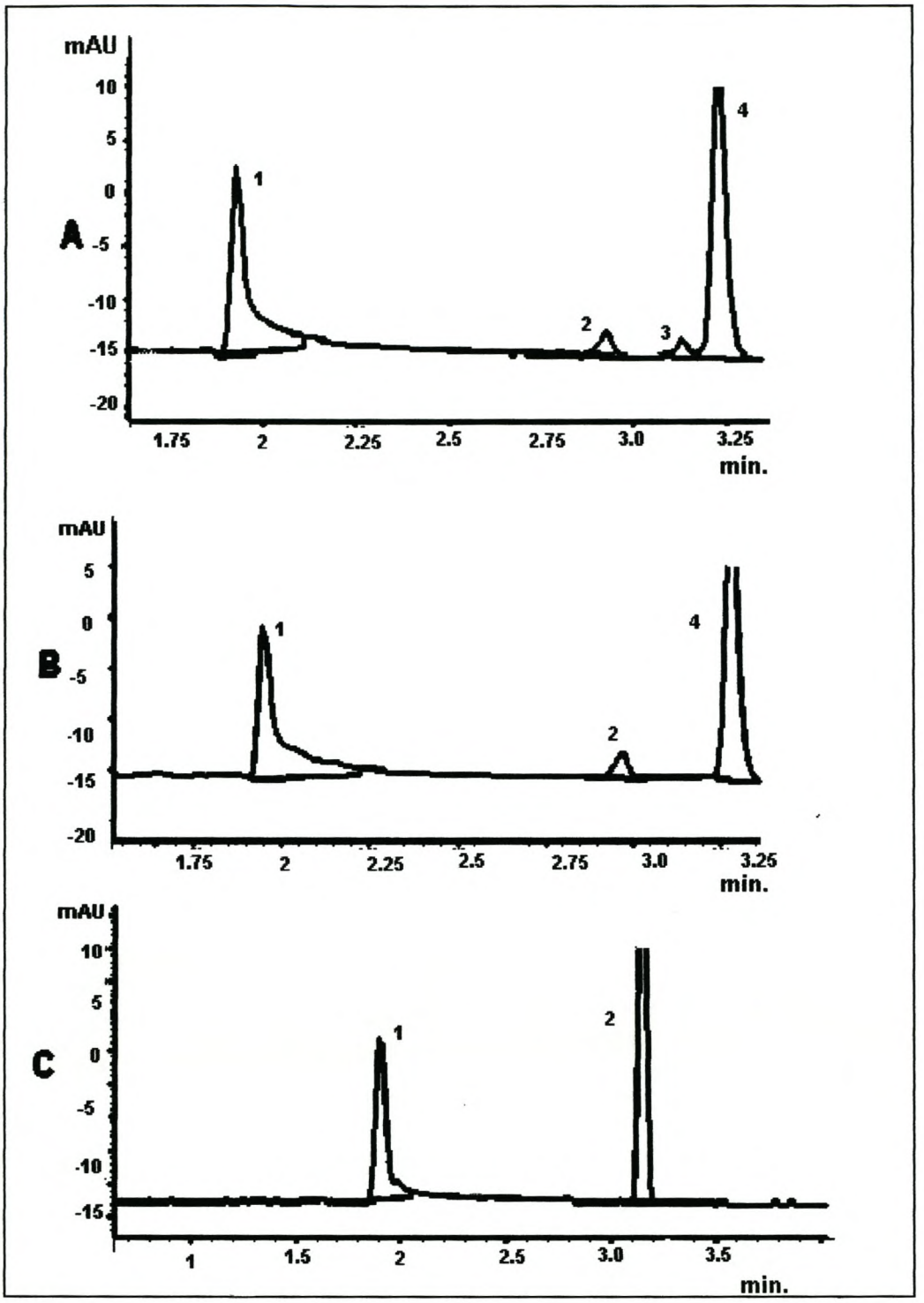

Figure 4.04 Separation of EDTA by CZE at pH 4.0 (A), 8.0 (B) and 10.0 (C).

Conditions: Column 45 mm × 50 μm i.d., injection: 50mbar during 3 s, detection: UV at 200 nm. Peaks: 1= $[HEDTA]^{3-}$, 2 = $[H_2EDTA]^{2-}$, 3 = $[H_3EDTA]^{-}$, 4 = Marker.

Figure 4.04 (A), (B) and (C) represent electropherograms of EDTA at pH values 4.0, 8.0 and 10.0, respectively. At pH 4.0, EDTA is in the forms $[HEDTA]^{3-}$, $[H_2EDTA]^{2-}$ and $[H_3EDTA]^{-}$. At pH 8.0, $[HEDTA]^{3-}$ and $[H_2EDTA]^{2-}$ are observed. At pH 8, it is also noted that the $[HEDTA]^{3-}$ peak is larger than the $[H_2EDTA]^{2-}$ peak. These results are comparable with the speciation calculations for EDTA using JESS (Figure 3.02). At pH 4 the concentration of $[EDTA]^{4-}$ is extremely small, hence the peak is not observed. The dominant species are $[HEDTA]^{3-}$ (83%) and $[H_2EDTA]^{2-}$ (17%). At pH 10.0 the same peaks are observed as at pH 8.0 except that the $[H_2EDTA]^{2-}$ peak has increased and is now larger than the $[HEDTA]^{3-}$ peak. As expected, the mobility of $[HEDTA]^{3-}$ is faster, due to its higher charge state, than $[H_2EDTA]^{2-}$ and $[H_3EDTA]^{-}$. In addition, the hydroxy groups interact with the ionized silanol groups on the walls of the capillary column and lead to slower migration times. The marker shifts in accordance with the direction as predicted in Figure 4.03. This is because as the pH decreases the EOF slows down owing to the dissociation of capillary surface silanol groups, hence the migration time of the peaks are observed later. This is true for all the electropherograms described below.

Furthermore, since the borate buffer was neutralized with NaOH, the ionic strength of the buffer increases, which results in a decreased μ_{EOF} and the electrophoretic mobilities of the analytes, as summarized in Table 4.04. When the EDTA was investigated in acidic medium at pH 2.0-6.0, however, the peaks for most analytes became broader and the migration times longer (Table 4.04). Common anions, such as nitrate did not interfere directly with the detection of the amino carboxylic acids or with their metal complexes

here, since their charge density is much greater and therefore these anions eluted more rapidly (typically less than 2 min).

Table 4.04 Obtained mobility values for EDTA

	Effective mobility (μ_e) (cm^2/Vs)			Migration times (min)		
pH	**$[HEDTA]^{3-}$**	**$[H_2EDTA]^{2-}$**	**$[H_3EDTA]^{-}$**	**$[HEDTA]^{3-}$**	**$[H_2EDTA]^{2-}$**	**$[H_3EDTA]^{-}$**
2			2.627			3.142
4	4.323	2.842	2.562	1.926	2.925	3.224
6	4.322	2.804		1.933	2.943	
8	4.235	2.803		1.949	2.968	
10	4.150	2.660		1.989	3.128	
12	3.993			2.090		

After obtaining these electropherograms at different pH values the plot of peak area vs. pH was constructed (Figure 4.05) and compared with the speciation data in Figure 3.02. Good agreement was obtained from speciation modelling studies although the modelled speciation diagrams were produced at different concentrations (0.1 M compared to 8 mM in the CE experiments). The general trend was the same in the protonation of the ligand at low pH and deprotonation at high pH. At the concentration at which the analytical determinations were done, the distribution diagram shows that one is able to speciate EDTA using capillary zone electrophoresis.

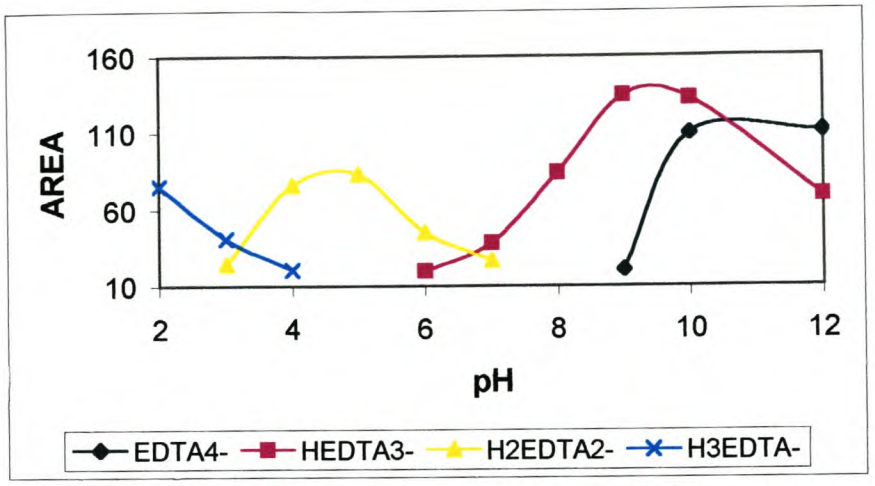

Figure 4.05 Speciation of EDTA using CZE. Total ligand concentration 8 mM.

The speciation graph in Figure 4.05 shows that $[EDTA]^-$ exists within the pH range 9-12, $[HEDTA]^{3-}$ within the pH range 6-12, $[H_2EDTA]^{2-}$ within the pH range 3-7, and $[H_3EDTA]^-$ within the pH range 2-4. At the concentration at which the analytical determinations were done, the distribution diagram shows that one is able to speciate EDTA using capillary zone electrophoresis.

The analysis of EDTA by CE under the different conditions was done to demonstrate the viability of the technique for the speciation of the ligands. EDTA complexes are kinetically very stable, even in the presence of competing metal-EDTA complexes at specific pH values. These processes were well studied by Martell, *et al.*[25]. The EDTA species existing at specified pH values, if detected, would be of significance for environmental monitoring.

The reproducibility of the method was studied by carrying out five consecutive runs. The standard deviations of peak areas were better than 4.5%.

Considering the similarities between EDTA, [S,S']-EDDS and EDDM, it is expected that a similar behavior would be observed for the latter two ligands.

4.5.3 Speciation of [S,S']-EDDS using capillary zone electrophoresis

[S,S']-EDDS has been identified as a biodegradable ligand, which can replace EDTA. It has already been used in countries like UK and Finland, hence speciation of [S,S']-EDDS was done using CE and the results compared with EDTA. The diagrams below show the electropherograms of 1 mM [S,S']-EDDS at various pH values.

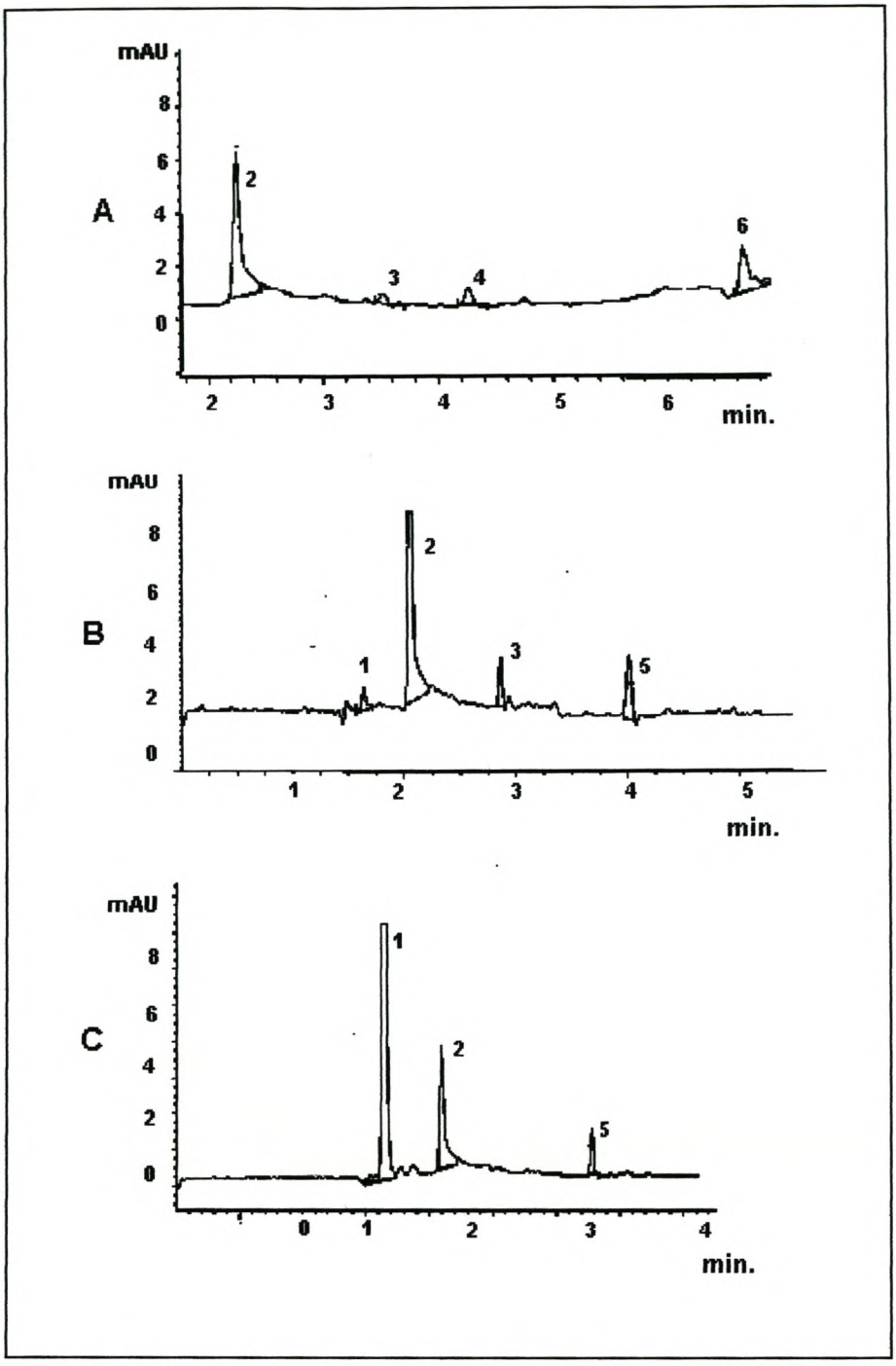

Figure 4.06 Separation of [S,S']-EDDS by CZE at pH 5.0 (A), 8.0 (B) and 10.0 (C).

Conditions: Same as in Figure 4.04. Peaks: 1 = $[EDDS]^{4-}$, 2 = $[HEDDS]^{3-}$,

3 = $[H_2EDDS]^{2-}$, 4 = $[H_3EDDS]^{-}$, 5 = $[OHEDDS]^{5-}$, 6= Marker

Figure 4.06 (A), (B) and (C) represent electropherograms of [S,S']-EDDS at pH values 5.0, 8.0 and 10.0. At pH 5.0, [S,S']-EDDS is present in three forms: $[HEDDS]^{3-}$, $[H_2EDDS]^{2-}$ and $[HEDDS]^{-}$. At pH 8.0, $[EDDS]^{4-}$, $[HEDDS]^{3-}$ $[H_2EDDS]^{2-}$ and $[OHEDDS]^{5-}$ are observed. At pH 10.0, $[EDDS]^{4-}$, $[HEDDS]^{3-}$ and $[OHEDDS]^{5-}$ are observed. At pH 8, EDDS forms mainly $[HEDDS]^{3-}$, hence the peak has a large peak area compared to the areas of the other peaks. When the pH is raised to 8.0, the $[EDDS]^{4-}$ amount increases and the hydroxy species of [S,S']-EDDS is observed. Table 4.05 shows the electrophoretic mobilities of [S,S']-EDDS at varied pH. The same trend is observed here as for EDTA.

Table 4.05 Obtained mobility values for EDDS

	Effective mobility (μ_e) (cm^2/Vs)				**Migration times (min)**			
pH	**$[HEDDS]^{3-}$**	**$[EDDS]^{4-}$**	**$[H_2EDDS]^{2-}$**	**$[H_3EDDS]^{-}$**	**$[HEDDS]^{3-}$**	**$[EDDS]^{4-}$**	**$[H_2EDDS]^{2-}$**	**$[H_3EDDS]^{-}$**
2				4.323				1.914
4	4.150		2.964	4.069	1.997		2.816	2.036
6	3.915		2.730	3.705	2.108		3.036	2.259
8	3.773	6.484	2.562		2.198	1.266	3.259	
10	3.705	6.483	2.358		2.241	1.281	3.517	

As expected [S,S']-EDDS showed a similar behavior to EDTA. Upon covering the entire pH range and plotting the relative peak areas of the different species vs. pH, the graph shown in Figure 4.07 was obtained.

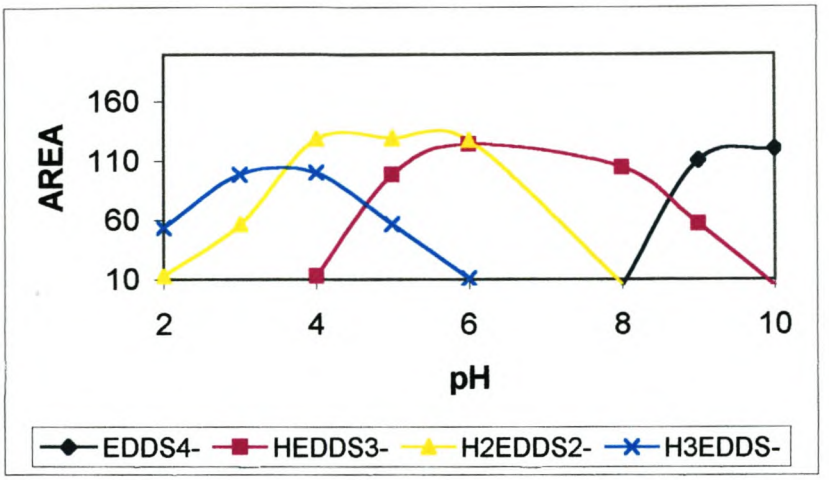

Figure 4.07 Speciation of EDDS using CZE. Total ligand concentration 8mM

The speciation graph in figure 4.07 shows that $[H_3EDDS]^-$ exists within the pH range 2-6. $[H_2EDDS]^{2-}$ is present within the pH range 2-8 and $[HEDDS]^{3-}$ within the pH range 4-10. [S,S']-EDDS, being proposed as a biodegradable replacement for EDTA, has similar properties to EDTA. As such, speciation of this ligand would be of significance in analytical determinations.

4.5.4 Speciation of EDDM using capillary zone electrophoresis

EDDM, was synthesized using the method by Schwarzenbach[26], and then tested. The resulting electropherograms are shown in Figure 4.08 (A), (B) and (C).

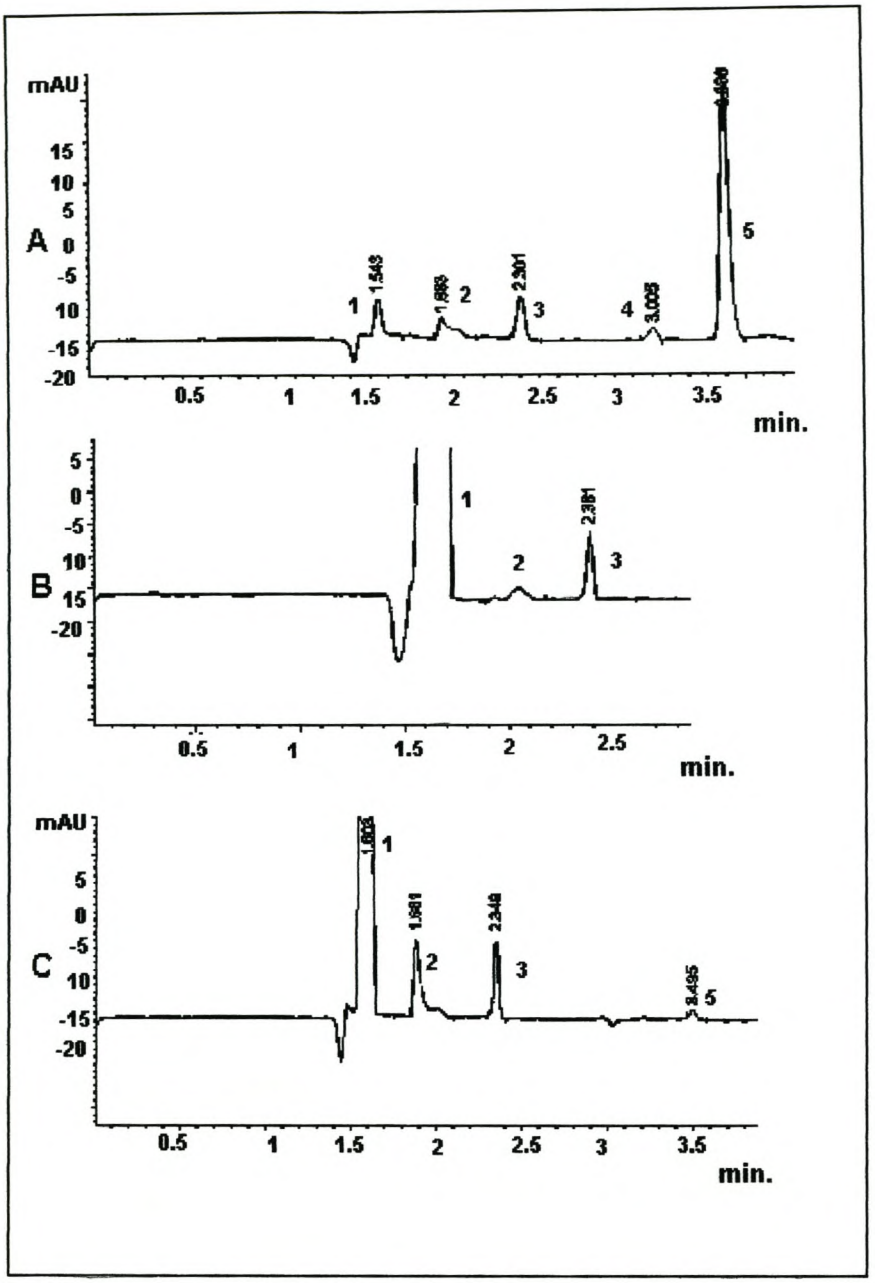

Figure 4.08 Separation of EDDM by CZE at pH 4.0 (A), 6.0 (B) and 8.0 (C). Conditions: Same as in Figure 4.04. Peaks: 1 = $[NO_3]^{2-}$, 2 = $[HEDDM]^{3-}$, 3 = $[H_2EDDM]^{2-}$, 4 = $[H_3EDDM]^{-}$, 5 = Marker

In figure 4.08 the electropherograms of EDDM at pH values 4.0, 6.0 and 8.0 are shown. At pH 4.0, $[HEDDM]^{3-}$, $[H_2EDDM]^{2-}$ and $[H_3EDDM]^{-}$ are observed. At pH 6.0 EDDM

exists in two forms: $[HEDDM]^{3-}$ and $[H_2EDDM]^{2-}$. At pH 8.0 the same peaks are observed as at pH 6.0, but the $[HEDDM]^{3-}$ peak is increased. These results correspond with the modelled speciation diagram in Figure 3.04. Table 4.06 shows the electrophoretic mobilities of EDDM, which follows the same trends as [S,S']-EDDS and EDTA.

Table 4.06 Obtained mobility values for EDDM

	(Effective mobility) μ_e (cm^2/Vs)			**Migration times (min)**		
pH	**$[HEDDM]^{3-}$**	**$[H_2EDDM]^{2-}$**	**$[H_3EDDM]^-$**	**$[HEDDM]^{3-}$**	**$[H_2EDDM]^{2-}$**	**$[H_3EDDM]^-$**
2			2.767			2.982
4	4.415	3.640	2.766	1.883	2.301	3.005
6	4.414	3.517		1.891	2.349	
8	3.915	3.516		2.114	2.361	
10	3.773			2.186		

The speciation graph in Figure 4.09 shows that $[H_3EDDM]^-$ exists within the pH range 2-4, $[H_2EDDM]^{2-}$ within the pH range 4-8, $[HEDDM]^{3-}$ within the pH range 6-10 and $[EDDM]^{4-}$ within the pH range 9-12.

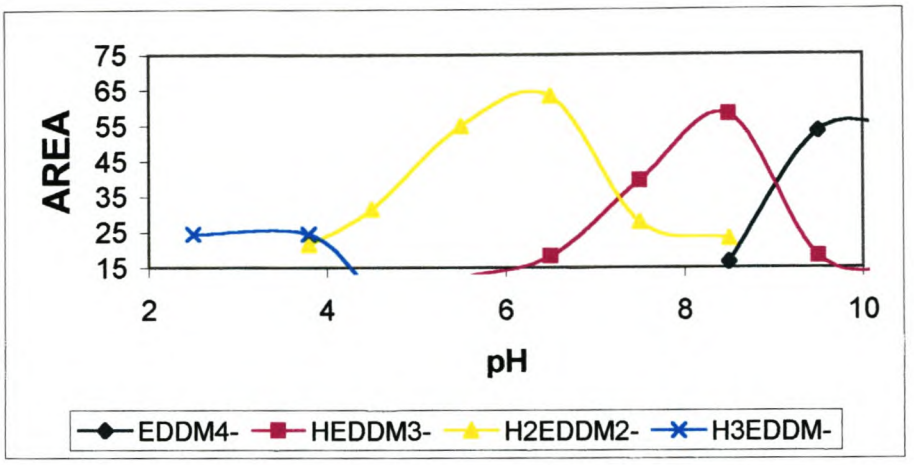

Figure 4.09 Speciation of EDDM using CZE. Total ligand concentration 8mM

EDDM, being a biodegradable ligand, can also be applied as a replacement for EDTA, and has indeed been used in certain applications like binding metal ions in industry. EDDM was used to further act as evidence for the viability of capillary zone electrophoresis for the speciation of the ligands.

Table 4.07 shows the pH regions for the different forms of each ligand.

Table 4.07 pH regions in which different forms of the ligands EDTA, [S,S']-EDDS and EDDM exist.

Species	EDTA	[S,S']-EDDS	EDDM
Y^{4-}	9-12	8-12	9-12
HY^{3-}	6-12	4-10	8-10
H_2Y^{2-}	3-7	2-8	4-9
H_3Y^{-}	2-4	2-6	2-4

Y= Ligand

4.5.5 Speciation of divalent metal ions (Cu, Pb, Cd and Zn) with EDTA, EDDS and EDDM

Separation of CuEDTA complex was performed using a borate electrophoretic buffer at various pH values. The obtained peaks were sharp, and the migration times short. Results of the separations at pH values 3.0, 5.0 and 11.0 are shown in Figure 4.10. The electropherograms in Figure 4.10 illustrate baseline resolution of the model components within 5 min. In order of migration times, the complexes eluted as follows: first $[CuEDTA]^{2-}$, followed by $[CuHEDTA]^{-}$ and finally $[CuOHEDTA]^{3-}$ (Table 4.08). Although migration times were somewhat variable, analyte identity was readily established by calculating the electrophoretic mobilities using equation (4.1). CZE migration times are a combination of electrophoretic migration and electroosmotic flow. With conventional CZE buffers, mobile cations contained in the Stern-layer are repelled by the positive injection electrode, resulting in an electroosmotic flow toward the detector. It is known that divalent copper can be incorporated, either ionically or perhaps even covalently, into the fused silica surface although the exact nature of this association remains poorly understood. The presence of divalent cations and/or cationic surfactants alters the Stern-layer structure, which may result in a diminished magnitude (or even reversal) of EOF. Negatively charged polyaminocarboxylic acid-copper complexes were repelled from the negative injection electrode and therefore displayed an electrophoretic migration toward the detector. The polyaminocarboxylic acid-copper complexes migrated faster than, and in an opposite direction to, the EOF.

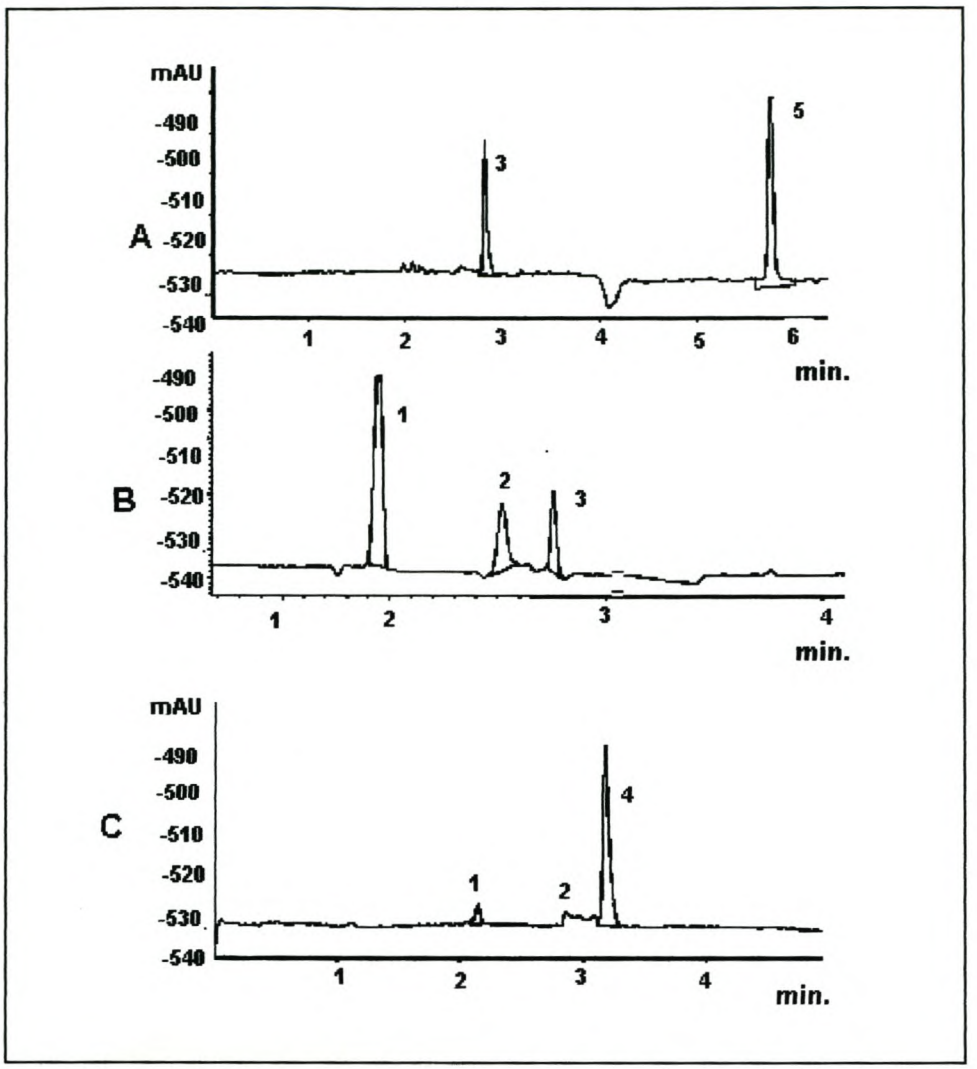

Figure 4.10 Separation of CuEDTA by CZE at pH 3.0 (A), 5.0 (B) and 11.0 (C), respectively. Conditions: Same as in Figure 4.04. Peaks: 1 = $(NO_3)^{2-}$, 2 = $[CuEDTA]^{2-}$,3 = $[CuHEDTA]^{-}$, 4 = $[CuOHEDTA]^{3-}$, 5 = Marker

From the electropherogram it is observed that at pH 5.0 (Figure 4.10(B)) CuEDTA is present in two forms: $[CuHEDTA]^{-}$ and $[CuEDTA]^{2-}$. As the pH is reduced to 3.0 (Figure 4.10(A)) the $[CuEDTA]^{2-}$disappeares and only the protonated peak is observed $[CuHEDTA]^{-}$. When the pH is increased to 11.0 the complex hydrolyses to form

$[CuOHEDTA]^{3-}$ while the $[CuEDTA]^{2-}$ peak starts disappearing (Figure 4.10(C)). These results are in good agreement with the distribution-pH diagrams (Figure 3.05), which showed that in the pH range 3.0-12.0, the species obtained were present. The migration times of the copper complexes did not change significantly with pH (Table 4.08) as was also observed by Jen J-F., *et al.* when they studied[22] vanadium complexes at various pHs. As the ionic strength of the buffer is increased, the effective mobility is expected to decrease[27]. The same observations are obtained in table 4.09 for CuEDDS species.

Table 4.08 Obtained mobility values for CuEDTA

	Effective mobility (μ_e) (cm^2/Vs)			**Migration times (min)**		
pH	**$[CuEDTA]^{2-}$**	**$[CuHEDTA]^{-}$**	**$[CuOHEDTA]^{2-}$**	**$[CuEDTA]^{2-}$**	**$[CuHEDTA]^{-}$**	**$[CuOHEDTA]^{3-}$**
2		3.458			2.397	
4	3.007	3.457		2.755	2.408	
6	2.964	3.294		2.808	2.519	
8	2.882		2.695	2.864		3.062
10	2.842		2.627	2.937		3.173

Upon covering the whole pH range (2.0-12.0) and plotting the relative peak areas of the different species of CuEDTA vs. pH, the graph shown in Figure 4.11 was obtained.

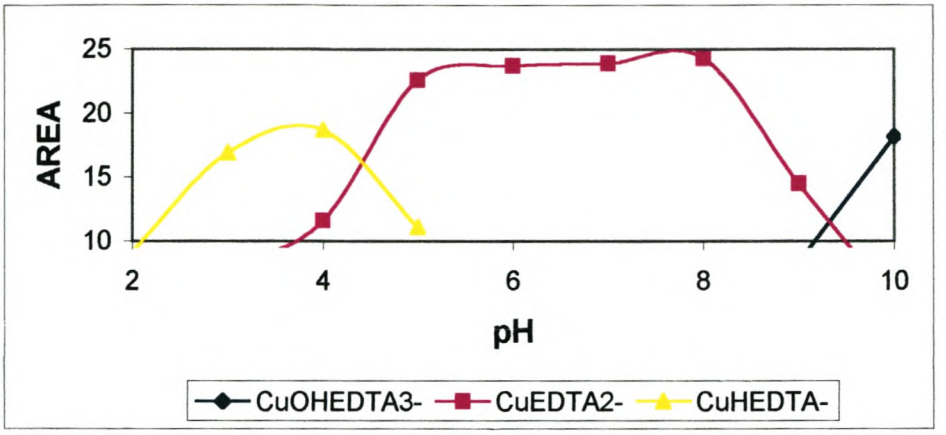

Figure 4.11 Speciation of CuEDTA using CZE. Total metal concentration: 100 ppm, total ligand concentration 8mM.

The speciation graph in Figure 4.11 shows that $[CuHEDTA]^-$ exists within the pH range 2-5, $[CuEDTA]^{2-}$ within the pH range 4-9 and $[CuOHEDTA]^{3-}$ within the pH range 9-12. At the concentration at which the analytical determination was done, the distribution diagram shows that one is able to speciate CuEDTA by this method. The Cu metal ion was also complexed with EDDS and with EDDM, and the results compared with the CuEDTA results.

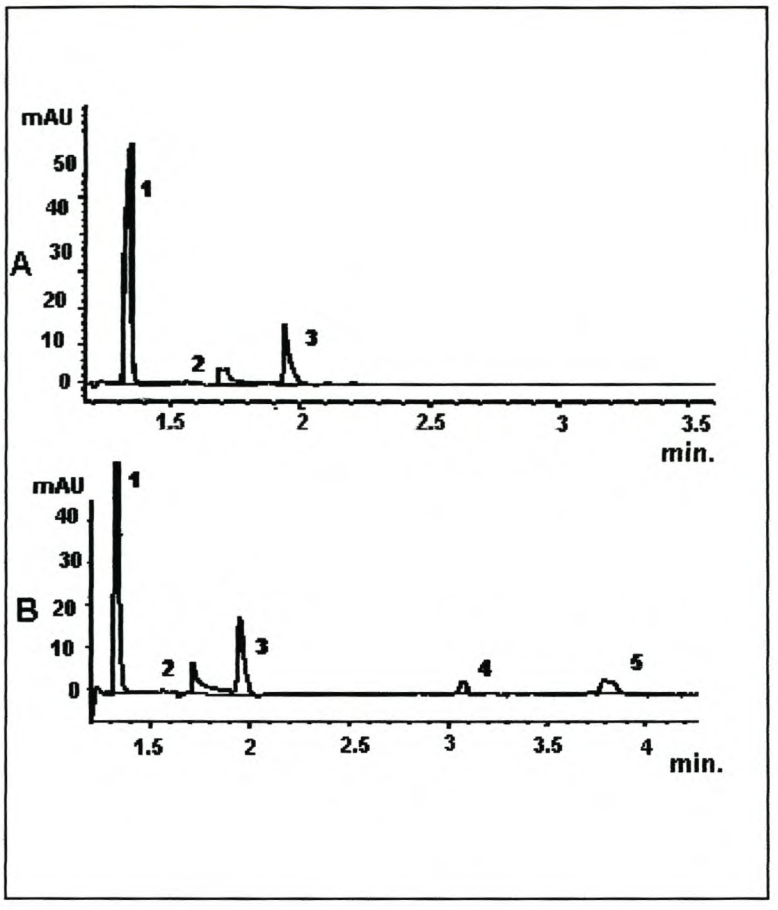

Figure 4.12 Separation of CuEDDS by CZE at pH 5.0 0 (A) and 12.(B), respectively. Conditions: Same as in Figure 4.04. Peaks: 1 = $(NO_3)^{2-}$, 2= $[CuEDDS]^{2-}$, 3 = $[CuHEDDS]^{-}$, 4 = $[CuOHEDDS]^{3-}$, 5 = Marker

Figure 4.12 represents electropherograms of CuEDDS at pH values 5.0 (A)and 12.0 (B). At pH 5.0 $[CuHEDDS]^{-}$ and $[CuEDDS]^{2-}$ are observed. At pH 12.0 CuEDDS is present in three forms: $[CuOHEDDS]^{3-}$, $[CuHEDDS]^{-}$ and $[CuEDDS]^{2-}$. Difficulties in quantification were noted and can be caused by complexes exchanging aminocarboxylate ligands for potential ligands (*e.g.* borate) within the capillary electrolyte[27]. Comparison of the results with those of CuEDTA (Figure 4.10) shows that the same speciation peaks are

observed for CuEDTA, except that the protonation peak was still present at high pH in the case of CuEDDS. This is because the differences in the effective mobilities of CuEDDS and CuHEDDS are so small that separation of these peaks could not be achieved[24]. The effect of complexing agents on the effective electrophoretic mobilities of chelates is shown in Table 4.09.

Table 4.09 Obtained mobility values for CuEDDS

	Effective mobility (μ_e) (cm^2/Vs)			**Migration times (min)**		
pH	**$[CuEDDS]^{2-}$**	**$[CuHEDDS]^{-}$**	**$[CuOHEDDS]^{3-}$**	**$[CuEDDS]^{2-}$**	**$[CuHEDDS]^{-}$**	**$[CuOHEDDS]^{3-}$**
2	4.940	4.415		1.691	1.898	
4	4.823	4.323		1.702	1.902	
6	4.822	4.322		1.713	1.924	
8	4.821	4.235	2.594	1.724	1.946	3.196
10	4.820	4.235	2.593	1.738	1.968	3.202
12	4.716	4.150	2.592	1.753	1.986	3.214

These results show a good agreement with the speciation graph in Figure 3.08. Upon covering the whole pH range and plotting the relative peak areas of the different species vs. pH, the graph shown in Figure 4.13 was obtained.

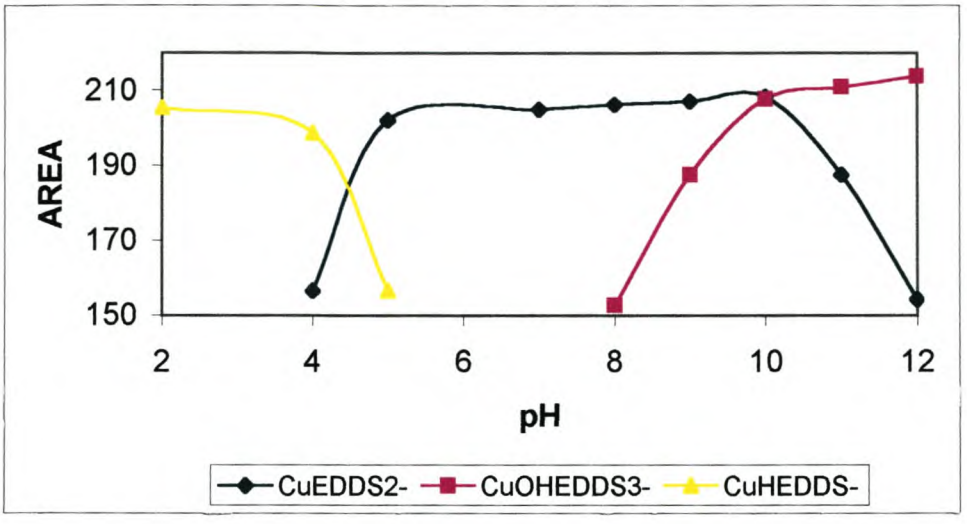

Figure 4.13 Speciation of CuEDDS using CZE. Total metal concentration: 100 ppm, total ligand concentration 1mM.

The species distribution graph in Figure 4.13 shows that $[CuHEDDS]^-$ exists within the pH range 2-5, $[CuEDDS]^{2-}$ within the pH range 4-12 and $[CuOHEDDS]^{3-}$ within the pH range 8-12. Comparison of the results with CuEDTA indicates that when the pH is increased, the effect of formation of mixed hydroxy complexes is much faster for CuEDDS compared to CuEDTA (*i.e.* pH 8 and 9). This is because the complex of CuEDTA is more stable compared to CuEDDS (*i.e.* 18.8 and 18.5 for CuEDTA and CuEDDS, respectively) and according to Schwedt G. *et al.*[28]less stable complexes have a tendency to hydrolyse quicker than the more stable ones.

Cu forms a much less stable complex when complexed with EDDM compared to EDTA and EDDS. Although the EDDM ligand has three functional groups in metal chelate formation, it is sterically impossible for these groups to coordinate to the metal ion forming two chelate rings, and this can be confirmed by its stability constant value, which

is 13.00. This can also be seen from the speciation data of CuEDDM in Figure 3.14 where only the $[CuEDDM]^{2-}$ distribution diagram is observed at the concentration at which the speciation is done. The protonation peak is not observed while the hydrolysis peak was seen below pH 10. Figure 4.14 shows the electropherograms of CuEDDM at both low and high pH.

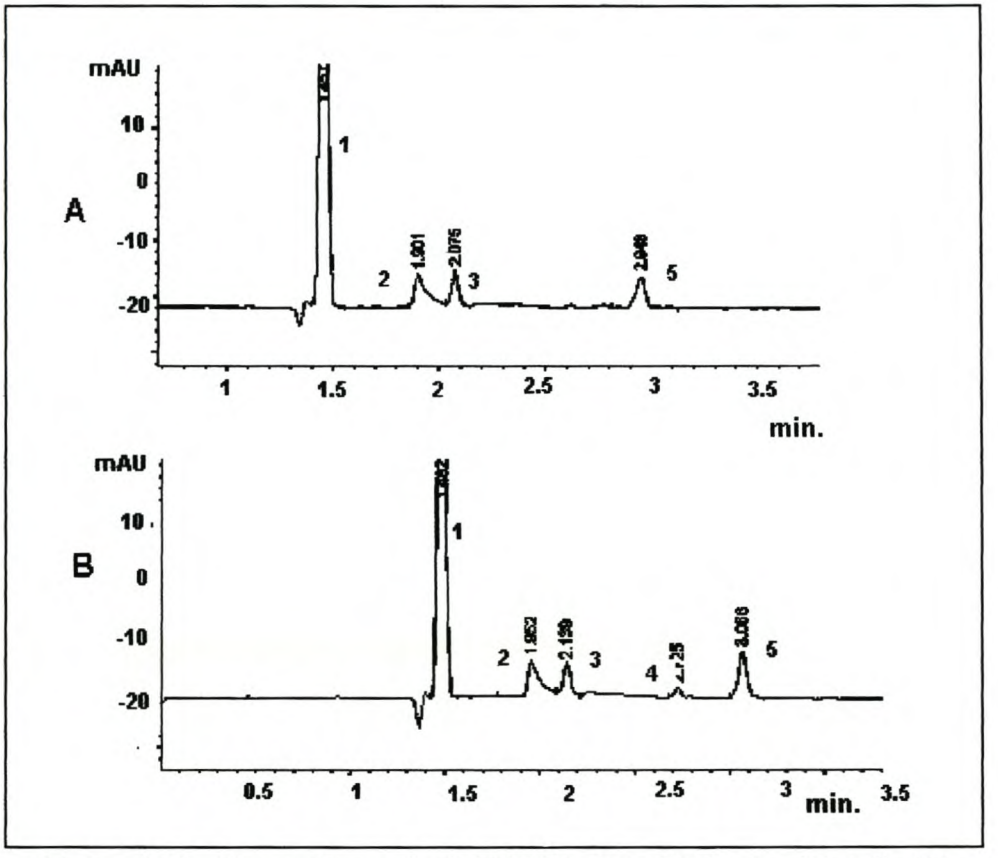

Figure 4.14 Separation of CuEDDM by CZE at pH 3.0 (A) and 11.0 (B), respectively. Conditions: Same as in Figure 4.04. Peaks: 1= $(NO_3)^{2-}$, 2= $[CuEDDM]^{2-}$, 3= $[CuHEDDM]^{-}$, 4 = $[CuOHEDDM]^{3-}$, 5 = Marker

The electropherograms show two peaks at pH 3.0: $[CuEDDM]^{2-}$ and $[CuHEDDM]^{-}$. At pH 11.0 an additional third peak is observed: $[CuOHEDDM]^{3-}$. The mobilities of the metal-EDDM complexes were consistently lower than those of the corresponding metal-

EDTA complexes, indicating that they moved more slowly through the electrolyte (Table 4.10). This was to be expected since, although smaller in size, the metal-EDDM complexes also possess a smaller charge than the metal-EDTA complexes and therefore a smaller charge density.

Complexation of divalent cations with a medium complexing agent leads to a complete separation only when the ligand is used at stiochiometric or high concentrations.

Table 4.10 Obtained mobility values for CuEDDM

	(Effective mobility (μ_e) (cm^2/Vs)			**Migration times (min)**		
pH	**$[CuEDDM]^{2-}$**	**$[CuHEDDM]^-$**	**$[CuOHEDDM]^{3-}$**	**$[CuEDDM]^{2-}$**	**$[CuHEDDM]^-$**	**$[CuOHEDDM]^{3-}$**
2	4.415	3.990		1.864	2.069	
4	4.323	3.989		1.901	2.075	
6	4.322	3.988		1.919	2.083	
8	4.321	3.997		1.926	2.096	
10	4.320	3.915	3.192	1.934	2.113	2.614
12	4.235	3.914		1.952	2.139	

Differences in the effective mobilities of CuEDDM and CuHEDDM were so small that separation of those peaks could not be achieved, as was the case for CuEDDS. This can be seen in the speciation diagram in Figure 4.15, where both peaks are between pH 2-12, while the $[CuOHEDDM]^{3-}$ peak was hardly noticeable since it was only observed at pH 10 with the peak area less than 5 %. For weak chelating agents, solutions containing divalent metal ions are expected to be problematic because of high rates of exchange. Substitution with inert trivalent metal ions such as Cr^{3+} can yield quantifiable CE

electropherograms. Divalent metal ions, which yield lower log K values than trivalent metal ions, are more likely to yield problematic CE analysis[28]. Upon covering the whole pH range and plotting the relative peak areas of the different species of CuEDDM vs. pH, the graph shown in Figure 4.15 was obtained.

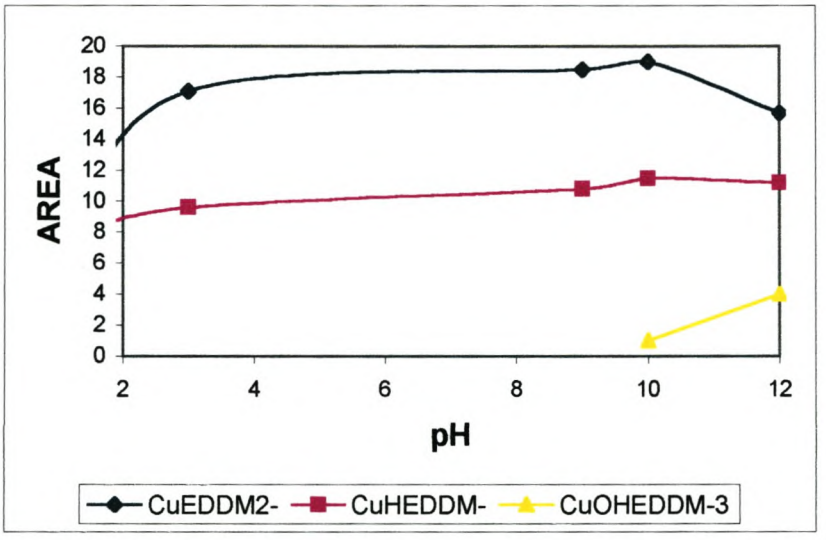

Figure 4.15 Speciation of CuEDDM using CZE. Total metal concentration: 100 ppm, total ligand concentration 8 mM.

A similar approach as to CuEDTA, CuEDDS and CuEDDM was taken in all subsequent determinations. Table 4.11 shows the obtained effective mobility values for PbEDTA.

Table 4.11 Obtained mobility values for PbEDTA

	(Effective mobility) (μ_e) (cm^2/Vs)			Migration times (min.)		
pH	**$[PbEDTA]^{2-}$**	**$[PbHEDTA]^{-}$**	**$[PbOHEDTA]^{3-}$**	**$[PbEDTA]^{2-}$**	**$[PbHEDTA]^{-}$**	**$[PbOHEDTA]^{3-}$**
2		2.804			2.943	
4		2.803			2.965	
6	3.294	2.767		2.512	2.987	
8	3.347			2.487		
10	3.294			2.534		
12	3.097		2.231	2.673		3.718

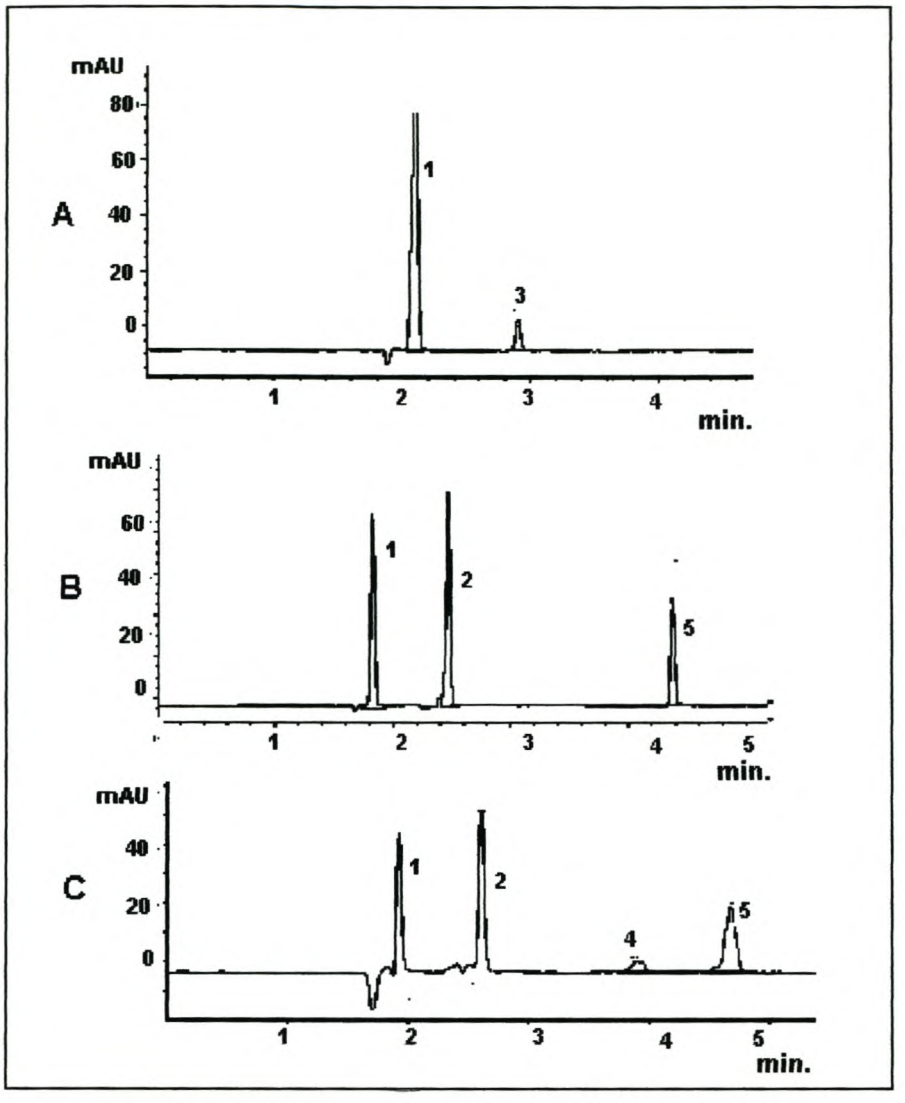

Figure 4.16 Separation of PbEDTA by CZE at pH 3.5 (A), 9.0 (B) and 12.0 (C), respectively. Conditions: Same as in Figure 4.04. Peaks: 1 = $(NO_3)^{2-}$, 2 = $[PbEDTA]^{2-}$, 3 = $[PbHEDTA]^{-}$, 4 = $[PbOHEDTA]^{3-}$, 5 = Marker

Figure 4.16 represent electropherograms of PbEDTA at pH values 3.5, 9.0 and 12.0. At pH 9.0 only $[PbEDTA]^{2-}$ is observed, at pH 12.0 PbEDTA is present in two forms: $[PbOHEDTA]^{3-}$ and $[PbEDTA]^{2-}$ and at pH 3.5 only the $[PbHEDTA]^{-}$ peak is observed. Upon covering the whole pH range and plotting the relative peak areas of the different species vs. pH, the graph shown in Figure 4.17 was obtained.

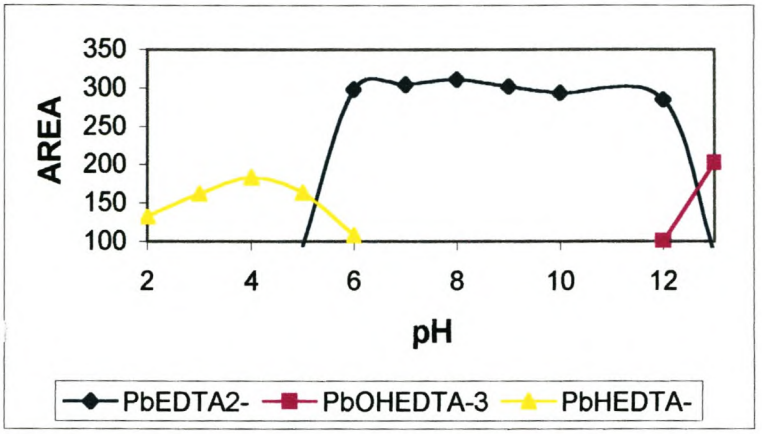

Figure 4.17 Speciation of PbEDTA using CZE. Total metal concentration: 100 ppm, total ligand concentration 8 mM.

The speciation graph in Figure 4.17 shows that $[PbHEDTA]^-$ exists within the pH range 2-6, $[PbEDTA]^{2-}$ within the pH range 2-12 and $[PbOHEDTA]^{3-}$ above pH 12. At the concentration at which the analytical determination was done, the distribution diagram shows that PbEDTA could be speciated by this method.

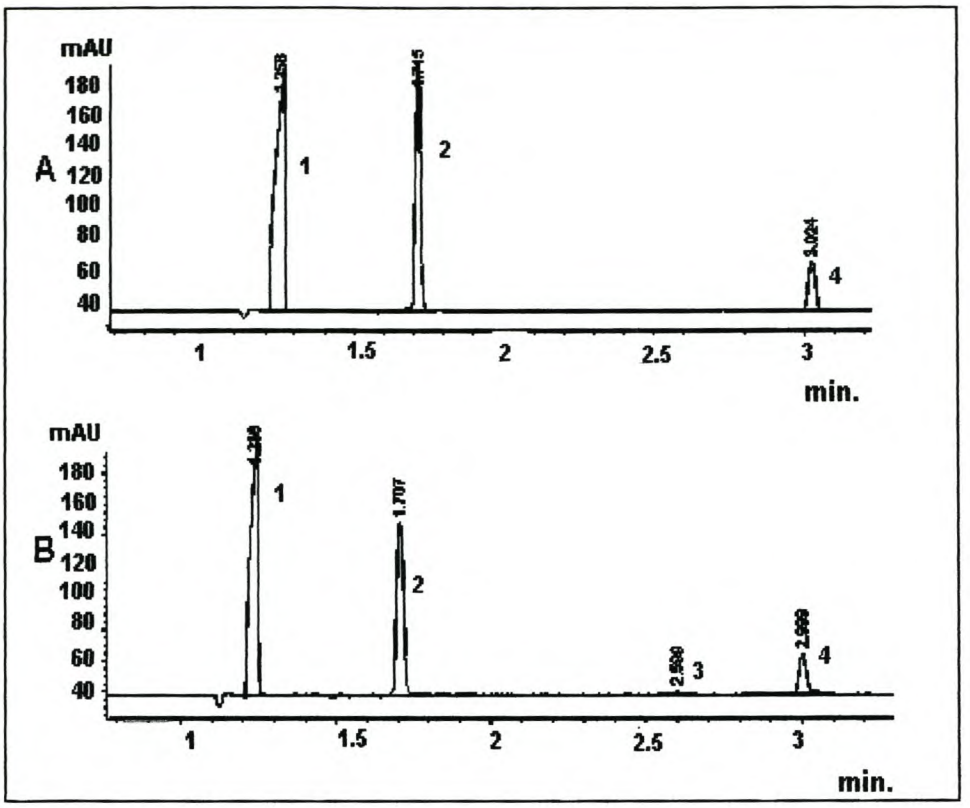

Figure 4.18 Separation of PbEDDS by CZE at pH 8.0 (A) and 12.0 (B). Conditions: Same as in Figure 4.04. Peaks: 1 = $(NO_3)^{2-}$, 2 = $[PbEDDS]^{2-}$, 3 = $[PbOHEDDS]^{3-}$, 4 = Marker

Figure 4.18 represents an electropherogram of PbEDDS at pH values 8.0 and 12.0. At pH 12.0 PbEDDS is present in two forms: $[PbOHEDDS]^{3-}$ and $[PbEDDS]^{2-}$. At pH 6.0 only $[PbEDDS]^{2-}$ is observed. These results are in good agreement with the speciation graph in Figure 3.09. Upon covering the whole pH range and plotting the relative peak areas of the different species vs. pH, the graph shown in Figure 4.19 was obtained. At pH 12.0 PbEDDS forms mainly $[PbEDDS]^{2-}$, hence the peak has a large area compared to the $[PbOHEDDS]^{3-}$ peak. The obtained mobility values are listed in table 4.12. The marker shifts in accordance with the direction as predicted in figure 4.03. This is because

as the pH decreases the EOF slows down, hence the migration time of the peaks is observed later.

Table 4.12 Obtained mobility values for PbEDDS

	Effective μ_e (cm^2/Vs)		Migration times (min.)	
pH	**$[PbEDDS]^{2-}$**	**$[PbOHEDDS]^{3-}$**	**$[PbEDDS]^{2-}$**	**$[PbOHEDDS]^{3-}$**
2	4.940		1.683	
4	4.939		1.695	
6	4.826		1.701	
8	4,825	3.517	1.704	2.379
10	4.824	3.347	1.708	2.480
12	4.823	3.192	1.715	2.599

The species distribution graph in Figure 4.19 shows that $[PbEDDS]^{2-}$ exists above pH 2 and $[PbOHEDDS]^{3-}$ above pH 8.

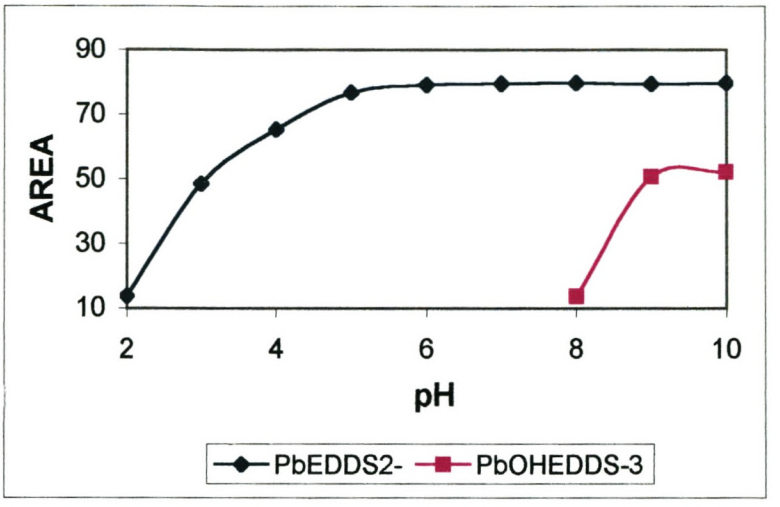

Figure 4.19 Speciation of PbEDDS using CZE. Total metal concentration: 100 ppm, total ligand concentration 1 mM

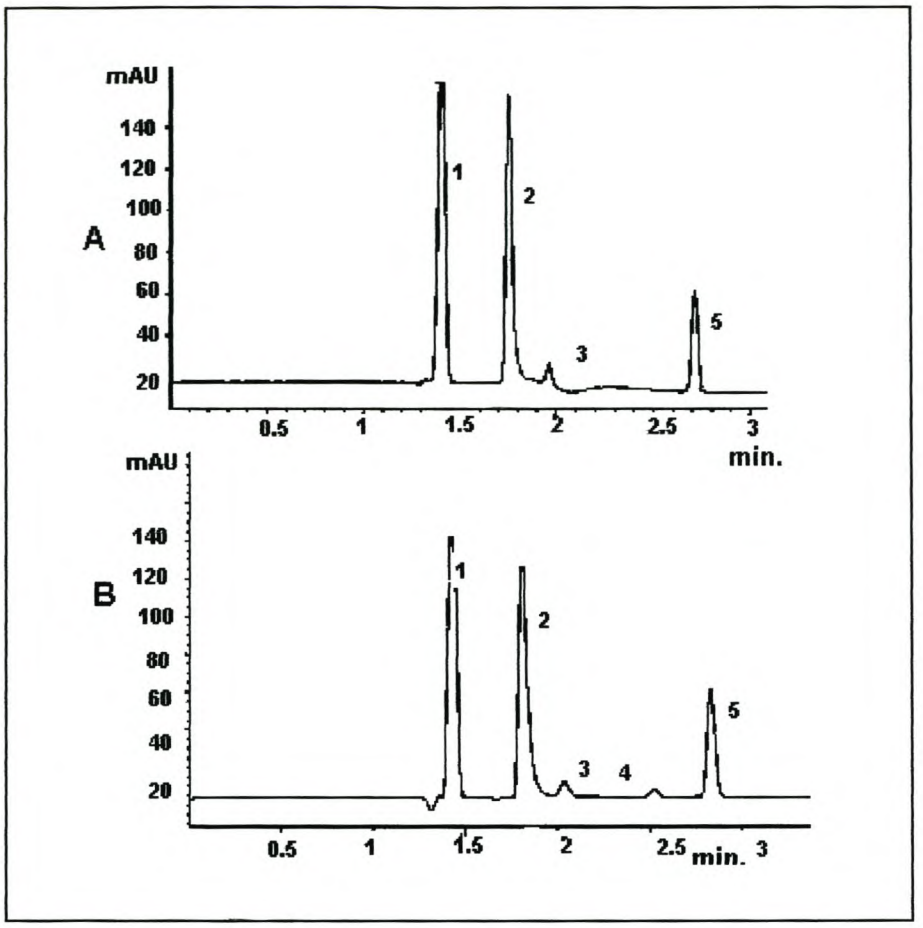

Figure 4.20 Separation of PbEDDM by CZE at pH 5.0 (A) and 12.0 (B). Conditions: Same as in Figure 4.04. Peaks: 1 = $(NO_3)^{2-}$, 2 = $[PbEDDM]^{2-}$, 3 = $[PbHEDDM]^{-}$, 4 = $[PbOHEDDM]^{3-}$, 5 = Marker

Figure 4.20 shows the electropherogram of PbEDDM at pH values 5.0 and 12.0. At pH 5.0 PbEDDM is present as $[PbEDDM]^{2-}$ and $[PbHEDDM]^{-}$. At pH 12.0 the $[PbOHEDDM]^{3-}$, peak is also observed. PbEDDM forms a weak complex (*i.e.* K value is 11.1), hence it behaves like CuEDDM, such that the complex peak PbEDDM and the protonation peak PbHEDDM are inseparable. Table 4.12 shows the obtained mobilities.

Table 4.13 Obtained mobility values for PbEDDM

	Effective mobility μ_a) (cm^2/Vs)			Migration times (min.)		
pH	**$[PbEDDM]^{2-}$**	**$[PbHEDDM]^-$**	**$[PbOHEDDM]^{3-}$**	**$[PbEDDM]^{2-}$**	**$[PbHEDDM]^-$**	**$[PbOHEDDM]^{3-}$**
4	5.061	4.511		1.653	1.850	
6	4.940	4.415		1.694	1.872	
8	4.825	4.414		1.702	1.894	
10	4.716	3.773	3.402	1.745	2.215	2.432
12	4.611	3.705	3.347	1.783	2.236	2.496

Upon covering the whole pH range and plotting the relative peak areas of the different species vs. pH, the graph shown in Figure 4.21 was obtained.

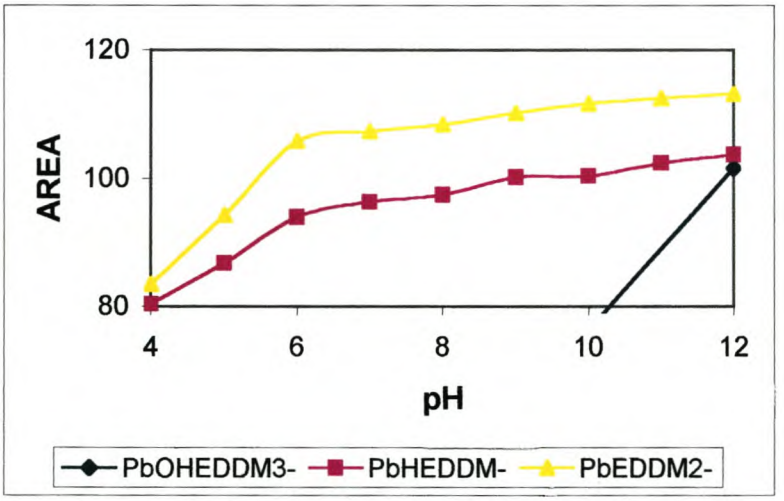

Figure 4.21 Speciation of PbEDDM using CZE. Total metal concentration: 100 ppm, total ligand concentration 8 mM

The species distribution graph in Figure 4.21 shows that both $[PbHEDDM]^-$ and $[PbEDDM]^{2-}$ exists within the pH range 4-12 and $[PbOHEDDM]^{3-}$ within the pH range 10-12.

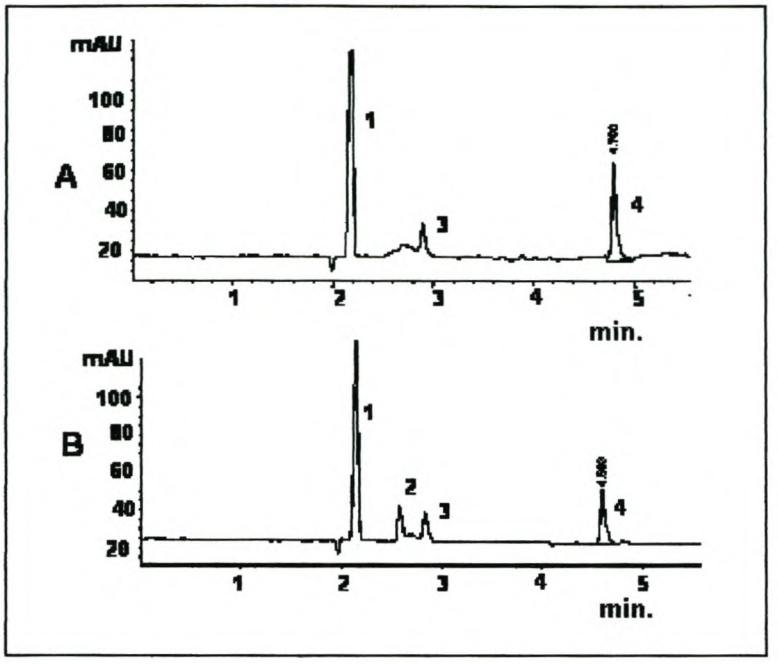

Figure 4.22 Separation of CdEDTA by CZE at pH 3.0 (A) and 10.0 (B), respectively. Conditions: Same as in Figure 4.04. Peaks: 1 = $(NO_3)^{2-}$, 2 = $[CdEDTA]^{2-}$, 3 = $[CdHEDTA]^-$, 4 = Marker

Figure 4.22 represents an electropherogram of CdEDTA at pH 3.0 and 10.0. At pH 10.0 CdEDTA is present in two forms: $[CdHEDTA]^-$ and $[CdEDTA]^{2-}$. When the pH is reduced to 3.0 the $[CdEDTA]^{2-}$ starts disappearing and only the $[CdHEDTA]^-$ peak is observed. The hydroxy peak is not observed in the pH range 2-12. This is confirmed by the speciation data of CdEDTA in Figure 3.07. As the stability of the metal ligand (M-L) complexes decreases, so does the ability of CE to yield quantifiable peaks[25]. Table 4.14 shows the obtained mobility values.

Table 4.14 Obtained mobility values for CdEDTA

	Effective mobility (μ_e) (cm^2/Vs)		Migration times (min)	
pH	**$[CdEDTA]^{2-}$**	**$[CdHEDTA]^-$**	**$[CdEDTA]^{2-}$**	**$[CdHEDTA]^-$**
2		2.964		2.810
4		2.923		2.842
6	3.192	2.922	2.613	2.853
8	3.191	2.882	2.618	2.875
10	3.144	2.881	2.624	2.893

Upon covering the whole pH range and plotting the relative peak areas of the different species vs. pH, the graph shown in Figure 4.23 was obtained.

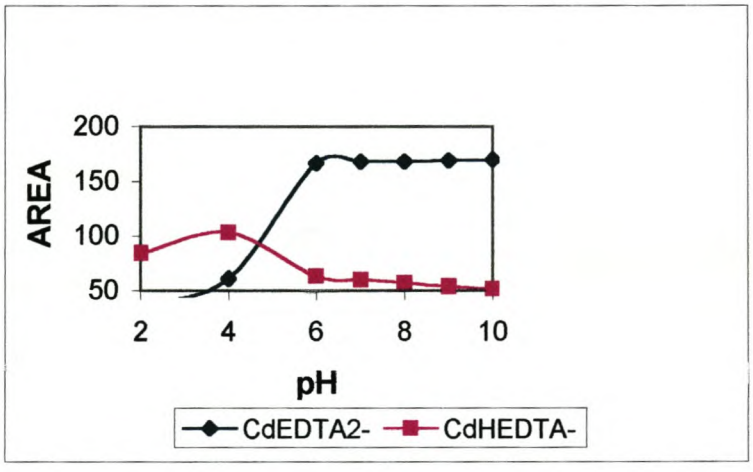

Figure 4.23 Speciation of CdEDTA using CZE. Total metal concentration 100 ppm, total ligand concentration 8mM.

The speciation diagram in Figure 4.23 shows that $[CdHEDTA]^-$ exists within the pH range 2-6 and $[CdEDTA]^{2-}$ above pH 4.

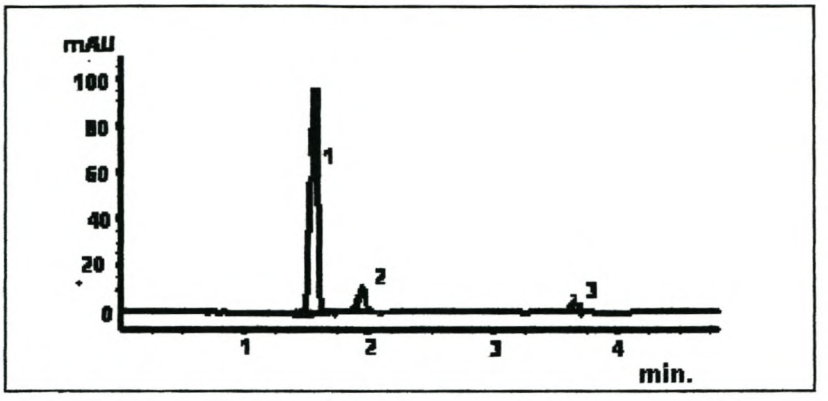

Figure 4.24 Separation of CdEDDS by CZE at pH 8.0. Conditions: Same as in Figure 4.04. Peaks: 1 = $(NO_3)^{2-}$, 2 = $[CdEDDS]^{2-}$, 3 = Marker

Figure 4.24 represents an electropherogram of CdEDDS at pH 8.0. At this pH only $[CdEDDS]^{2-}$ is observed, and until pH < 2, These results were evaluated with the speciation graph of CdEDDS (Figure 3.10), where no other peak was observed between pH 2 and 10 except for the $[CdEDDS]^{2-}$ peak and the Cd^{2+}, which is not observed because of the direction of the EOF. Upon covering the whole pH range and plotting the relative peak areas of the different species vs. pH, the graph shown in figure 4.25 was obtained.

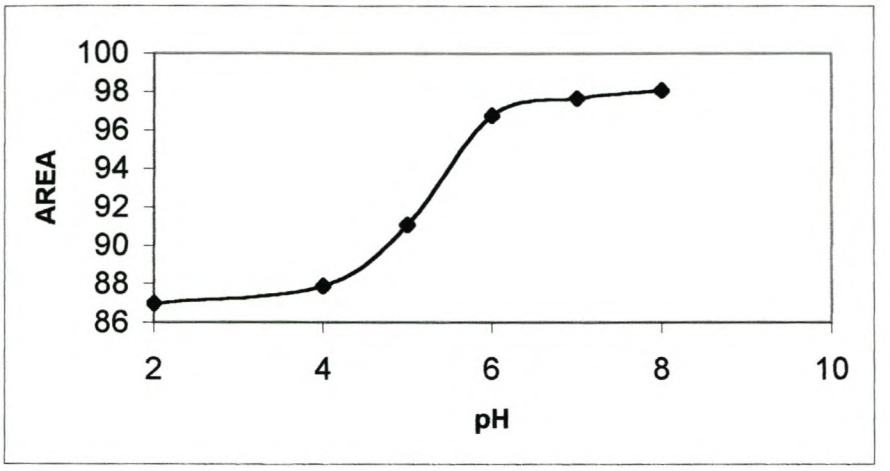

Figure 4.25 Speciation of CdEDDS using CZE. Total metal concentration: 100 ppm, Total ligand concentration 0.1M, Temperature 25°C

The speciation diagram in Figure 4.25 shows that $[CdEDDS]^{2-}$ exists above pH 4.

The same results were obtained for CdEDDM as for CdEDDS. The obtained electropherograms and speciation diagrams are shown in Figures 4.27 and 4.28. Table 4.15 and 4.16 show the obtained mobilities for CdEDDS and CdEDDM, respectively.

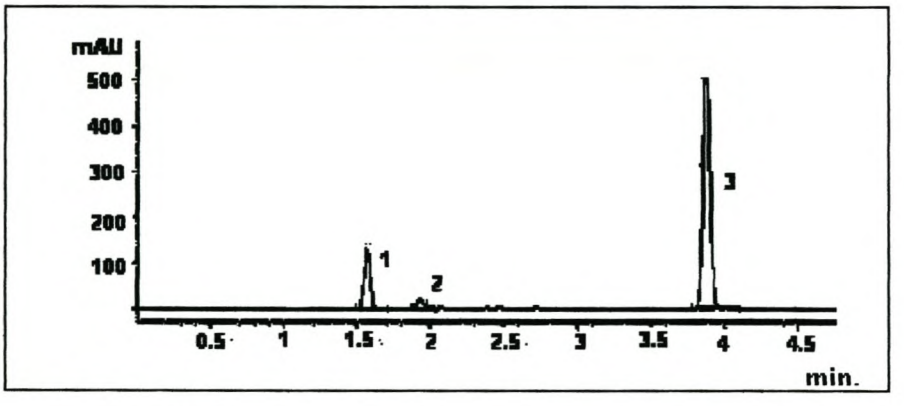

Figure 4.26 Separation of CdEDDM by CZE at pH 9.0. Conditions: Same as in Figure 4.05. Peaks: 1= $(NO_3)^{2-}$, 2= $[CdEDDM]^{2-}$, 3 = Marker

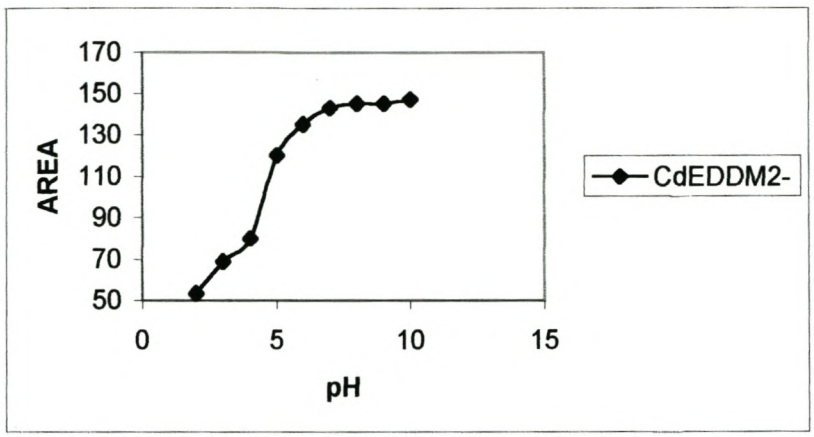

Figure 4.27 Speciation of CdEDDM using CZE. Total metal concentration: 100 ppm, Total ligand concentration 0.1M, Temperature 25°C

Table 4.15 Obtained mobility values for CdEDDS

	Effective mobility (μ_e) (cm^2/Vs)	**Migration times (min.)**
pH	**$[CdEDDS]^{2-}$**	**$[CdEDDS]^{2-}$**
4	4.235	1.952
6	4.234	1.973
8	4.150	1.994
10	4.069	2.036

Table 4.16 Obtained mobility values for CdEDDM

	Effective mobility (μe) (cm^2/Vs)	**Migration times (min.)**
pH	**$[CdEDDM]^{2-}$**	**$[CdEDDM]^{2-}$**
4	4.235	1.952
6	4.234	1.973
8	4.150	1.994
10	4.069	2.036

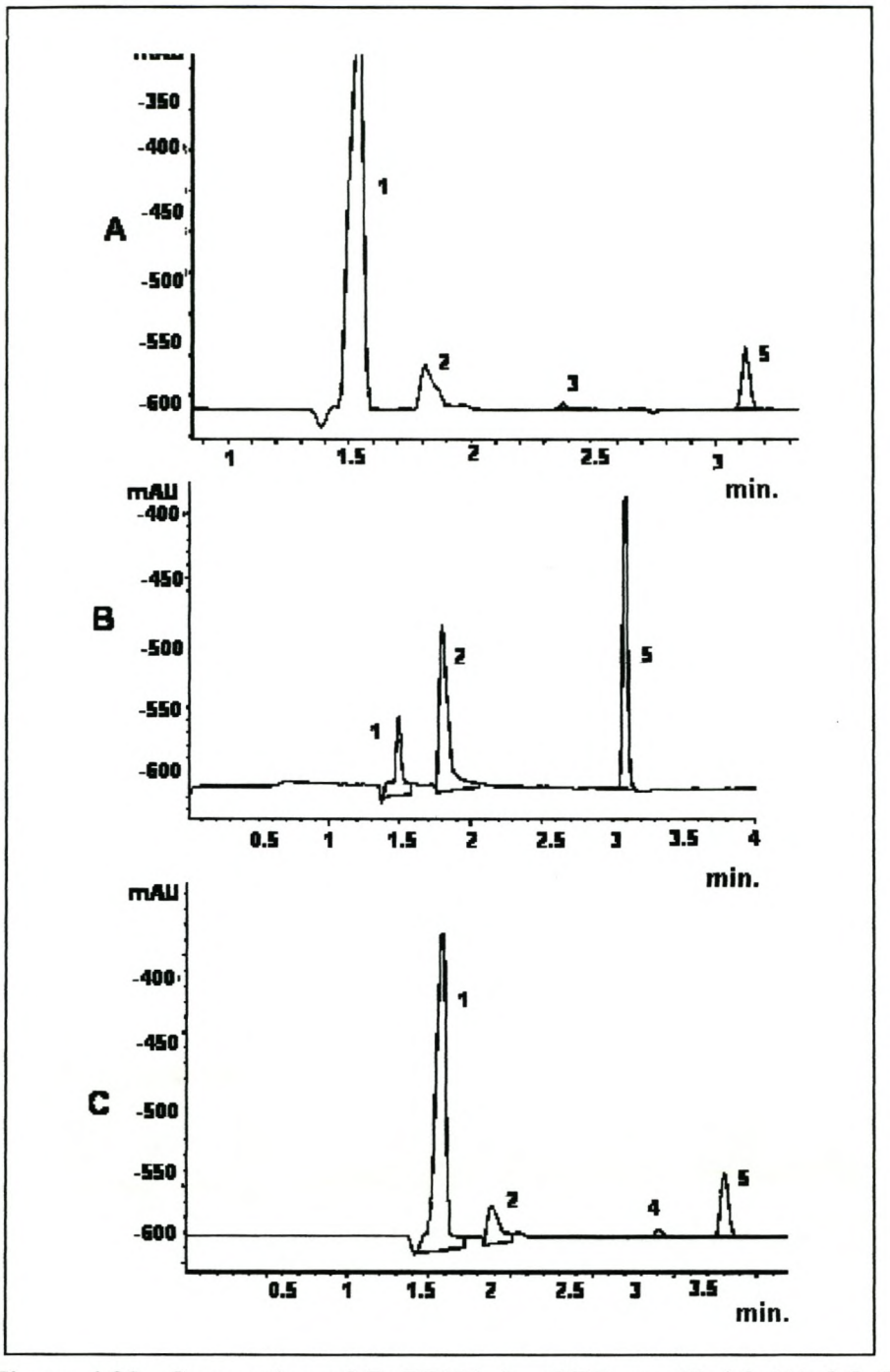

Figure 4.28 Separation of ZnEDTA by CZE at pH 4.0 (A) 9.0 (B) and 12.0 (C), respectively. Conditions: Same as in Figure 4.04. Peaks: 1 = $(NO_3)^{2-}$, 2 = $[ZnEDTA]^{2-}$, 3 = $[ZnHEDTA]^{-}$, 4 = $[ZnOHEDTA]^{3-}$, 5 = Marker

Figure 4.28 represents an electropherogram of ZnEDTA at pH values 4.0, 9.0 and 12.0. At pH 9.0 only $[ZnEDTA]^{2-}$ is observed, *i.e.* it is nearly 100% complexed, while at pH 4.0, $[ZnHEDTA]^{-}$ and $[ZnEDTA]^{2-}$ are observed and at pH 12.0 ZnEDTA is present in two forms: $[ZnOHEDTA]^{3-}$ and $[ZnEDTA]^{2-}$. Table 4.17 shows the obtained mobility values.

Table 4.17 Obtained mobility values for ZnEDTA

	Effective μ_e (cm^2/Vs)			**Migration times (min.)**		
pH	**$[ZnEDTA]^{2-}$**	**$[ZnHEDTA]^{-}$**	**$[ZnOHEDTA]^{3-}$**	**$[ZnEDTA]^{2-}$**	**$[ZnHEDTA]^{-}$**	**$[ZnOHEDTA]^{3-}$**
2	5.061	3.843		1.650	2.153	
4	4.940	3.517		1.683	2.375	
6	4.826	3.458		1.706	2.397	
8	4.825			1.736		
10	4.611		2.882	1.794		2.867
12	4.415		2.842	1.879		2.908

Upon covering the whole pH range and plotting the relative peak areas of the different species vs. pH, the graph shown in Figure 4.29 was obtained.

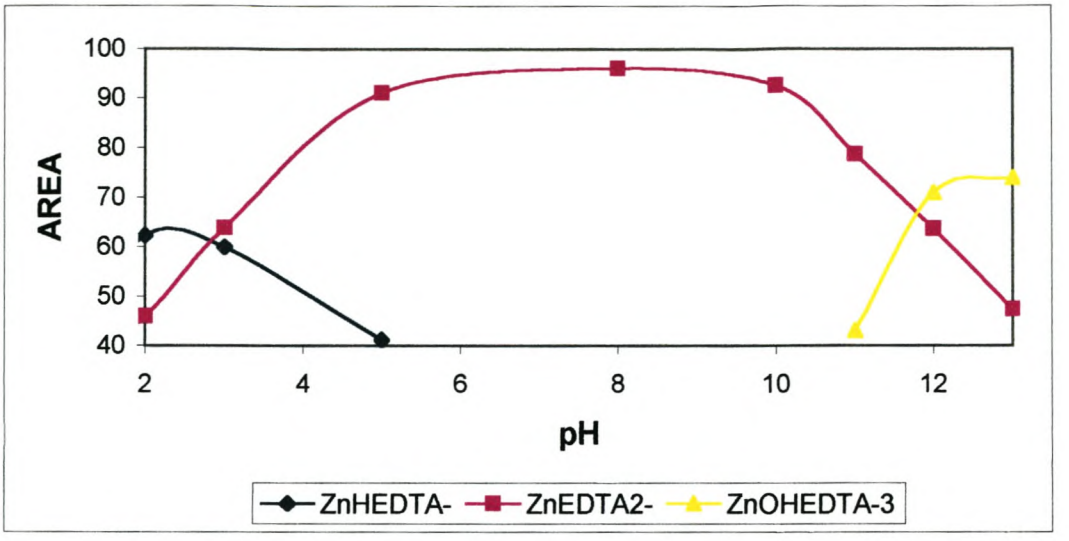

Figure 4.29 Speciation of ZnEDTA using CZE. Total metal concentration: 100 ppm, total ligand concentration 8mM.

The speciation graph shows that $[ZnHEDTA]^-$ exists within the pH range 2-6, $[ZnEDTA]^{2-}$ within the pH range 4-12 and $[ZnOHEDTA]^{3-}$ within the pH range 11-12.

For ZnEDDS and ZnEDDM, the same results were obtained as for CdEDDS and CdEDDM. The obtained electropherograms and distribution species-pH diagrams are shown in Figures 4.30 and 4.31 for ZnEDDS and figure 4.32 and 4.33 for ZnEDDM. The obtained effective mobilities are tabulated in table 4.18.

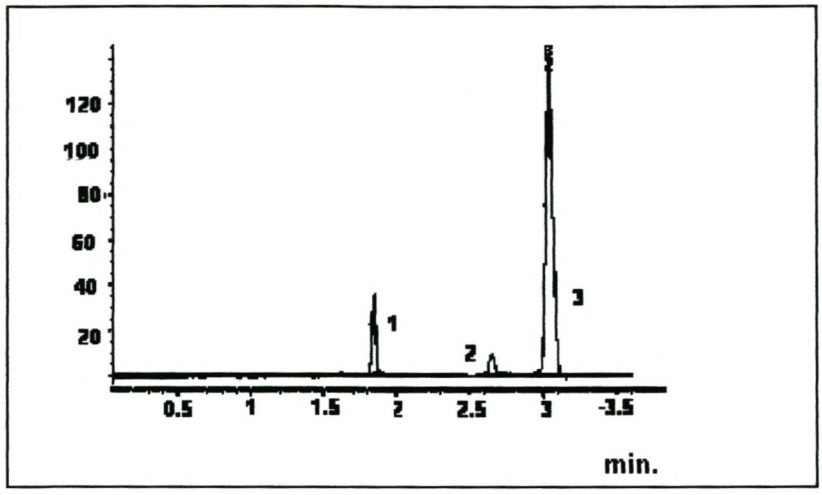

Figure 4.30 Separation of ZnEDDS by CZE at pH 8.0. Conditions: Same as in Figure 4.04. Peaks: 1= $(NO_3)^{2-}$, 2= $[ZnEDDS]^{2-}$, 3= Marker

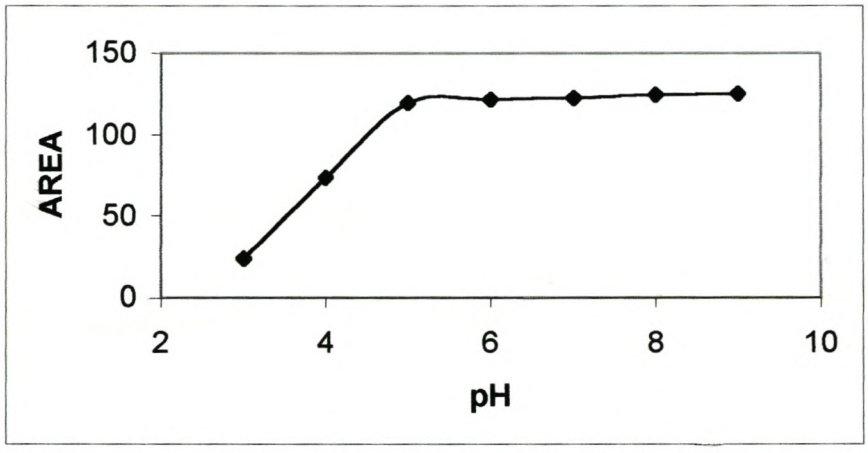

Figure 4.31 Speciation of ZnEDDS using CZE. Total metal concentration: 100 ppm, Total ligand concentration 0.1M, Temperature 25°C

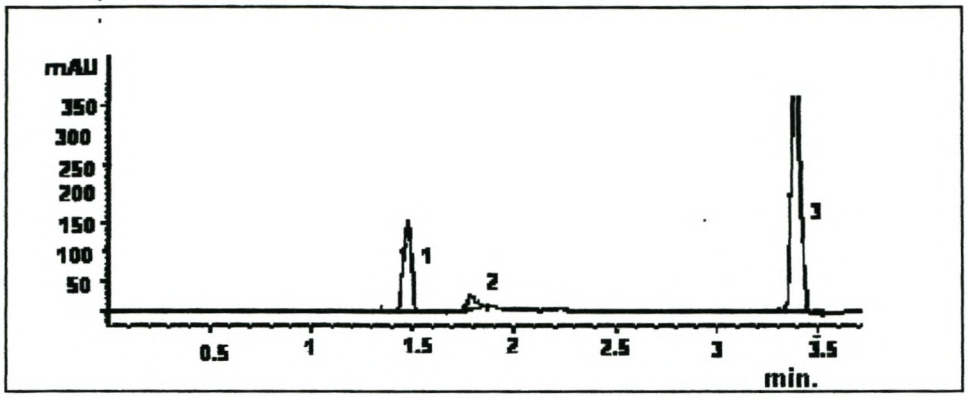

Figure 4.32 Separation of ZnEDDM by CZE at pH 8.0. Conditions: Same as in Figure 4.04. Peaks: 1= $(NO_3)^{2-}$, 2= $[ZnEDDM]^{2-}$, 3= Marker

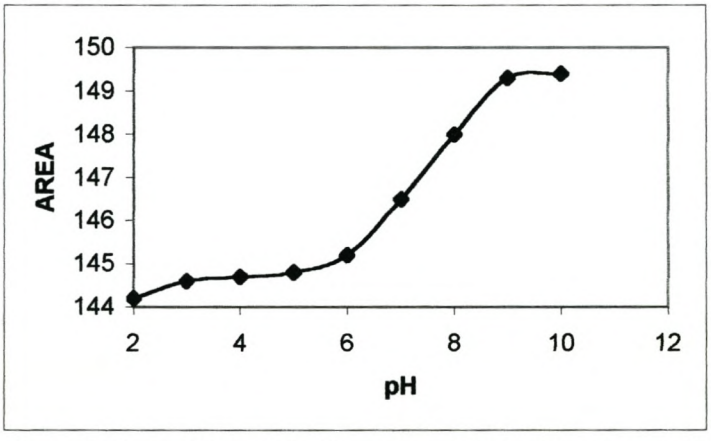

Figure 4.33 Speciation of ZnEDDM using CZE. Total metal concentration: 100 ppm, Total ligand concentration 0.1M, Temperature 25°C

Table 4.18 Obtained mobility values for ZnEDDS and ZnEDDM

	Effective μ_e (cm^2/Vs)	Migration times (min)	Effective μ_e (cm^2/Vs)	Migration times (min)
pH	**$[ZnEDDS]^{2-}$**	**$[ZnEDDS]^{2-}$**	**$[ZnEDDM]^{2-}$**	**$[ZnEDDM]^{2-}$**
2	3.051	2.732	4.511	1.842
4	3.050	2.738	4.510	1.847
6	3.007	2.744	4.509	1.851
8	3.006	2.749	4.414	1.873
10	3.005	2.754	4.413	1.892
12	3.004	2.761	4.323	1.917

4.5.6 Speciation of trivalent metal ions (Fe and Cr) with EDTA

Strong complexing agents form stable metal complexes when complexed with divalent metals but, in the case of transition metals, anionic complexes with similar charge are formed, therefore the separation selectivity is very poor[29].

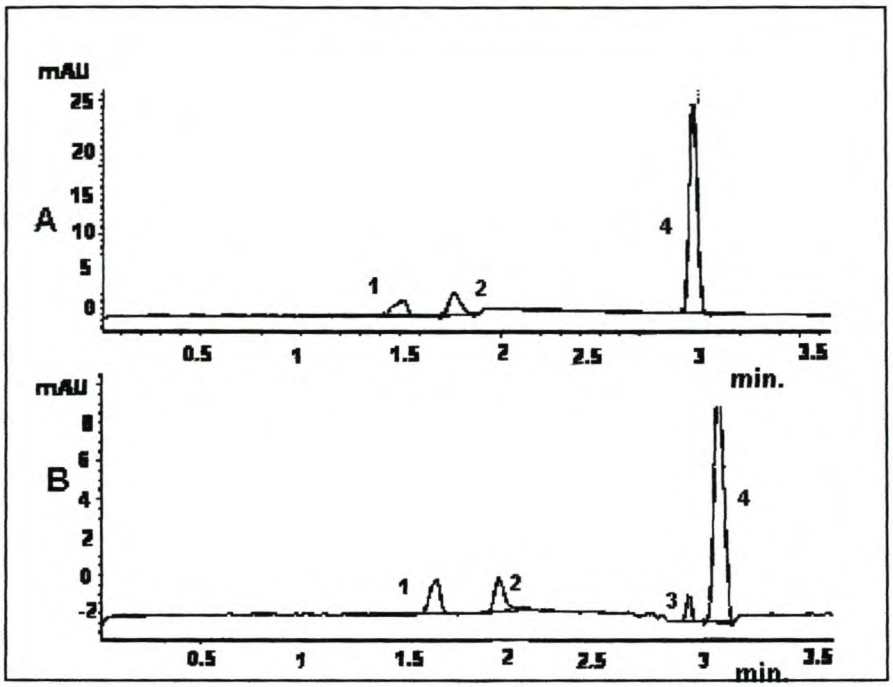

Figure 4.34 Separation of FeEDTA by CZE at pH 12.0 (A) and 5.0 (B), respectively. Conditions: Same as in Figure 4.04. Peaks: 1 = $[FeEDTA]^-$, 2 = FeHEDTA, 3 = $[FeOHEDTA]^{2-}$, 4 = Marker

Figure 4.34 represent electropherograms of FeEDTA at pH values 5.0 and 12.0. At pH 5.0 FeEDTA is present in two forms: FeHEDTA and $[FeEDTA]^-$. At pH 12.5 $[FeOHEDTA]^{2-}$, FeHEDTA and $[FeEDTA]^-$ are observed. The formation of metal HEDTA complexes under basic conditions allowed the detection of trivalent metal complexes under CE conditions because the ionization of the hydroxy group of HEDTA gave complexes a net negative charge. It has been shown that under basic conditions the ethanolic proton of the hydroxy group of HEDTA takes part in bond formation with metals that form hexadentate structures[18]. The migration behavior of the complexes generally follow the charge number and the mass of the complexes. In addition, equivalent ionic conductance of metal ions is suggested to affect the migration behavior

with metal complex ions that have higher equivalent ionic conductance migrating faster. The same is valid for the CrEDTA complex. The obtained effective mobilities for FeEDTA are listed in table 4.19.

Table 4.19 Obtained mobility values for FeEDTA

	Effective mobility (μ_e) (cm^2/Vs)			**Migration times (min.)**		
pH	**$[FeEDTA]^-$**	**FeHEDTA**	**$[FeOHEDTA]^{2-}$**	**$[FeEDTA]^-$**	**FeHEDTA**	**$[FeOHEDTA]^{2-}$**
2	5.929	4.611		1.403	1.792	
4	5.764	4.502		1.452	1.834	
6	5.608	4.415		1.469	1.867	
8	5.607	4.414		1.498	1.893	
10	5.461	4.323	2.804	1.534	1.926	2.943
12	4.940	4.069	2.803	1.679	2.039	2.976

Upon covering the whole pH range and plotting the relative peak areas of the different species vs. pH, the graph shown in Figure 4.34 was obtained.

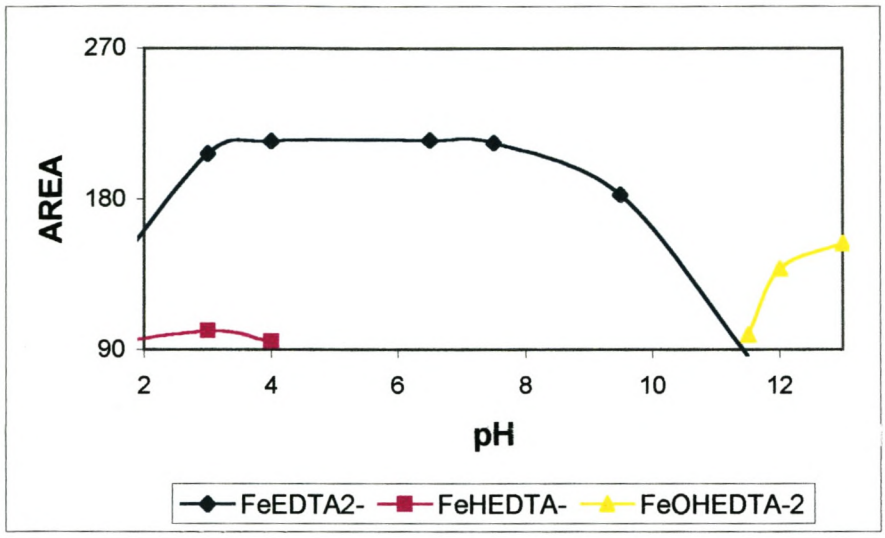

Figure 4.35 Speciation of FeEDTA using CZE. Total metal concentration: 100 ppm, total ligand concentration 8 mM.

The speciation graph shows that FeHEDTA exists within the pH range 2-4, $[FeEDTA]^-$ within the pH range 2-12 and $[FeOHEDTA]^{2-}$, above pH. FeEDTA exists only as hydroxy species when the pH exceeds 12.

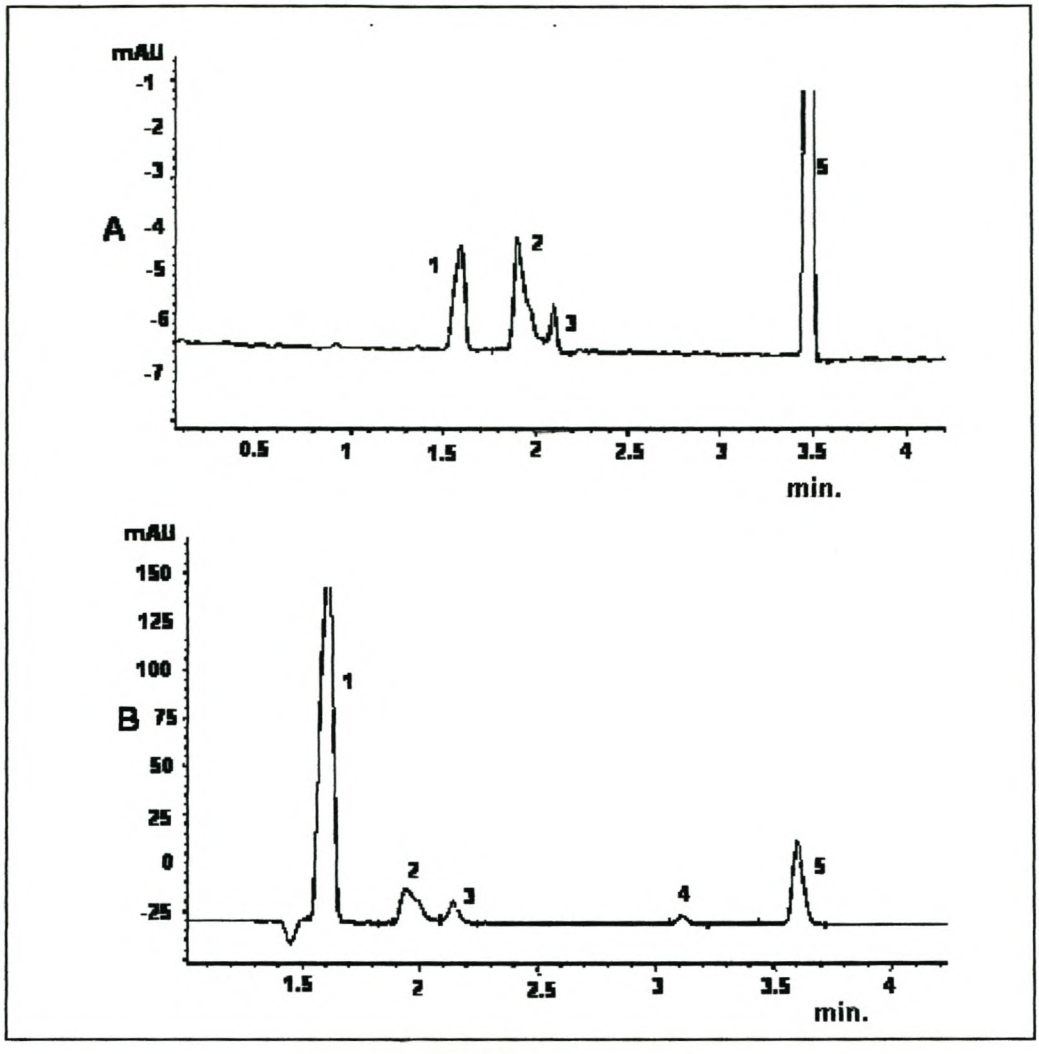

Figure 4.36 Separation of CrEDTA by CZE at pH 4.0 (A) and 12.0 (B). Conditions: Same as in Figure 4.04. Peaks: 1 = $(NO_3)^{2-}$, 2 = $[CrEDTA]^-$, 3 = CrHEDTA, 4 = $[CrOHEDTA]^{2-}$, 5 = Marker

Figure 4.36 represent electropherograms of CrEDTA by CZE at pH 4.0 (A) and 12.0 (B). At pH 4.0 CrEDTA is present in two forms: CrHEDTA and $[CrEDTA]^-$. At pH 12.0 $[CrOHEDTA]^{2-}$, CrHEDTA and $[CrEDTA]^-$ are observed. The obtained effective mobilities are listed in table 4.20.

Table 4.20 Obtained mobility values for CrEDTA

	μ_{EOF} (cm^2/Vs)			Migration times		
pH	**$[CrEDTA]^-$**	**CrHEDTA**	**$[CrOHEDTA]^{2-}$**	**$[CrEDTA]^-$**	**CrHEDTA**	**$[CrOHEDTA]^{2-}$**
2	4.415	4.150		1.894	1.986	
4	4.323	3.990		1.903	2.099	
6	4.322	3.915		1.914	2.114	
8	4.321	3.914	2.842	1.923	2.127	2.904
10	4.320	3.913	2.695	1.930	2.138	3.096
12	4.319	3.843	2.694	1.938	2.142	3.108

Upon covering the whole pH range and plotting the relative peak areas of the different species vs. pH, the graph shown in figure 4.37 was obtained.

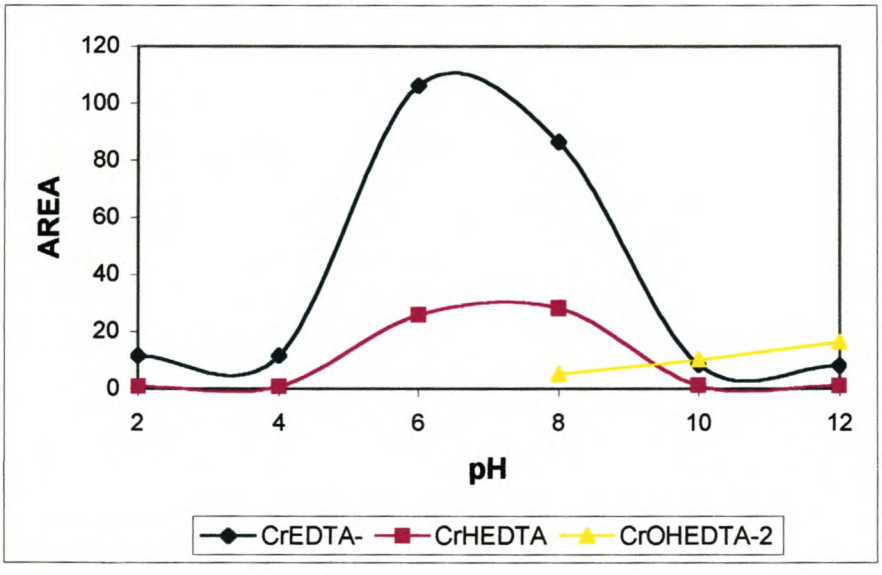

Figure 4.37 Speciation of CrEDTA using CZE. Total metal concentration: 100 ppm, Total ligand concentration 8 mM.

3.7 Conclusions

The results of this study have shown that it is possible to speciate the relatively inert ligand EDTA by making use of CE in the CZE mode. EDTA, being an environmentally important ligand could be detected in its various ionic forms at a specified pH. The CE results closely follows the modelled speciation curves, using accepted speciation models. The biodegradable analogues of EDTA *i.e.* EDDS and EDDM have shown to be equally useful. The method of slowing down the EOF to speciate these ligands by CE has been demonstrated. The speciation distribution curves for both EDDS and EDDM closely follow the predicted model for these two ligands. In all cases, the separation could be effected within 6 minutes.

For all the metal ligand complexes separated in this work using the borate electrophoretic buffer, the following chelate-forming reactions with metal cations M^{n+} can be written for different pH conditions:

At pH 2.0-4.0

$$MY^{m-} + H^{n+} = M(H)Y^{(m-n)-}$$

At pH 6.0-8.0

$$M^{n+} + H_2Y^{2-} = MY^{n-4} + 2H^+$$

At pH 8.0-12.0

$$MY^{m-} + OH^- = M(OH)Y^{(m+1)-}$$

EDDS has the same complexing groups as the EDTA, but is a smaller molecule and forms faster migrating complexes with higher charge-to-size ratio. EDDM forms higher charged and therefore faster migrating complexes as EDDS and EDTA.

Metal EDDM complexes hydrolysed faster than M-EDTA and M-EDDS complexes and this is due to the fact that the M-EDDM complexes are less stable. Because the EDDM ligand having three functional groups in the metal chelate formation, it is sterically impossible for these groups to coordinate to the metal ion forming two chelate rings.

The effective mobilities of all metal chelates increase with increasing pH. In addition, the pH influence is more significant for M^{3+} than M^{2+} chelates. This corresponds with the stronger tendency of these analytes to form mixed hydroxy complexes.

For Cu complexes of EDDS and EDDM, the effective mobilities of CuEDDS, CuHEDDS, CuEDDM and CuHEDDM are very small compared to CuEDTA and CuHEDTA, hence the separation was not achieved.

Also since the borate buffer was neutralized with NaOH, the ionic strength of the buffer increased which resulted in a decreased μ_{EOF} and the electrophoretic mobilities of the analytes. Whereas when the complexes were investigated in acidic medium at pH 2.0-6.0, the peaks for most analytes became broader and the migration times were longer. Also common anions such as nitrate did not interfere directly with the detection of the amino carboxylic acids studies here or with their metal complexes, since their charge density was much larger and these anions therefore eluted more rapidly.

From the electropherogram results it was shown that:

- The migration time t decreased as the pH was decreased.
- The results agree favourably with the speciation data.
- The effective mobilities of the complexes decreased with an increase in ionic strength.
- The complexes followed the same trend as they eluted according to the charge ratio.

CZE was demonstrated to be an attractive method for speciation validation because of the following advantages:

- CE provides efficient separations with high resolution and can have excellent detection limits for small sample sizes.
- Separation was achieved within short analysis time.
- Low operation cost.
- Small solvent consumption.

References

1. Skoog D. A., Holler F. J., Nieman T. A., *Principles of Instrumental Analysis*, Saunders College Publishing, United States of America, 1998.
2. Heiger D. N., *High Performance Capillary Electrophoresis – An Introduction*, Hewlett Packard Company, France, 1992.
3. Liu Y., Pietrzyk D. J., *Journal of Chromatography A*, 1998, **804**, 337.
4. Landers J. P., *Handbook of Capillary Electrophoresis*, CRC Press, Baton Raton, FL, 2nd ed., 1996.
5. Padarauskas A., Olsauskaite V., Schwedt G., *Journal of Chromatography A*, 1998, **800**, 369.
6. Lauer H.H., Ooms J.B., *Analytica Chimica Acta*, 1991, **250,** 45.
7. Jorgenson J. W., Lukacs K. D., *Science*, 1983, **222**, 266.
8. Terabe S., Otsuka K., Ichikawa K., Tsuchiya A., Ando T., *Analytical Chemistry*, 1984,**56**, 113.
9. Kuhr W. G., *Analytical Chemistry*, 1990, **62,** 403.
10. Cohen A. S., Kerger B. L., *Journal of Chromatography*, 1987, **397**,409.
11. Cohen A. S., Najarian D. R., Paulus A., Guttman A., Smith J.A., Karger B. L., *Proceedings of the National Academy of Sciences.*, USA, 1988, **85**, 9660.
12. Worthy W., *Chemical Engineering News*, September 1990, 21.
13. Heiger D. N., Cohen A. S., Karger B. L., *Journal of Chromatography*, 1990, **516,** 33.
14. Hjerten S., *Journal of Chromatography* , 1985, **347**, 191.
15. O'Farrell P. H., *Journal of Biological Chemistry*, 1975, **250**, 4007.

16. Giannazza E., Astrua-Testori S., Giacon P., Righetti P. G., *Electrophoresis*, 1985, **6**, 332.

17. Sudor J., Novotny M. V., *Chem. Listy*, 1998, **92**, 1020.

18. Okemgbo A. A., Hill H. H., Metcalf S. G., Bachelor M., *Analytica Chimica Acta*, 1999, **396**, 105.

19. Pacakova V., Coufal P., Stulik K., *Journal of Chromatography A*, 1999, **834**, 257.

20. Huang X., Gordon M. J., Zare R. N., *Analytical Chemistry*, 1988, **60**, 375.

21. Gottlicher B., Bachmann K., *Journal of Chromatography A*, 1997, **780**, 63.

22. Jen J-F., Wu M-H, Yang T. C., *Analytica Chimica Acta*, 1997, **239,** 251.

23. Li S. F.Y., and Wang T., *Journal of Chromatography A*, 1995, **707**, 343.

24. Burgiser C. S., Stone A. T., *Environmental Science and Technology*, 1997, **31**, 2656.

25. Martell A. E., Hancock R. D., *Chemistry Reviews*, 1989, 89, 1875.

26. Crouch A. M., Polhuis M., *Journal of Molecular Structure*, 2000, **530**, 171.

27. Padarauskas A., Schwedt G., *Journal of Chromatography A*, 1997, **773**, 351.

28. Pozdniakova S., Padarauskas A., Schwedt G., *Analytica Chimica Acta*, 1997, **351,** 41.

29. Baraj B., Martinez M., Sastre A., Aguila M., *Journal of Chromatography A*, 1995, **695**, 103.

CHAPTER 5

AMPEROMETRIC DETECTION SYSTEM FOR CAPILLARY ELECTROPHORESIS

5.1 Introduction

Detection in capillary electrophoresis (CE) is a significant challenge as a result of the small dimensions of the capillary. Although CE requires only nanoliter volumes of sample it is not a "trace" analysis technique, since relatively concentrated analyte solutions or pre-concentration are often necessary. A number of detection methods have been used in CE, such as UV, fluorescence, *etc.* As in HPLC, UV-Visible detection is by far the most common detection method[1].

Table 5.01 contains a list of many of the detection methods investigated, along with their detection limits, their advantages and disadvantages. It has been reported that the concentration detection limits achieved with the commonly used UV absorbance detection are often too high for the typical demands of practical applications[2].

The UV Visible (diode array) and electrochemical detectors that were used in this study will now be discussed extensively, and the difference in concentration detection limits of the two detectors will be evaluated.

Table 5.01 Detection methods with their detection limits, their advantages/disadvantages

Methods	**Mass detection limits (moles)**	**Concentration detection limit (molar)**	**Advantages/Disadvantages**
UV-Vis absorption	10^{-13}-10^{-16}	10^{-5}-10^{-8}	-Universal -Diode array offers spectral information
Fluorescence	10^{-15}-10^{-17}	10^{-7}-10^{-9}	-Sensitive -Usually requires sample derivatization
Laser-induced fluorescence	10^{-18}-10^{-20}	10^{-14}-10^{-16}	-Extremely sensitive -Usually requires sample derivatization -expensive
Amperometry	10^{-18}–10^{-19}	10^{-10}-10^{-11}	-Sensitive -Selective but useful only for electroactive analytes -Requires special electronics and capillary modification
Conductivity	10^{-15}-10^{-16}	10^{-7}-10^{-8}	-Universal -Requires special electronics and capillary modification
Mass spectrometry	10^{-16}-10^{-17}	10^{-8}-10^{-9}	-Sensitive and offers structural information -Interface between CE and MS complicated

5.2 UV-Visible detection

Diode array detection (DAD) is an alternative to single or multiple wavelength detection. Instrumentally, a DAD consists of an achromatic lens system to focus light into the capillary. The beam is then dispersed by a diffraction grating and falls on the photodiode array. An array consists of numerous diodes, each of which is dedicated to measuring a narrow-band spectrum. DAD in CE offers similar advantages over single-wavelength detection as it does in HPLC[3].

Importantly, DAD optics can yield detection limits, sensitivity, and a linear detection range that equals or exceeds that of single or multiple wavelength detectors. With respect to spectral analysis, DAD also has significant advantages over rapid scanning detectors. The primary advantage of the DAD is the increased confidence with which the purity and identity of a peak can be established[3]. Unlike in the scanning design, the signal-to-noise ratio of spectral data is independent of the number of wavelengths acquired, the bandwidth of individual wavelengths is not predetermined, and on-line spectra are available at all times.

DAD can greatly simplify analysis of electrophoretic data. When developing a new electrophoretic method there is usually little or no information regarding the required detector conditions, and in particular no optimal wavelength. Using a conventional variable wavelength detector, the sample must be injected repeatedly, changing the detector wavelength each time to make sure that all solutes are detected. With a diode-array an entire wavelength range can be selected, for example from 190 to 600 nm with a bandwidth of 400 nm. In a single analysis, all solutes absorbing within this range will be detected.

One of the disadvantages of DAD, however, is that it is not selective and the sensitivity is not sufficient for trace element analysis[4].

5.3 Electrochemical detection (EC)

EC techniques were first introduced to CE in 1987 by Ewing *et al.* [5,6] using the end-column detection approach with capillaries of 25 μm i.d. and carbon fiber electrodes. This configuration allowed CEEC to be performed without incorporating an electrical-field decoupler. Cassidy *et al.*[7] succeeded in extending this approach to capillary dimensions of 10 and 25 μm i.d. More recently it has been demonstrated that end-column CEEC can be performed without the need of an electrical-field decoupler using capillaries with 50 μm and even 75 μm i.d., which are commonly used with other detection methods. The latter achievements simplify the routine application of CEEC measurements significantly[2]. Subsequently, dozens of reports have appeared, demonstrating the strengths of CE with EC and its applicability for many important analytes. Without question, the past two decades have seen a great increase in the use of electrochemically based methods to solve analytical problems.[8]

Electrochemical detectors are usually constructed in the laboratories where they are used. The components required for setting up an amperometric detection system for CE are rather simple and inexpensive. However, the two main challenges of CEEC are to achieve a precise and stable alignment of the working electrode relative to the capillary column and proper consideration of effects that may rise from interference of the high voltage (HV) electric field with the detection circuit[2].

One approach to reduce the effects of the HV electric field on the detection circuit is based on the implementation of a fracture near the capillary end through which the electrophoresis circuit is grounded. The typical CEEC layout, shown in Figure 5.01 is a schematic representation of the electrochemical detector.

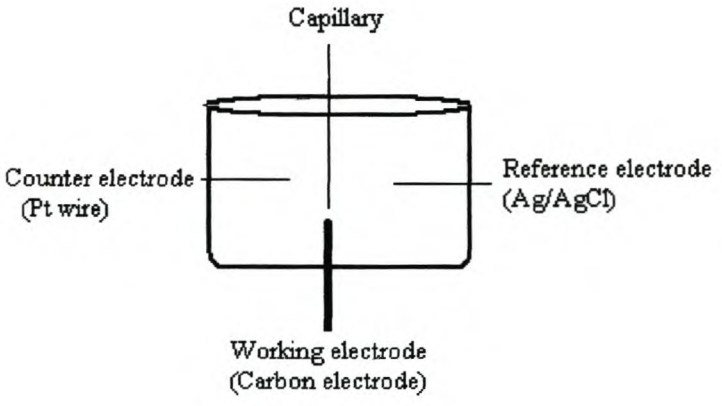

Figure 5.01 Schematic representation of the electrochemical detector

Except for the electrodes and the elements introduced for their decoupling and alignment, none of the equipment is different from that used in other CE and EC instrumentation. The EC electronics is simply a potentiostat similar to those developed earlier for use in HPLC[9] and available commercially from a number of suppliers. Of course, because of the small size of the working electrodes employed in CEEC, the potentiostat must be able to measure current in the 10-100 pA range, which is somewhat smaller than what is encountered in analogous HPLC experiments. EC is a reusable, sensitive and low cost analytical device[10]. Another aspect of practical relevance is the size and geometry of the working electrode and its alignment relative to the capillary outlet. Most initial CEEC arrangements were based on carbon fiber electrodes positioned inside the capillary end

and the implementation of an electric-field decoupler, which involved an interruption of the separation capillary. Although carbon and metal fibers are still being used, disk electrodes of various sizes are gaining increasing importance. This is mainly due to the fact that they are more robust than fiber electrodes and can be mechanically polished which facilitates long time use.

Basically, there are three EC systems suitable for sensitive detection of metal ions, *i.e.* amperometric (AD), conductometric (CD) and potentiometric detection (PD).

The salient features of the three-electrochemical detection methods: amperometry, conductometry and potentiometry are summarized in Table 5.02. The amperometric detector, which was used in this work, is detailed.

Table 5.02 Electrochemical detection methods for capillary electrophoresis

Method	**Features**
Amperometry	-Good detection limits. -Only possible for electroactive ions. -Different electrodes needed for different species. -Stability sometimes problematic.
Conductometry	-Available commercially. -Universal, but particularly good for small ions. -Detection limits not always adequate. -No adaptation of electrodes to sample necessary.
Potentiometry	-For lipophilic ions only. -Different electrodes required for anions and cations. -Relatively difficult electrode preparation.

Amperometry, measuring the redox current at an electrode to which a fixed potential is applied, is the most commonly employed electrochemical means of detection in capillary electrophoresis[11]. The use of amperometric electrochemical detection techniques was first introduced by Ewing in 1987[12]. Amperometric detection with a microelectrode is potentially one of the most sensitive detection techniques because it allows very good detection limits, often better than 10^{-7} mol, for CE separation. This method was the one that was used in this study. Amperometric detection in CE has been accomplished by either off-column or end-column detection[13].

Note that the term EC in the context of chromatography and electrophoresis often has the exclusive connotation of an amperometric detector[14]. It is only applicable to redox-active species. Most often it has been used oxidatively but reduction is sometimes also feasible. The range of species determined includes many organic species with electro-active groups, such as amino acids, peptides, neurotransmitters, pharmaceuticals, chlorinated phenols, and carbohydrates as well as inorganic anions such as sulfur-containing species and heavy metal cations[15].

5.4 Modes of electrochemical detection

There are two modes of EC, namely "end-column" and "off-column" detection. These terms are used to specify the respective absence and presence of a decoupler, respectively.

For end-column detection an electrode is placed directly at the end of the separation capillary without a conductive joint[14] (Figure 5.02A). If the width of the capillary is small

(*i.e* 25 μm i.d. or less), its ohmic resistance is very high. Therefore, the CE current is low in magnitude and nearly the entire CE high voltage is dropped across the capillary itself. In order to improve the sensitivity and to eliminate the noise from mechanical vibrations, precise alignment and stabilization of the working electrode are required.

However, in this method, because the detector is not isolated from the separation voltage used in CE, the actual detection potential is influenced by the electric field present at the end of the separation capillary. In addition, small fluctuation in the voltage of the power supply used for separation can translate into noise at the end-column detection, and the electrode must re-equilibrate each time the separation voltage is turned on. Due primarily to these factors, concentration detection limits using end-column detection have been reported to be consistently higher than those obtained by off-column detection. The major disadvantage of end-column compared to off-column detection is that there is a 1-2 order of magnitude loss of sensitivity with the former[16].

For optimization of end-column CEEC, a detailed knowledge of effects of the HV electric field on detection performance and insights into hydrodynamic voltammetry of electroosmotically driven systems are necessary.

For the off-column mode, a conductive junction between the separation and detection capillary is used to isolate the high voltage applied to the separation capillary from the EC system[17]. The decoupling of the CE and EC systems is accomplished by creating a small opening or fracture in the capillary wall *ca.* 1 cm before the exit end. This effectively divides the capillary into two sections: a "separation capillary" before the fracture and a "detection capillary" beyond it (Figure 5.02B).

A potential problem with this approach is band broadening due to the pressure generated by the detection capillary[18].

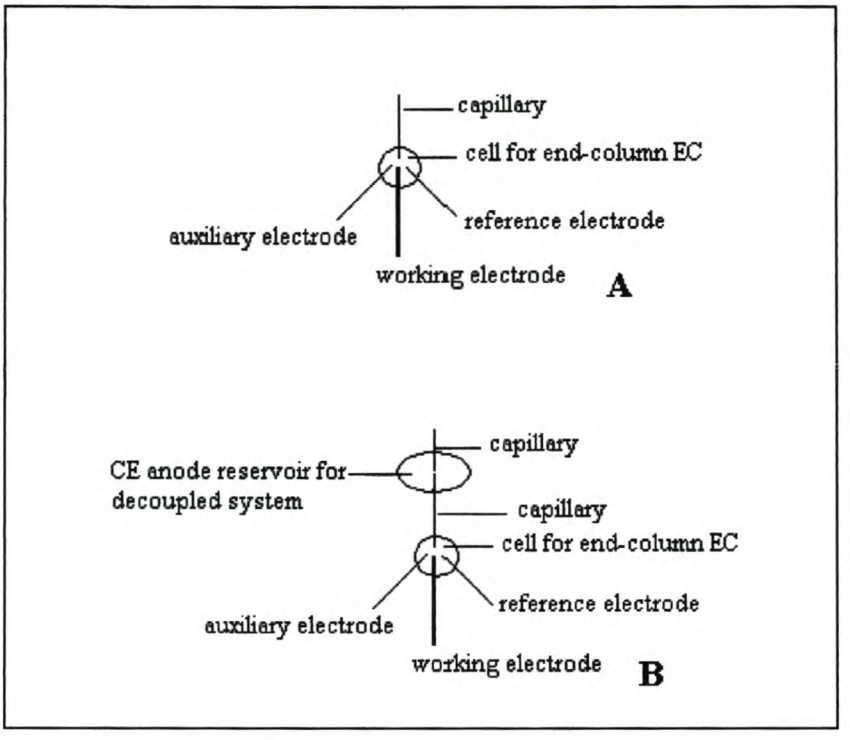

Figure 5.02 Schematic representation of the end-column (A) and off-column (B) detectors.

Although satisfactory results can be obtained from both modes of EC, these modes have seldom been applicable to routine analysis[17]. This is primarily due to the difficulty in finding an appropriate material to make the conductive junction, and the fairly elaborate work needed for the construction of a reliable and sophisticated electrochemical cell.

5.5 Capillary alignment

A number of specific alignment strategies have been devised and demonstrated[2]. These have been shown both to simplify the operations involved in establishing the optimum alignment initially and to improve the stability and reproducibility with which it can be maintained. The positioning of the electrode to the capillary outlet is the most important

parameter for optimization of detection performance as it determines the characteristics of mass transport toward the electrode and the effect of ohmic potential drop resulting from the electrophoretic current on actual detection potential[2].

The different EC system arrangements

1. Wall-jet arrangement – EC electrode is placed at the end of the capillary.
2. On-capillary electrodes – EC electrode is permanently attached to the capillary tip.
3. In-capillary electrode – EC electrode is physically inserted into a capillary in a short distance.

5.5.1 Wall-jet electrodes (WJE)

In CEEC successful alignment usually depends on the exact placement, relative to one another, of two very small objects, the capillary opening and a microelectrode surface, both of which are difficult to see clearly with the naked eye. The WJE approach attempts to simplify this task by making one of the objects, the electrode, much larger. This is accomplished by using a flat, disk-shaped electrode in place of the cylindrically shaped wire or fiber microelectrode usually employed in CEEC. As with the microelectrodes above, the larger electrode is aligned with the capillary with the aid of a micro positioning device. However, this operation in practice is only slightly more involved than simply pushing the flat tip of the wall-jet electrode up against the capillary outlet and checking the placement by a test injection of analyte. With this design, the electrode is large enough to be seen and electrode placement with respect to the capillary is easy to

reproduce over the course of an extended series of CE experiments[18]. This type of configuration offers several practical advantages, including easier electrode/capillary alignment, and greater stability and reproducibility. Moreover, it is possible to obtain the higher current response of a macroelectrode with the low background current by using an array electrode[19].

These advantages have been verified in a number of subsequent wall-jet CEEC systems employing different electrode materials and capillary/electrode combinations, ranging from a 75 μm capillary with a 500 μm electrode (used in this study) to a 13 μm capillary paired with a 90 μm electrode (Figure 5.03).

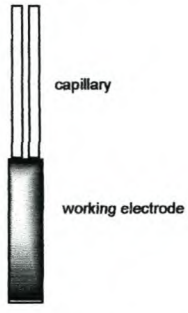

Figure 5.03 Schematic representation of the wall-jet electrode.

5.5.2 In-capillary and on-capillary electrodes

One of the principal methods employed to alleviate alignment difficulties involves the physical insertion of the EC electrode a short distance into a capillary opening to create what has been termed an "in-capillary" electrode (ICE) configuration[20]. The electrode must be smaller than the i.d of the capillary for this approach to be feasible. Although electrodes as small as 1 μm have been used with 2 μm i.d. capillaries, this requirement generally limits the use of this method to larger capillaries with i.d.s of at least 50 μm. A schematic presentation of an in-capillary electrode is shown in Figure 5.04A.

An on-capillary electrode (OCE) is permanently attached to the capillary tip. The obvious way to completely avoid alignment issues is to incorporate both the capillary and the electrode into a single integrated unit[8] whose subsequent placement in the detection cell is not critical. OCE's essentially render alignment issues completely moot. Very recently, two reports describing fabrication methods for such "on-capillary" electrodes have appeared, the first by Zhong and Lunte,[21] and the second by Voegel and Baldwin[10](Figure 5.04B).

Although a degree of manipulative skill on the part of the experimenter, including some reliance on microscopes and micropositioners, is still required for construction of this OCE, the system proved quite rugged in operation, with the useful life of the OCE normally outlasting that of the capillary itself. A real advantage of this approach is that it can be adapted to make a batch of OCE's simultaneously (so far, as many as 21 at a time). Further, the OCE method can be used to create a wide range of different OCE's, either by sputter-coating different metals or by altering the Au and Pt coatings by conventional electrode modification schemes. With this method, the alignment is no longer an issue as the integrated capillary/electrode unit is simply inserted into the terminating electrophoresis buffer reservoir at the start of the CE experiment[22].

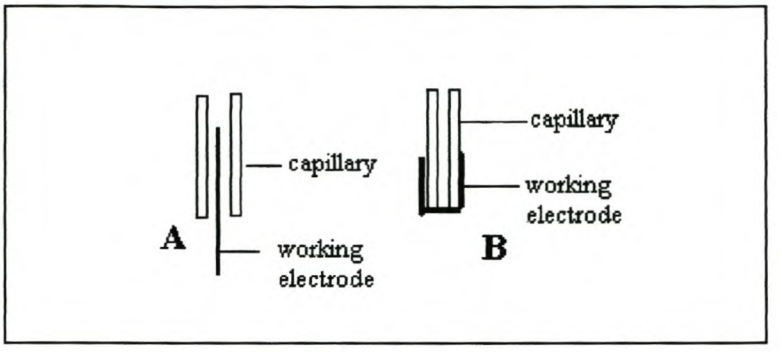

Figure 5.04 Schematic representation of in-capillary (A) and on-capillary (B) electrodes.

In all cases, wall-jet was employed using the end-column configuration.

5.6 Why is EC not popular?

- High voltage applied in CE is considered being incompatible with EC perceive the separation and the resulting current in the capillary instinctively[14]. One possible approach is to locate the detector and counter electrodes opposite and exactly perpendicular, to the length of the capillary, so that the voltage gradient along the capillary length is not pressed on the detector[14].
- Commercially available UV-Vis detectors can be adapted relatively easily to be used with capillaries, a convenient route chosen by many instrument manufacturers.
- For EC, care has to be taken to eliminate or minimize interference of the applied high voltage and resulting current. This is exactly what was considered difficult to achieve[14].

- The application of EC in CE for reducible substances is rare compared to that for oxidizable substances. This is because, for determination of electrochemical reducible substances, the interference of coexisting oxygen in the solution, which can also be reduced at the same working electrode and produces high noise, has to be considered[12].
- Problems arise from the need to isolate the small detection potential from the CE voltage and current, and requirements for precise alignment of the capillary and electrodes[23,24].
- There is the question of how small EC detection potentials and currents are influenced by, and can be shielded or "decoupled" from, the much larger CE voltage and current.
- The issue of capillary/electrode alignment must be addressed in a manner that leads to acceptable analytical performance without making the CEEC experiment an unduly complex or burdensome operation to perform. The problem here is that the microelectrode must be placed very close to the capillary opening to ensure maximum interaction with the analyte species and maximum sensitivity.
- Alignment must be able to be maintained over the course of several experiments and to be reproduced on a daily basis if CEEC is to provide useful and attractive quantitative analytical capabilities.
- A critical mass of analytically significant applications must be developed for CEEC. This will require that CEEC-compatibility can be constructed from a variety of different materials in addition to the electrochemist's conventional choice of carbon. This includes noble and transition metal electrodes that often

respond to a wider range of analytes than carbon as well as chemically modified electrodes (CME's), which can be designed to target specific analyte compounds or families[18].

- The major drawback of EC is its inherent selectivity, which generally limits analysis to easily oxidizable or reducible species[13].
- One general limitation of EC is, the fact that the detector electrodes are in direct contact with the sample solution and may therefore deteriorate due to corrosion or fouling.
- The number of analytically important species that are electroactive at modest potentials at the carbon electrodes conventionally used in CEEC, is relatively small[15].
- The use of EC detection schemes often requires a high degree of manipulative skill on the part of the analyst in order to align the microelectrode and capillary opening initially and then to maintain that alignment reproducibly over the course of hours of CEEC operation[1].

Some of these difficulties have been addressed, at least in part, by the creation of electrochemically active electrodes that respond to a wider range of analytes. For example, the use of chemically modified electrodes has made it feasible to employ electrodes that more specifically target individual analyte species.

The problem of alignment can be dealt with by using a wall-jet electrode configuration in which the working electrode is the flat tip of a 100 μm (or larger) wire or a disk-shaped macro-electrode that is simply pushed up against the much smaller capillary outlet. With such an arrangement, the electrodes are large enough to

be seen and electrode placement with respect to the capillary opening is not critical and easy to reproduce over time. This problem can also be resolved by using an "on-capillary electrode".

5.7 Experimental

5.7.1 Instrumentation

Electrophoresis in the capillary was driven by a high-voltage supply (Model HCN 7E-35000, F. u. G. Elektronik, Rosenheim-Langenfunzen, Germany) capable of delivering 0±30 kV. The outlet end of the capillary was always kept grounded through a platinum wire in the amperometric detection cell. Experiments were carried out using fused-silica capillaries (Polymicro Technology, Phoenix, AZ, USA) of 75 μm i.d. (375 μm o.d.) and 102 cm long (90 cm to the detector). The solutes were injected in the hydrodynamic mode by overpressure (100 mbar).

Amperometric detection at a constant potential was performed with a BAS LC-4CE amperometric detector (West Lafayette, IN, USA). The construction of the complete CE system was done in house. End-column detection was employed using a laboratory-made wall-jet cell configuration. A conventional three-electrode system was used with the mercury carbon composite working electrode at the end of the separation capillary. The reference electrode was a Ag/AgCl reference electrode and the auxiliary electrode was a platinum wire. CE experiments were performed with a Prince programmable injector from Lauer Labs (Emmen, The Netherlands). Data analysis was executed with DAX 32 software (Eindhoven, The Netherlands). All experiments were conducted under ambient conditions.

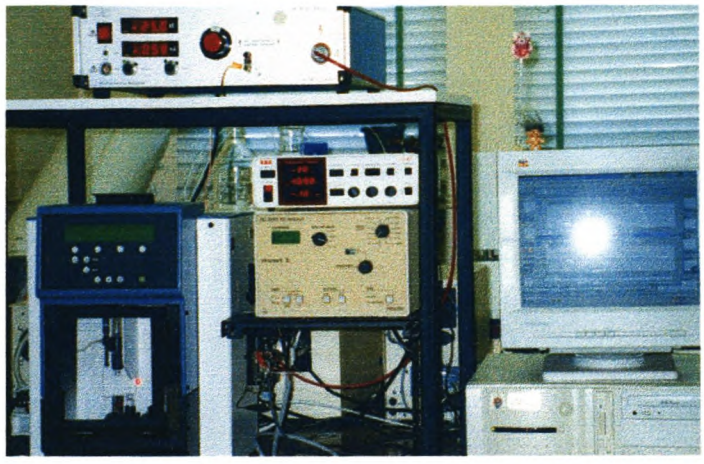

The following parameters were generally used throughout:

Amperometric detector system

Potential	:	-1 600 mV
Filter	:	0.1 Hz
Range	:	20 µA

CE Instrument

Potential	:	-25 kV
Injection time:		2 s
Pressure	:	100 mbar
Wavelength:		200 nm

5.7.2 Stripping Voltammetry

All stripping voltammetry experiments were carried out using a BAS CGME Controlled Growth Mercury Electrode System attached to a BAS 50B Potentiostat. The three electrode system consisted of a mercury modified carbon composite working electrode, a platinum auxiliary electrode and a Ag/AgCl reference electrode. Experiments were carried out in an electrochemical cell holding 10 ml of air saturated 1.15 mM mercury solution under ambient conditions.

The following parameters were generally used throughout:

Initial potential	:	-2000 mV
High potential	:	-200 mV
Scan rate	:	100 mV/s
Sensitivity	:	1 μA/V
Deposit time	:	240 s

5.7.3 Reagents and chemicals

The chemicals used were as given in *Chapter 4*.

5.74 Deposition of mercury

0.015M Hg^{2+} stock solution: Triple distilled mercury (0.3 g) was dissolved with several drops of concentrated nitric acid and was diluted to 100 ml with distilled water.

5.8 Results and discussion

A simple end-column electrochemical detector was designed and attached to an available commercial capillary electrophoresis instrument with UV detection to detect different metal complexes. The working electrode positioning was easily achieved without micropositioners. The alignment between working electrode and capillary outlet was very reproducible; the R.S.D. obtained was lower than 6.0% for about 100 μm gap distance. In this mode, the non-electroactive and electroactive compounds could be detected simultaneously by UV and electrochemical detection. This is the first time that the electrochemical determination of biodegradable complexes using capillary zone electrophoresis (CZE) was attempted. Using both detection systems, a linear range was obtained for concentrations lower than 100.0 ppm. The borate buffer 0.020 M at pH 8.20 and containing 0.030 M of hexadecyltrimethylammonium bromide (CTAB) was used, to obtain selectivity additional separation by the zone distribution process. The separation was performed with a wall-jet configuration cell. Amperometric detection has been used for metal complexes analysis[25]. The use of carbon amalgamated mercury has been reported[26]. The similar procedure is used on determination of metal complexes at carbon/mercury amalgam electrodes. Chemically modified electrodes (CME's) that contain a surface-bound redox mediator are often utilized to lower over-potential for the redox processes of various compounds. CME's have shown advantages over conventional bare electrodes in terms of mechanical stability, improved selectivity and protection from potential fouling effects. The use of modified electrodes and the ability to operate at reduced potentials is especially useful for the analysis of complex environmental samples where interfering compounds may adversely affect detection

selectivity[19]. It has also been shown to be effective in catalyzing the oxidation of several analytes at substantially reduced potentials[27]. For all the metal complexes the detection limits were lower than those obtained by UV detection.

During the analysis, the detection electrode was positioned close to the channel outlet because of the large diameter of the detecting electrode (0.3 mm) compared to the internal width of the channel outlet (75 μm). Good electrochemical efficiency was achieved without precise micro-alignment. However, to ensure the reproducibility of the results obtained, the distance between the detecting electrode and channel outlet was controlled by monitoring the detector's background current before the sample was introduced to the separation channel. A close distance should influence the background current (sloping baseline) owing to incomplete decoupling of the detecting electrode from the high separation field. In contrast, too large a distance reduces electrochemical efficiency as well as separation efficiency, mainly due to the increased post-capillary diffusional broadening at large channel-electrode distances. Wang *et al.*[17] reported that the response of the detecting electrode decreased about 10-fold upon increasing the spacing between the electrode and the channel exit from 60 to 240 μm.

In this thesis, the distance between the detecting electrode and the channel exit was adjusted until a relatively flat background current with a fluctuation of about ±3 nA was attained at various separation potentials.

Each metal complex was analyzed five times to determine the reproducibility of the peak area and migration time for all analytes under optimum conditions in this experiment.

A series of standard solutions of EDDS and EDDM with a concentration range 10 ppb-1 ppm were tested to determine the detection limits for all analytes at the mercury coated carbon electrode.

The buffer concentration influences the viscosity coefficient of the solution, the diffusion coefficient of the analytes and the zeta-potential of the inner surface of capillary tube. It affects not only the resolution and migration time of the analytes but also the peak area. Hence concentrations greater than 1000 ppb were not determined since the concentration had a negative effect on the detection limits because the peak area of all the analytes decrease and the effect of Joule heating become pronounced.

Figure 5.05 shows electropherograms of CuEDDS under optimum conditions at a mercury-amalgamated CCE with concentration range of 10 to 1000 ppb. The same trend was observed for CrEDDS and PbEDDS. Detection limits ranging from 0.05-0.3 μM were obtained. The detection limits were evaluated on the basis of a signal-to-noise ratio of 3.

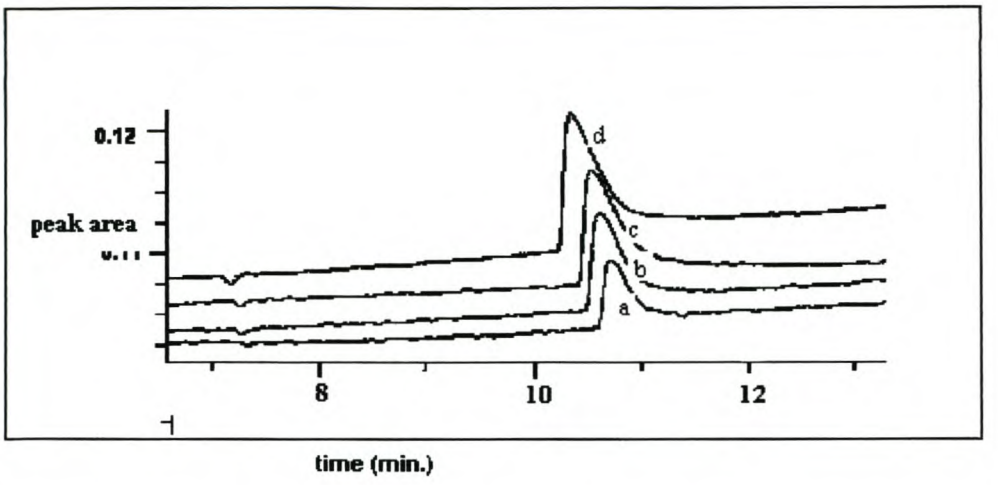

Figure 5.05 Electropherogram of CuEDDS determined by CZE at various concentrations between 10 and 1000 ppb from a-d, respectively. Conditions: Column 112 cm × 50 μm i.d., working electrode: 30 mm diameter carbon disk electrode, injection: 50mbar during 3 s, working potential -1.0V.

For CuEDDS, peak tailing increased and peak broadening was observed as the concentration was increased. An increase in the peak area is observed as the concentration is increased. The response for a series of five injections of PbEDDS, CrEDDS and CuEDDS resulted in relative standard deviations of the currents of 0.95%, 0.963% and 1.29%, respectively. A linear relationship holds between the peak current detected and the concentration in the 20-200 ppb range with correlation coefficients (r) > 0.998 with an applied voltage of -1.0V (vs. Ag/AgCl). The obtained detection limits for EC and UV detection, based on signal-to-noise (S/N) ratio of 3 are listed in table 5.03.

Table 5.03 Detection limits of PbEDDS, CrEDDS and CuEDDS for EC and UV detection

Metal ligand	Detection limit (μM) for EC	Detection limit (μM) for EC
PbEDDS	0.005	1.0
CrEDDS	0.016	3.846
CuEDDS	0.016	3.147

Speciation of the metal complexes using the CE method is sensitive when an electrochemical detector is used. Between 200 ppb and 1 ppm not much change was observed in the peak area of the metal complexes.

A calibration curve was constructed by determining the peak area for 3 replicated injection of each metal complex. Figure 5.06 shows a linear relationship between the peak area and the concentrations for CuEDDS and PbEDDS, while for CrEDDS the response was reasonably stable. It can also be observed from Figure 5.05 that the resolution (R_s) increased with increasing buffer concentration. As it is known, higher buffer concentrations result in higher ionic strength, which leads to an increase in current in the capillary and joule heating. Concurrently, higher buffer concentration with slow electroosmotic flow results in longer migration times.

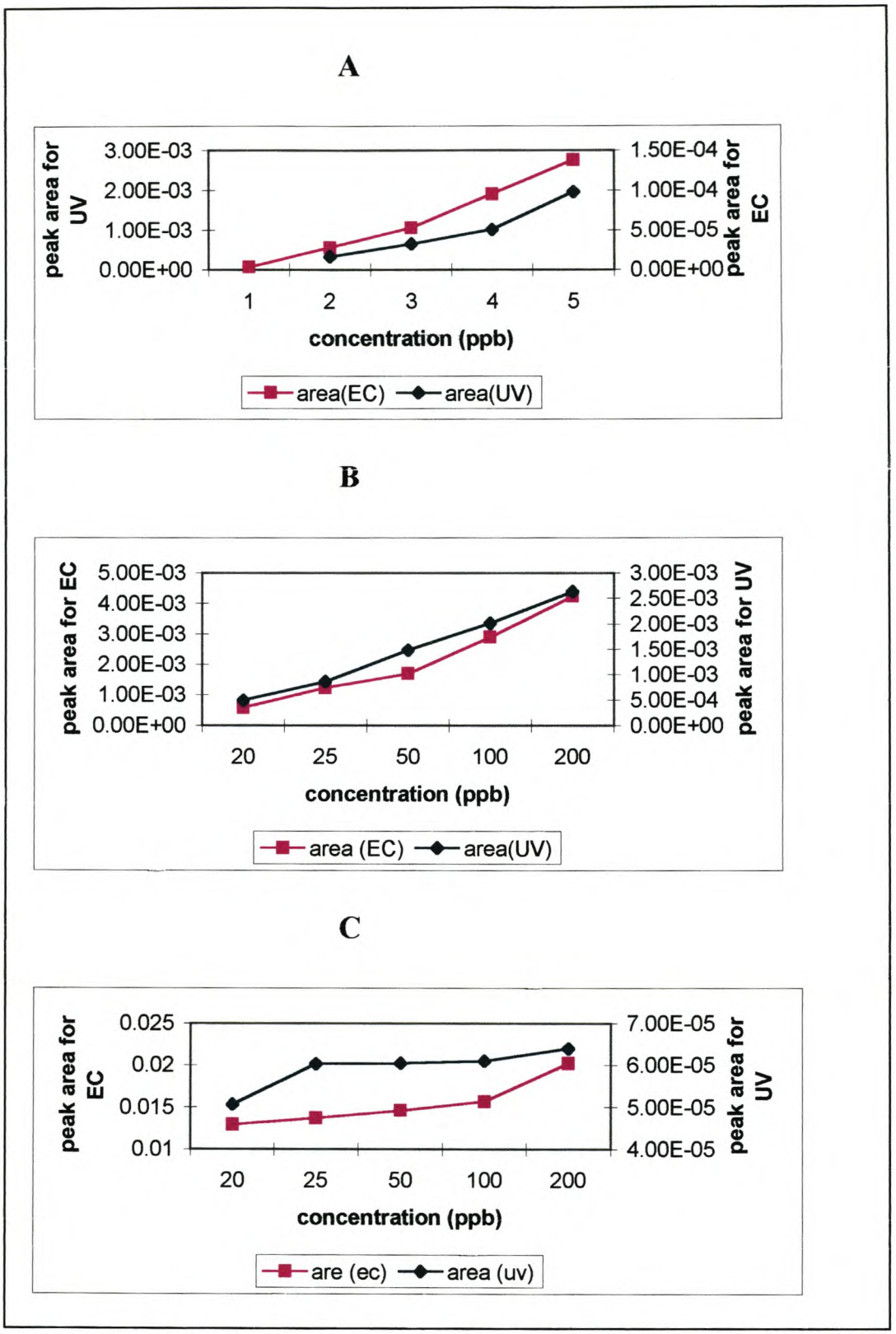

Figure 5.06 Graph of peak area vs. concentration for CuEDDS (A), CrEDDS (B) and PbEDDS (C) using EC and UV detection.

Figure 5.06 shows the differences in peak areas for the CuEDDS, CrEDDS and PbEDDS complexes when using UV and EC detectors. It can be seen from the graph that the peak area obtained using the EC is much greater than when the UV detector is used. From the graphs it can be seen that the peak area increases linearly at concentrations lower than 100 ppb while at higher concentrations the peak area increases much slower.

A similar approach was taken in all subsequent determinations. Table 5.04 shows the obtained detection limits for CdEDDM, CrEDDM and FeEDDM.

Table 5.04 Detection limits of CdEDDM, CrEDDM and FeEDDM for EC and UV detection

Metal ligand	**Detection limit (μM) for EC**	**Detection limit (μM) for UV**
CdEDDM	0.009	1.780
CrEDDM	0.016	3.846
FeEDDM	0.018	3.581

Figure 5.07 shows the obtained electropherograms for CdEDDM and FeEDDM.

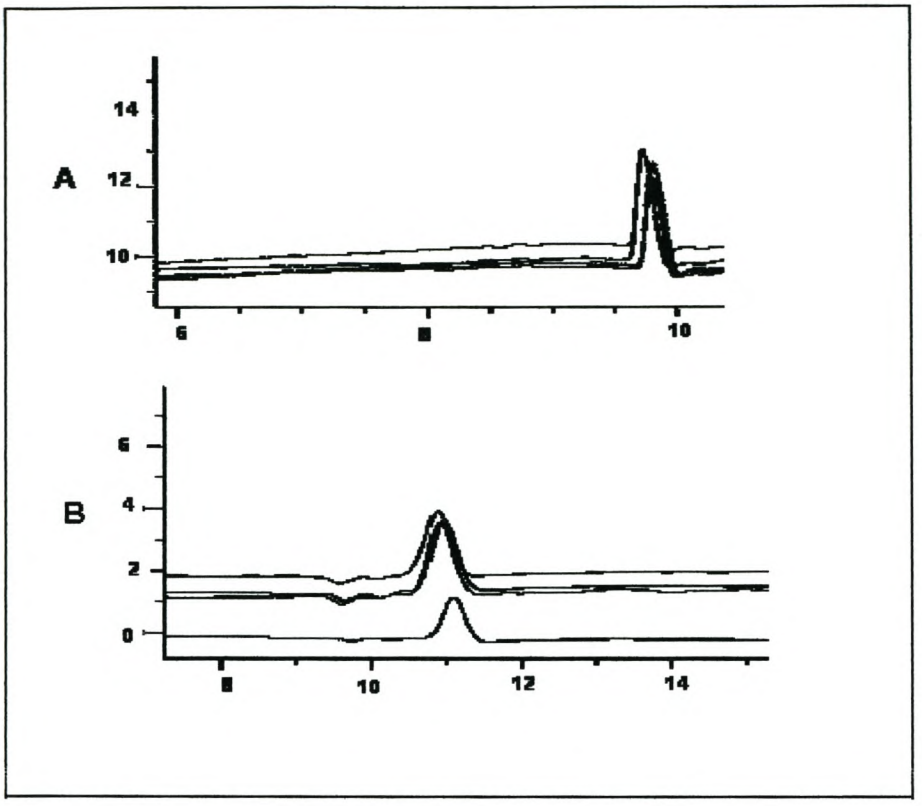

Figure 5.07 Electropherograms of CdEDDM (A) and FeEDDM (B) obtained by CZE at different concentrations between 10 and 1000 ppb. Conditions: Same as in Figure 5.05.

From the electropherograms it can be observed that the same trend was obtained as for CuEDDS, where the area of the peak increased with an increase in concentration. Figure 5.08 shows the obtained calibration graphs for CdEDDM, CrEDDM and FeEDDM, respectively for concentration vs. area.

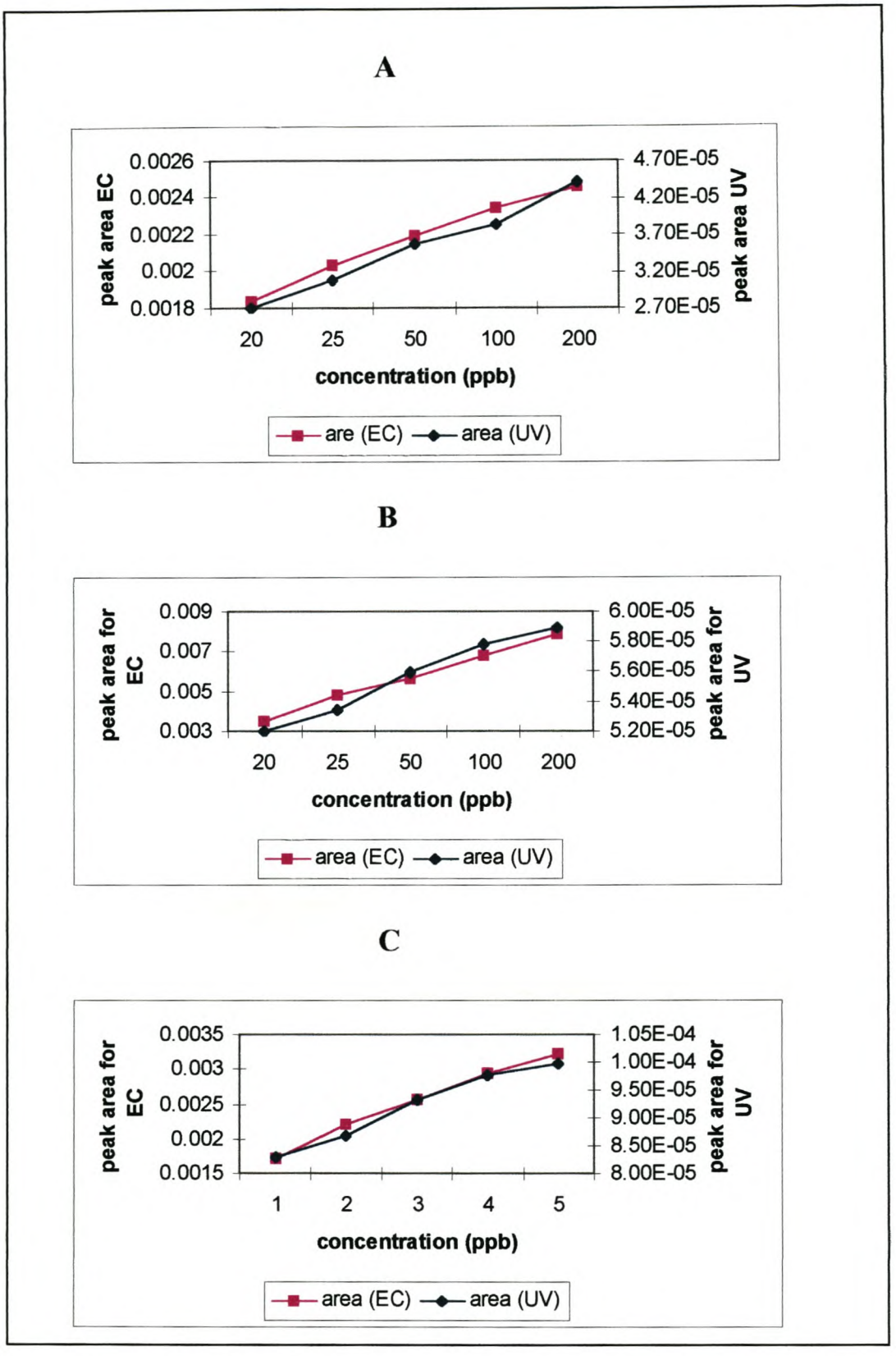

Figure 5.08 Graph of peak area vs. concentration for CdEDDM (A), CrEDDM (B) and FeEDDM (C) using EC and UV detection.

From the calibration graphs it can be seen that the EC detector is more sensitive than the UV detector.

5.9 Conclusions

A new and useful electrochemical cell, designed to maintain a reliable operation at capillary electrophoresis flow rates, has been developed. The primary advantage of this electrochemical cell assembly is its easier construction compared with other end-column electrochemical detectors, in which a micropositioner is needed. The electrochemical cell could also be easily coupled to available commercial capillary electrophoresis equipment, in which no special modifications are needed on its original design.

The combined detection with both UV detector and electrochemical detector was performed. The UV detection was on-column, while the amperometric detection was end-column. Such a combined detection approach shows very good versatility and selectivity. In addition, it is very easy to position the working electrode and the outlet of the capillary column. Metal complexes could be detected by electrochemical and UV detection system simultaneously.

The utility of the system was demonstrated in the detection of various polyaminocarboxylate complexes. The detection limit of these complexes was between 0.005-0.02 $\mu moll^{-1}$ for amperometric detection and > 1 $\mu moll^{-1}$ for UV detection.

CE coupled with electrochemical detection using Hg-modified CCE has proven to be suitable for the determination of metal complexes. The electrode described, consisting of Hg deposited in a carbon composite, represents a very effective and simple method for constant potential amperometric detection of polyaminocaroxylates in CE. The

performance of the mercury amalgamated electrode has demonstrated desirable properties, namely stability and versatility, *i.e.* ease of incorporation of redox catalyst. The alkaline condition that prevails present no problem for electrochemical detection with the Hg amalgamated CCE. Based on the diversity of chemical modifiers available, the Hg amalgamated CCE coupled with CE offer great promise for future CE applications.

The combination of the electrochemical techniques with electrophoretic separation was generally found not to be a problem when using capillaries of 75 μm diameter and electrical decoupling was not necessary. The electrochemical detection used in this study provides a high selectivity for only electro-active substances. The study also demonstrates that the end-column electrochemical detection produces lower detection limits compared to UV detection.

References

1. Hua L., Tan S. N., *Analytica Chimica Acta*, 2000, **403**, 179-186.
2. Matysik F-M., *Analytical Chemistry*, 2000, **72**, 2581-2586.
3. Heiger D. N., Kaltenbach P., Slevert H-J. P., *Electrophoresis,* **15**, 1994, 1234-1247.
4. Weber G., Messerschmidt J., Alt F., *Fresenius Journal of Analytical Chemistry,* 1998, 209-214.
5. Huang X., Zare R. N., Sloss S., Ewing A. G., *Analytical Chemistry*, **63,** 1991, 189.
6. Sloss S., Ewing A. G., *Analytical Chemistry*, **65**, 1993, 577.
7. Lu W., Cassidy R. M., Baranski A. S., *Journal of Chromatography*, **640**, 1993, 433-440.
8. Baldwin R. P., *Journal of Pharmaceutical and Biomedical Analysis*, 1999, **19,** 69-81.
9. Voegel P. D., Baldwin R. P., *Electrophoresis,* 1997, **18**, 2267-2278\
10. Heiger D. N., Kaltenbach P., Slevert H-J. P., *Electrophoresis,* **15**, 1994, 1234-1247.
11. Kappes T., Galliker B., Schwartz M. A., Hauser P. C., *Trends in Analytical Chemistry,* **20(3),** March 2001, 2526-2536.
12. Voegel P. D., Zhou W., Baldwin R. P., *Analytical Chemistry*, 1997, **951**, 957.
13. Sato K., Jin J-Y. Takeuchi T., Miwa T., Takekoshi Y., Kanno S., Kawase S., *Analyst,* 2000, **125**, 1041-1043.

14. Kappes T., Hauser P. C., *Electroanalysis*, 2000, **12(13),** 165-170.

15. Kappes T., Hauser P. C., Galliker B., and Schwartz M. A., *Science Direct*, March 2001, **20(3),** 133-139.

16. Zhong M., Lunte S. .M., *Analytical Chemistry,* **68**, 1996, 2488-2493.

17. Wang A., Fang Y., *Electrophoresis*, 2000, **21**, 1281-1290.

18. Lacher N. A., Garrison K. E., Martin R. S., Lunte S. M., *Electrophoresis,* 2001, **22**, 2526-2536.

19. Liu J., Zhou W., You T., Li F., Wang E., Dong S., *Analytical Chemistry*, **68,** 1996, 3350-3353

20. Dempsey E., Lunte S. M., *The Analyst,* 2001, **126**, 277-280.

21. Voegel P. D., Zhou W., Baldwin R. P., *Analytical Chemistry*, **69**,1997, 951-957.

22. Wallingford R. A., Ewing A. G., *Analytical Chemistry*, **59**, 1987, 1762-1766.

23. Voegel P. D., Baldwin R. P., *Electrophoresis,* 1998, **19**, 2226-2232.

24. Vogt C., Klunder G. L., *Fresenius Journal of Analytical Chemistry*, 2001, **370,** 316-331.

25. Kappes T., Schierle P., Hauser P. C., *Analytica Chimica Acta,* 1997, **350**, 141-147.

26. Kappes T., Hauser P. C., *The Analyst,* 1999, ***124***, 1035.

27. Martin R. S., Crawron A. J., Forgarty B. A., Regan F. P., Dempsey E., Lunte S. M., *The Analyst,* 2001, **126**, 277-280.

CHAPTER 6

OVERALL CONCLUSIONS AND RECOMMENDATIONS

6.1 Overall conclusions

The main objectives of the project were to develop a simple analytical technique to speciate polyaminocarboxylic acid ligands and their complexes. Speciation is essential in a better understanding of reactions in the environment and industry as discussed in *Chapter 3*.

Speciation can be determined using such techniques like Computer Simulated Modelling, stripping voltammetry *etc.*, but so far there is no analytical technique that is able to speciate sufficiently. Capillary zone electrophoresis was the method of choice since it has been used before by Burgisser and Stone[1] for the determination of a variety of amino carboxylic acids at 185 nm that had the ability to simultaneously determine the chelate metal complex thus allowing speciation to be readily studied.

Chapter 4 discusses extensively the obtained electropherograms. Data are compared with the speciation graphs obtained using JESS. From the results it can be concluded that CZE can speciate polyaminocarboxylic acids and their complexes since the same trend was observed for as in JESS.

After developing the analytical method for speciation an electrochemical detector was developed to improve the method. A wall jet end-column detector was developed to improve the detection limits of the complexes. From *Chapter 5*, it can be concluded from the results that the electrochemical detector improved the method since lower detection limits were obtained compared to the detection limit of UV detector.

6.2 Recommendations

- Chiral speciation of biodegradable ligands can be done using CZE since these biodegradable ligands have chiral centres.
- Converting area to concentration (having suitable standards) of the speciation diagrams obtained using CZE for quantitative analysis.
- Synthesis of new biodegradable complexes *e.g.* EDDG.

6.3 Outputs

Papers published, submitted or in preparation

1. Khotseng L E, Polhuis M, Williams D R, Crouch A M, A Comparative Study of Cyclic Voltammetry with Potentiometric Analysis for Determining Formation Constants for Polyaminocarboxylate-metal Ion Complexes, Analytica Chimica Acta. 448 (2001), 231-237.

2.Crouch A M, Khotseng L E, Polhuis M, Williams D R, A Voltammetric Study of the Metal Complex Formation Constants for [S,S']-Ethylenediamine-N,N'-disuccinic Acid with Selected Transition Metals, Electrochimica Acta (submitted).

3.Crouch A M, Khotseng L E, Polhuis M, Williams D R, A Voltammetric Study of Metal Complex Formation Constants of Ethylenediamine -N, N'-dimalonic Acid Complexes, Fresenius. Journal of Analytical Chemistry (submitted).

4.Khotseng L E, Sandra P, Crouch A. M, Speciation of the Ligands EDTA, EDDS and EDDM by Capillary Zone Electrophoresis, Prepared for Electrophoresis.

5.Khotseng L E, Sandra P, Crouch A. M, Speciation of Biodegradable Complexes by Capillary Zone Electrophoresis, Completed for Electrophoresis.

6.Khotseng L E, Sandra P, Crouch A. M Electrochemical Determination of Aminopolycarboxylate Ligands at Mercury Carbon Composite Electrode and Amperometric Detection in Capillary Electrophoresis, Completed for the Analyst.

Conference contributions

1.Khotseng L E, Polhuis M, Crouch A M, Ethylenediamine disuccinic Acid; A New Ligand for an Old Process, Inorganic 99, Stellenbosch, South Africa, January 1999

2.Crouch A M, Polhuis M, Khotseng L E, Electrochemistry and Speciation of Ethylendiamine Disuccinic Acid (EDDS) and its Complexes with Transition Metals, Environmental. Science & Pollution Research -International, Special Issue 1, 2000.

3.Khotseng L E, Polhuis M, Crouch A. M, Electrochemistry and Speciation Studies of Polyaminocarboxylate Complexes, 35th Convention of SACI, 24-29 September 2000, Potchefstroom, South Africa

4.Crouch A M, Polhuis M, Khotseng L E, Katata L, Electrochemistry and Separation of Readily Biodegradable Ligands, 6th International Symposium on Applied Bioinorganic Chemistry, Cardiff, UK, 20-23 June 2001

5.Khotseng L, Crouch A. M, Separation of Biodegradable Complexes using Capillary Zone Electrophoresis, 36th Convention of SACI, 1-5 July 2002, Port Elizabeth, South Africa

6.Khotseng L E, Crouch A M, An Electrochemical Detector for Capillary Electrophoresis: Separation and Detection of Biodegradable Metal Complexes, Analytica 2002, 4 - 10 December 2002, Stellenbosch, South Africa

References

1. Burgisser C. S., and Stone A. T., *Environmental Science and Technology,* 31 (9), (1997) 2656.